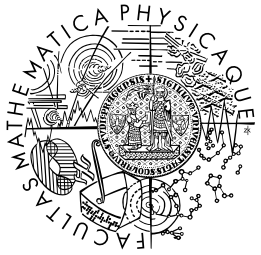

FACULTY
OF MATHEMATICS
AND PHYSICS
Charles University

MASTER THESIS

Lukáš Honsa

Periodically driven quantum systems

Institute of Particle and Nuclear Physics

Supervisor of the master thesis: prof. RNDr. Pavel Cejnar, Dr., DSc.

Study programme: Physics

Study branch: Theoretical Physics

Prague 2022

I declare that I carried out this master thesis independently, and only with the cited sources, literature and other professional sources. It has not been used to obtain another or the same degree.

I understand that my work relates to the rights and obligations under the Act No. 121/2000 Sb., the Copyright Act, as amended, in particular the fact that the Charles University has the right to conclude a license agreement on the use of this work as a school work pursuant to Section 60 subsection 1 of the Copyright Act.

In ..... date ....

Author's signature

I am deeply grateful to Professor Pavel Cejnar for his kind advice, continuous support and for giving me a nice and interesting topic for my master's thesis.

Title: Periodically driven quantum systems

Author: Lukáš Honsa

Institute: Institute of Particle and Nuclear Physics

Supervisor: prof. RNDr. Pavel Cejnar, Dr., DSc., Institute of Particle and Nuclear Physics

Abstract: We present theoretical methods for studying quantum mechanical systems subjected to fast periodic driving and apply them to model systems with long-range interaction. We provide a comparison between the methods and insight facilitated by these methods. The methods recently occurred in scientific papers, which supports the need for a scrutinized exposition of the theory. One of the main objects of the theory is a so-called Floquet Hamiltonian—an artificial stationary Hamiltonian describing important features of a quantum system. The methods construct Floquet Hamiltonians in the form of series in the powers of the time period. We present the spectra of Floquet Hamiltonians—the so-called quasienergy spectra—computed by the methods and computed numerically (with higher precision). The quasienergy spectra were computed using various approximations of Floquet Hamiltonians and compared. We discuss an interesting topic of the classical limit of an artificial stationary system. We also mention the kicked rotor system and its connection with the kicked top system—one of our model systems. In summary, the method characterized by simultaneous construction of a Floquet Hamiltonian and a so-called kick operator (operator capturing fast changes of the system) was found universal and accurate. The thesis presents an elaborated theoretical background for future study of the systems in more specific areas of physics and manifests the strengths and weaknesses of the methods.

Keywords: Floquet Hamiltonian quasienergies periodic driving

Contents

Introduction

In quantum mechanics, the dynamical problem of systems with a time-dependent Hamiltonian is hard to solve. Besides a few analytically solvable problems (e.g. the problem in section 1.2), a solution is usually reached via some perturbation approaches. This thesis studies a particular group of time-dependent systems—the periodically driven systems. A quite efficient theory, called Floquet theory, is suitable for handling these problems. In addition, we study these systems in the regime of a short time period in which we can describe the problem by non-trivial series in the powers of the time period.

The history of the Floquet theory goes back to mathematician G. Floquet and his work on differential equations with periodic coefficients [1] released in 1883. This theory was applied to time periodic quantum systems, e.g. in [2]. Providing a self-consistent description of the theory from the quantum mechanical point of view is one of the goals of this thesis.

Like any other physical model, the time-periodic systems described here can be subjected to experimental tests. One of the examples is described in [3], where the evolution of a quantum mechanical state is presented and a comparison between numerical and experimental results is provided.

A central object of the Floquet theory is a so-called Floquet Hamiltonian. It transforms (at least partly) the dynamical problem with a time-dependent periodic Hamiltonian into a problem with an artificial stationary Hamiltonian. And it is this object that we put under scrutiny in this thesis. A Floquet Hamiltonian provides a so-called quasienergy spectrum that enables further physical insight into the behaviour of periodically driven systems.

Periodically driven systems are still the focus of active research [4, 5, 6]. Papers [7, 8] discuss periodically driven systems in connection with analogues of quantum phase transitions in excited spectra—the so-called exited-state quantum phase transitions [9, 10, 11]. One of the goals of this thesis is to learn enough information about periodically driven quantum systems as a preparation for studying signatures of exited-state quantum phase transitions in these systems.

The structure of this work is the following: The first chapter presents two examples of simple periodically driven systems and explains some rudiments of the sophisticated approach discussed later. This chapter is intended as an elementary introduction to the topic of periodic driving in quantum mechanics.

The second chapter is a detailed description of the theory that describes periodically driven systems. Methods for constructing Floquet Hamiltonians by series in powers of the time period are also presented. Various versions of the famous Baker–Campbell–Hausdorff (BCH) formula are used. This chapter represents a synthesis of approaches described in various papers, but it also contains a non-trivial amount of our own insight and calculations.

The last chapter describes several examples of many-body periodically driven systems with long-range interaction and studies the capability of the theory to accurately describe the systems, i.e. the convergence of the series for Floquet Hamiltonians in the regime of a short time period. In several parts of the third chapter, we digress in order to present physically interesting related topics, i.e.

classical limits, the chaotic regime of the systems and the non-uniqueness of quantization of the kicked rotor system. All numerical calculations in this chapter represent our own results. Besides verifying older results presented in the literature, we performed some new calculations (like the exact and effective classical dynamics and the evolution of the Wigner distributions of the kicked top system). Also, the derivation of some Floquet Hamiltonians for harmonic driving is new in this work.

Unless otherwise stated, throughout this thesis we use such units that $\hbar = 1$.

1. Effective description of simple systems

Before we proceed to examine systems with many spins, we will examine a single-spin-$\frac{1}{2}$ system. This will enable us to grasp the concept of the effective description of periodically driven systems. We will use the spin-$\frac{1}{2}$ operator $\widehat{\vec{S}} = \widehat{\vec{\sigma}}/2$, where $\widehat{\vec{\sigma}}$ is the vector of Pauli matrices.

1.1 Delta-driven single-spin system

Here we present a simplistic model of one delta-driven spin. The Hamiltonian of the system reads[1]

$$\widehat{H}(t) = \kappa\widehat{I} + pT\widehat{\sigma}_x \sum_{n=-\infty}^{+\infty} \delta(t - n \cdot T), \tag{1.1}$$

where $\widehat{I}$ is an identity operator, p and κ are parameters of the system and T is a period of the driving. The summands $\delta(t-n\cdot T)$ are delta functions and present some impulsive driving of the system, e.g. homogeneous magnetic field switched on for an infinitesimal duration.

The term multiplying the sum of the delta functions commutes with the time-independent term of the Hamiltonian[2]

$$\left[p\widehat{\sigma}_x, \kappa\widehat{I}\right] = 0, \tag{1.2}$$

which makes the time evolution exceptionally simple.

The evolution operator reads

$$\widehat{U}(t^+, 0^+) \overset{\text{def}}{=} \lim_{\epsilon\to 0^+} \widehat{U}(t+\epsilon, 0+\epsilon) \tag{1.3}$$

$$= \lim_{\epsilon\to 0^+} e^{\left[-i\int_{0+\epsilon}^{t+\epsilon} \widehat{H}(t')\mathrm{d}t'\right]}. \tag{1.4}$$

If $t = n \cdot T, n \in \mathbb{Z}$, the sign t^+ means that we consider the time just after the realisation of the delta function. In other times the superscript + could be omitted. Mathematically, we ensure the fact that we mean the time just after the realisation of the delta function by doing a limit approaching the time t from the right.

[1] Although the part $\kappa\widehat{I}$ of the Hamiltonian (1.1) is trivial, it allows us to show the formalism we will construct in the next chapter. Also the term $\kappa\widehat{I}$ could be seen as a multiple of the z projection of the total spin operator squared that is in the case of spin-$\frac{1}{2}$ particle equal to $\frac{1}{4}\widehat{I}$.

[2] If we replace the delta functions by some approximate form (e.g. Cauchy form $\delta_\Delta(x) = \pi^{-1}\Delta/(\Delta^2 + x^2)$, $\Delta \ll 1$), the Hamiltonian at different times commutes $\left[\widehat{H}(t), \widehat{H}(t')\right] = 0$, $\forall t, t' \in \mathbb{R}$.

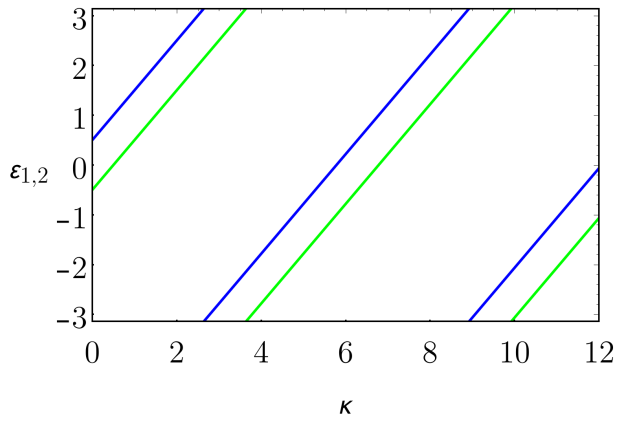

Figure 1.1: The quasienergies mapped to the first Brillouin zone ε_1 and ε_2 for the system described by the Hamiltonian (1.1) with the period $T = 1$ and parameter $p = 0.5$. Dependence on the parameter κ.

We evaluate the integral of the sum of the delta functions separately

$$\begin{aligned} \lim_{\epsilon\to 0^+} \sum_{n=-\infty}^{+\infty} \int_{0+\epsilon}^{t+\epsilon} \delta(t' - n\cdot T)\mathrm{d}t' &= \sum_{n=1}^{+\infty} \theta(t - n\cdot T), t \geq 0 \\ &= \lfloor t/T \rfloor, \end{aligned} \tag{1.5}$$

where we used the Heaviside step function defined the following way

$$\theta(x) = \begin{cases} 0 & \text{if} \quad x < 0, \\ 1 & \text{if} \quad x \geq 0 \end{cases} \tag{1.6}$$

and we also used the floor function defined by

$$\lfloor x \rfloor = m \quad \text{if} \quad x \in [m, m+1), m \in \mathbb{Z}. \tag{1.7}$$

The evolution operator reads

$$\begin{aligned} \widehat{U}(t^+, 0^+) = &\quad e^{-i\left(pT\lfloor t/T\rfloor \widehat{\sigma}_x + \widehat{I}\kappa t\right)} \\ = &\quad e^{-i\kappa t} e^{-ipT\lfloor t/T\rfloor \widehat{\sigma}_x}. \end{aligned} \tag{1.8}$$

Using the known expansion of exponential function

$$e^{-ipT\lfloor t/T\rfloor \widehat{\sigma}_x} = \sum_{n=0}^{\infty} \frac{(-ipT\lfloor t/T\rfloor \widehat{\sigma}_x)^n}{n!}, \tag{1.9}$$

we find another expression for the evolution operator

$$\widehat{U}(t^+, 0^+) = e^{-i\kappa t} \cdot \left[\cos\left(pT\lfloor t/T\rfloor\right) - i\sin\left(pT\lfloor t/T\rfloor\right)\widehat{\sigma}_x\right]. \tag{1.10}$$

For periodically driven systems, the evolution operator evolving the system for the duration of one period $\widehat{U}(T^+, 0^+)$ is of special importance. Another important class of operators are operators called Floquet Hamiltonians. In this case, one member of the class of Floquet Hamiltonians is some operator $\widehat{G}_s$ that satisfies

$$\widehat{U}(T^+, 0^+) = e^{-i\widehat{G}_s T}. \tag{1.11}$$

Since the system is exceptionally simple, we easily find

$$\widehat{G}_s = \frac{1}{T}\int_{0^+}^{T^+} \widehat{H}(t)\mathrm{d}t = p\hat{\sigma}_x + \hat{I}\kappa. \tag{1.12}$$

In matrix form

$$\left(\widehat{G}_s\right) = \begin{pmatrix} \kappa & p \\ p & \kappa \end{pmatrix}. \tag{1.13}$$

The eigenvalues of the matrix (1.13) are especially important. The eigenvalues are

$$\tilde{\varepsilon}_{1,2} = \kappa \pm p. \tag{1.14}$$

Note that the eigenvectors of $\widehat{G}_s$

$$|x\pm\rangle = \frac{1}{\sqrt{2}}\begin{pmatrix} 1 \\ \pm 1 \end{pmatrix} \tag{1.15}$$

diagonalize also the operator $\widehat{U}(T^+, 0^+)$ with eigenvalues $e^{\mp i\tilde{\varepsilon}_{1,2}T}$. From equation (1.11), we see that for another Floquet Hamiltonian[3] its eigenvalues could differ from $\tilde{\varepsilon}_{1,2}$. Generally

$$\begin{aligned} \varepsilon_\alpha &= \tilde{\varepsilon}_1 + m_\alpha \cdot \frac{2\pi}{T}, m_\alpha \in \mathbb{Z}, \\ \varepsilon_\beta &= \tilde{\varepsilon}_2 + m_\beta \cdot \frac{2\pi}{T}, m_\beta \in \mathbb{Z}, \end{aligned} \tag{1.16}$$

is another pair of possible eigenvalues of a Floquet Hamiltonian of our system. The eigenvalues of a Floquet Hamiltonian are made unique by adding the multiples of $2\pi/T$ to them so they fit into the interval $(-\pi/T, \pi/T]$. The eigenvalues of a Floquet Hamiltonian adapted to the interval $(-\pi/T, \pi/T] \ni \varepsilon_1, \varepsilon_2$ are called quasienergies in the first Brillouin zone. The quasienergies in the first Brillouin zone for the period $T = 1$ and parameter $p = 0.5$ are depicted in figure 1.1.

1.2 Harmonically-driven single-spin system

An intriguing example of a periodically driven system described in [12] captures the physics of nuclear magnetic resonance (NMR). It describes a particle with a magnetic moment placed in a combined stationary (homogeneous) and variable (rotating) magnetic field. The system is described by the Hamiltonian[4][5]

$$\widehat{H}(t) = -\omega_0\widehat{S}_z - \omega_r\left(\widehat{S}_x\cos(\omega t) + \widehat{S}_y\sin(\omega t)\right). \tag{1.17}$$

[3]The proper definition of the Floquet Hamiltonian is given in the next chapter by (2.15).

[4]The constants ω_0 and ω_r describe the magnitudes of the applied magnetic fields the following way $\omega_0 = \gamma B_0$ and $\omega_r = \gamma|\vec{B}_r|$, where B_0 and $\vec{B}_r$ are elucidated in figure 1.2 and γ is a gyromagnetic ratio. The gyromagnetic ratio for an electron is $\gamma_e \approx -1.761\cdot 10^{11}$ s^{-1} T^{-1}, $\gamma_e\hbar \approx -1.159\cdot 10^{-4}$ eV T^{-1} and for a proton $\gamma_p \approx 2.675\cdot 10^8$ s^{-1} T^{-1}, $\gamma_p\hbar \approx 1.761\cdot 10^{-7}$ eV T^{-1}.

[5]Considering the NMR, a spin precession is launched by setting $\omega = -\omega_0$ and switching on the rotating part of the magnetic field in short pulses.

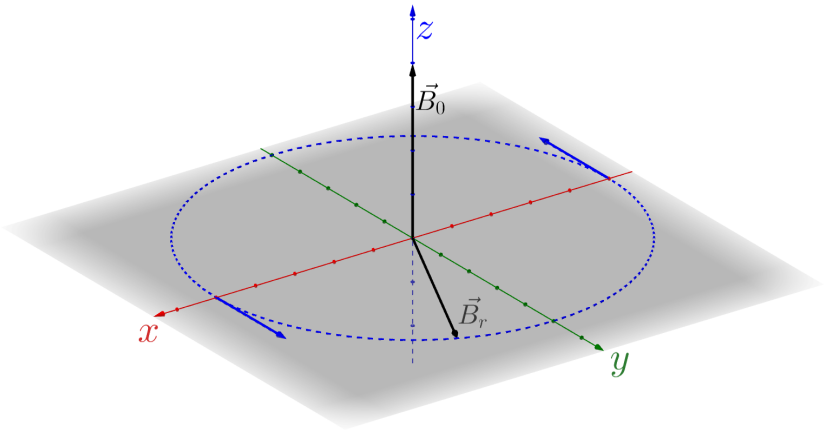

Figure 1.2: The rotating $\vec{B}_r(t) = \omega_r\gamma^{-1}(\cos(\omega t), \sin(\omega t), 0)^T$ and homogeneous $\vec{B}_0 = (0, 0, \omega_0\gamma^{-1})^T$ magnetic field from the NMR example. The constant γ is the gyromagnetic ratio.

The stationary and rotating magnetic field are visualized in figure 1.2.

Since the Hamiltonian at different times does not commute, i.e.

$$\begin{aligned}\left[\widehat{H}(t), \widehat{H}(t')\right] = \; & i\omega_0\omega_r \left[\sin(\omega t) - \sin(\omega t')\right] \widehat{S}_x \\ & + i\omega_0\omega_r \left[\cos(\omega t') - \cos(\omega t)\right] \widehat{S}_y \\ & + i\omega_r^2 \sin\left[\omega(t' - t)\right] \widehat{S}_z,\end{aligned} \tag{1.18}$$

the construction of the time evolution is not trivial.

We notice, using the well known formula[6]

$$e^{\widehat{A}}\widehat{B}e^{-\widehat{A}} = \widehat{B} + \sum_{k=1}^{\infty} \frac{1}{k!} \underbrace{\left[\widehat{A}, \left[\widehat{A}, \ldots \left[\widehat{A}, \widehat{B}\right]\right] \ldots\right]_k}_{\text{k commutators}}, \tag{1.19}$$

that the time dependence of the Hamiltonian could be eliminated by similarity transformation. The following relations hold

$$\begin{aligned} & e^{i\alpha\widehat{S}_z}\widehat{S}_x e^{-i\alpha\widehat{S}_z} \\ = \; & \widehat{S}_x + \frac{1}{1!}(i\alpha)^1\left[\widehat{S}_z, \widehat{S}_x\right] + \frac{1}{2!}(i\alpha)^2\left[\widehat{S}_z, i\widehat{S}_y\right] + \frac{1}{3!}(i\alpha)^3\left[\widehat{S}_z, \widehat{S}_x\right] + \ldots \\ = \; & \widehat{S}_x - \frac{\alpha}{1!}\widehat{S}_y - \frac{\alpha^2}{2!}\widehat{S}_x + \frac{\alpha^3}{3!}\widehat{S}_y + \frac{\alpha^4}{4!}\widehat{S}_x - \frac{\alpha^5}{5!}\widehat{S}_y + \ldots \qquad (1.20) \\ = \; & \left(1 - \frac{\alpha^2}{2!} + \frac{\alpha^4}{4!} - \ldots\right)\widehat{S}_x - \left(\frac{\alpha}{1!} - \frac{\alpha^3}{3!} + \ldots\right)\widehat{S}_y \qquad (1.21) \\ = \; & (\cos\alpha)\widehat{S}_x - (\sin\alpha)\widehat{S}_y. \qquad (1.22)\end{aligned}$$

We write again the Hamiltonian using the aforementioned similarity transformation

$$\widehat{H}(t) = e^{-i\omega t\widehat{S}_z}\left(-\omega_0\widehat{S}_z - \omega_r\widehat{S}_x\right)e^{i\omega t\widehat{S}_z}, \tag{1.23}$$

[6]The identity (1.19) follows from (A.9) in appendix A.

where we used (1.22) with the substitution $\alpha = -\omega t$.

We try to translate the time-dependent problem into a time-independent problem, i.e. the time-independent Schrödinger equation, with some new Hamiltonian. We define the new state vector

$$|\phi(t)\rangle \stackrel{\text{def}}{=} e^{i\omega t\widehat{S}_z} |\psi(t)\rangle \tag{1.24}$$

and try to find the evolution equation for that state.

We express the following term (the left-hand side of the Schrödinger equation)

$$\begin{aligned} i\frac{\mathrm{d}}{\mathrm{d}t} |\phi(t)\rangle &= i\frac{\mathrm{d}}{\mathrm{d}t} \left[e^{i\omega t\widehat{S}_z} |\psi(t)\rangle \right] && (1.25)\\ &= -\omega \widehat{S}_z e^{i\omega t\widehat{S}_z} |\psi(t)\rangle + e^{i\omega t\widehat{S}_z} \widehat{H}(t) |\psi(t)\rangle && (1.26)\\ &= -\omega |\phi(t)\rangle + e^{i\omega t\widehat{S}_z} \widehat{H}(t) e^{-i\omega t\widehat{S}_z} e^{i\omega t\widehat{S}_z} |\psi(t)\rangle . && (1.27) \end{aligned}$$

Using (1.23) we reach

$$i\frac{\mathrm{d}}{\mathrm{d}t} |\phi(t)\rangle = \left[(-\omega - \omega_0) \widehat{S}_z - \omega_r \widehat{S}_x \right] |\phi(t)\rangle . \tag{1.28}$$

Equation (1.28) is the Schrödinger equation $i\partial_t |\phi(t)\rangle = \widehat{H}_r |\phi(t)\rangle$ with the new time-independent Hamiltonian

$$\widehat{H}_r = (-\omega - \omega_0) \widehat{S}_z - \omega_r \widehat{S}_x. \tag{1.29}$$

It is easy to realise that the evolution operator for the original states,

$$|\psi(t_2)\rangle = \widehat{U}(t_2, t_1) |\psi(t_1)\rangle , \tag{1.30}$$

factorizes the following way

$$\widehat{U}(t_2, t_1) = e^{-i\omega t_2 \widehat{S}_z} e^{-i\widehat{H}_r (t_2 - t_1)} e^{i\omega t_1 \widehat{S}_z}. \tag{1.31}$$

The factorization of the evolution operator $\widehat{U}(t_2, t_1)$ in equation (1.31) is essentially a transformation to a rotating reference frame then an evolution of a time-independent system and then a transformation back to the laboratory reference frame. The operator $e^{-i\omega t\widehat{S}_z}$ represents a counterclockwise rotation around the z-axis by the angle ωt. In the next chapters, we will see that a generalized version of this procedure applies to all time-periodic problems.

2. Effective Hamiltonian

In this chapter we outline some methods for constructing a Floquet Hamiltonian. A Floquet Hamiltonian is loosely speaking a time-independent Hamiltonian, capturing characteristics of a system with a time-dependent periodic Hamiltonian. In this work the term effective Hamiltonian means an approximate form of a Floquet Hamiltonian—the first few terms of a series expansion of a Floquet Hamiltonian.

The Hamiltonian $\widehat{H}(t)$ of the system is supposed to be periodic in time with the period T. Thus

$$\widehat{H}(t+T) = \widehat{H}(t). \tag{2.1}$$

We will consider the Hamiltonian of the system in the form of the Fourier expansion

$$\boxed{\widehat{H}(t) = \widehat{H}_0 + \widehat{V}_0 + \sum_{n=1}^{+\infty} \left(\widehat{V}_n e^{+in\omega t} + \widehat{V}_{-n} e^{-in\omega t} \right)}, \tag{2.2}$$

where $\widehat{H}_0$ and $\widehat{V}_0$ are time-independent. The Hermicity of $\widehat{H}(t)$ implies $\widehat{V}_n^\dagger = \widehat{V}_{-n}$.

In the following, we will suppose that the frequency of the driving $2\pi/T$ is high compared to the typical energy scale. It means that the system itself—its state vector—is evolving slowly compared to the "speed" of the driving.[1] More precisely, there will always be some "fast motion" part of the evolution of the state of the system but this fast motion part is becoming increasingly small when the period T goes to infinity. For the time being, we estimate the typical energy scale by an operator norm of the constant term in the Hamiltonian $||\widehat{H}_0 + \widehat{V}_0||$, i.e. $T \ll 1/||\widehat{H}_0 + \widehat{V}_0||$. A more precise discussion of the smallness of T will follow. Generally, we will obtain some approximate formulas for a Floquet Hamiltonian working well for a short time period T.

2.1 Introduction

When dealing with time-independent systems (Hamiltonians), we utilize the concept of stationary states. In adiabatic systems, the concept of stationary states could be in some sense preserved. In this thesis we neither deal with time-independent systems nor with adiabatic systems. A new formalism shall consequently be adopted. In this chapter we will define the states called Floquet modes. In some sense, we could consider the Floquet modes to be the generalized stationary states for our problem. In this section we try to motivate the reader and show the important properties of the time-periodic systems which justify the chosen (Floquet) formalism.

Firstly, we show that considering the full evolution of the system—prescribed by the evolution operator $\widehat{U}(t,0)$—to any final time $t \in \mathbb{R}$, only the operator $\widehat{U}(t,0)$ for $t \in (0,T]$ is needed. This tremendously simplifies the description and could be considered a consequence of the discrete symmetry in time of the system.

[1] We are close to the sudden approximation or diabatic limit, discussed e.g. in [13].

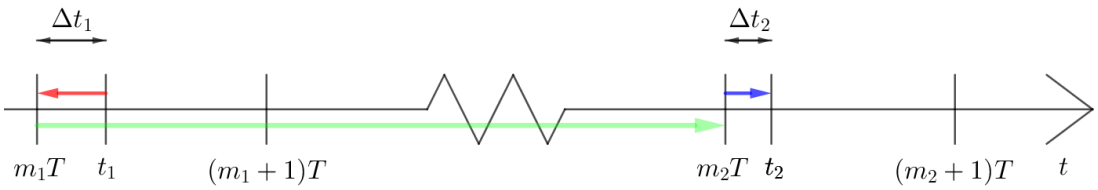

Figure 2.1: The important times facilitating factorization of the evolution operator, using equation (2.3), are depicted on the time axes. The action of the operators $\widehat{U}^\dagger(\Delta t_1, 0)$ (red), $\left[\widehat{U}(T,0)\right]^{m_2-m_1}$ (green) and $\widehat{U}(\Delta t_2, 0)$ (blue) is illustrated by coloured arrows.

From the Schrödinger equation for the evolution operator $\partial_t \widehat{U}(t,t') = \widehat{H}(t)\widehat{U}(t,t')$ and time periodicity of the Hamiltonian we get[2]

$$\widehat{U}(nT + t_2, nT + t_1) = \widehat{U}(t_2, t_1), n \in \mathbb{Z}. \tag{2.3}$$

For any $t_1, t_2 \in \mathbb{R}$ we find $\Delta t_{1,2} \in [0, T)$, $m_{1,2} \in \mathbb{Z}$ such that $t_1 = m_1 T + \Delta t_1$ and $t_2 = m_2 T + \Delta t_2$. Then using (2.3), we transcribe the evolution operator the following way

$$\widehat{U}(t_2, t_1) = \widehat{U}(\Delta t_2, 0) \left[\widehat{U}(T,0)\right]^{m_2-m_1} \widehat{U}^\dagger(\Delta t_1, 0). \tag{2.4}$$

The factorization is illustrated in figure 2.1. From equation (2.4) we see that only the evolution operator from zero to $t \in (0, T]$ is needed.

In many cases we restrict ourselves only to the evolution operator evolving the system for the duration of one period $\widehat{U}(T + t_s, t_s)$ called Floquet operator and we are only interested in the states at the stroboscopic times $t_s + nT, n \in \mathbb{N}_0$.

The systems in which we identify two significant operators $\widehat{A}$ and $\widehat{B}$ so that we can factorize the Floquet operator the following way

$$\widehat{U}(T + t_s, t_s) = e^{-i\widehat{A}} e^{-i\widehat{B}} \tag{2.5}$$

are of special importance since we can use the standard BCH formula for some further analysis. Systems having the property (2.5) are discussed in section 2.4.

Among others we study the properties of delta-driven systems. Delta-driven systems belong to archetypal systems used for studying chaos. Consequently, much effort has been dedicated to them. Delta-driven systems have also the factorizing property (2.5). Delta-driven systems are characterized as having the "driving" part of the Hamiltonian in the form

$$\widehat{V}(t) = \widehat{H}(t) - \widehat{H}_0 = \widehat{V}_P \cdot T \sum_{n=-\infty}^{+\infty} \delta\left(t - nT\right), \tag{2.6}$$

where $\widehat{V}_P$ is time-independent. As we have seen in our simplistic example in section 1.1, when considering the delta-driven systems, during the time period there are two significant moments which attract our attention. One of these moments is immediately before the realisation of the delta function and one is right after

[2] A verbose proof is given on the page 19.

the realisation of the delta function. These moments are connected with discontinuity in the formal objects of the theory (confer with the discontinuities of the floor function in section 1.1) and the appropriate objects should be constructed using the limits either from the left or from the right. Both of these moments are connected with the times $nT, n \in \mathbb{Z}$ so we should indicate whether we are taking the limit from the left or right (objects immediately before and right after the realisation of the delta function respectively). The Floquet operator $\widehat{U}(T+t_s, t_s)$ with $t_s = 0$ of a delta-driven system has the factorizing property (2.5). As we have seen in section 1.1 we need to choose whether we consider the time $t_s = 0$ before the realisation of the delta function or after the realisation of the delta function.

The central theorem of the Floquet formalism is Floquet's theorem. Floquet's theorem says that the evolving states of the system could be expressed as linear combinations of the Floquet states

$$\boxed{|\psi_\alpha(t)\rangle = e^{-i\varepsilon_\alpha t}\,|u_\alpha(t)\rangle}, \tag{2.7}$$

where the coefficients in the linear combinations are time-independent and each (Floquet mode) $|u_\alpha(t)\rangle$ is time-periodic with the period T. Floquet's theorem is closely connected with Bloch's theorem for periodic crystals, where the periodicity in space is considered. The values $\varepsilon_\alpha \in \mathbb{R}$ are eigenvalues of a so-called Floquet Hamiltonian. There is an ambiguity in the definition of the values ε_α—we can add integral multiples of $\omega = 2\pi/T$ to them. Also, the Floquet Hamiltonian is not uniquely defined, though the Floquet Hamiltonians have many universal properties. In finite-dimensional Hilbert space, the Floquet states (2.7) corresponding to all the eigenvalues of a Floquet Hamiltonian form a basis.

The Fourier transform form of the Hamiltonian (2.2)

$$\widehat{H}(t) = \widehat{H}_0 + \widehat{V}_0 + \sum_{n=1}^{+\infty} \left(\widehat{V}_n e^{+in\omega t} + \widehat{V}_{-n} e^{-in\omega t} \right)$$

is particularly expedient. In this thesis we consider harmonic driving, in which case only $\widehat{V}_1 = \widehat{V}_{-1}^\dagger$ and $\widehat{H}_0$ are non-zero and the other terms $\widehat{V}_n, n \neq \pm 1$ are equal to zero. Another extreme—all the terms $\widehat{V}_n$ are non-zero—presents a delta-driven system. Considering a delta-driven system, all the terms $\widehat{V}_n$ are the same $\widehat{V}_n = \widehat{V}_P, \forall n \in \mathbb{Z}$ and we get the time-periodic part of the Hamiltonian given by equation (2.6). Note that when considering (2.6) none of the $\widehat{V}_n$ depends on the time period T. We will see that the independence of $\widehat{V}_n$ on the time period T is a good requirement when expanding the formal objects of the theory (e.g. the Floquet Hamiltonian) in the powers of T.

We conclude this section by noting that the one-period average value of an observable $\widehat{A}$ in the Floquet state (2.7) has a meaningful definition, i.e.

$$\begin{aligned}
\overline{A}_\alpha &\overset{\text{def}}{=} \frac{1}{T}\int_0^T \langle\psi_\alpha(t)|\,\widehat{A}\,|\psi_\alpha(t)\rangle && (2.8)\\
&= \frac{1}{T}\int_0^T \langle u_\alpha(t)|\,e^{i\varepsilon_\alpha t}\widehat{A}e^{-i\varepsilon_\alpha t}\,|u_\alpha(t)\rangle && (2.9)\\
&= \frac{1}{T}\int_0^T \langle u_\alpha(t)|\,\widehat{A}\,|u_\alpha(t)\rangle\,. && (2.10)
\end{aligned}$$

2.2 Floquet theory

Here by the Floquet theory we mean the theory which stems from the work of the mathematician Gaston Floquet (1847–1920) on linear differential equations with periodic coefficients [1, 14] and which is appropriate for the description of time-periodic quantum mechanical systems. We synthesize reviews of this theory from various sources. Since one of our goals is to compare various ways how to construct the building blocks of the Floquet theory, e.g. a Floquet Hamiltonian, we need to really do the synthesis rather than rely on one source. The main sources we use in this section (in the order of relevance to this text) are [14], [15], [16], [17] and [18].

2.2.1 Essentials

Bloch's theorem

A useful tool of solid state physics is Bloch's theorem:

The eigenstates ψ of the one-electron Hamiltonian $\widehat{H} = -\hbar^2\nabla^2/(2m) + U(\widehat{\vec{r}})$, where $U(\widehat{\vec{r}} + \vec{R}) = U(\widehat{\vec{r}})$ for all $\vec{R}$ in a Bravais lattice, can be chosen to have the form of a plane wave times a function with the periodicity of the Bravais lattice:

$$\psi_{n\vec{k}} = e^{i\vec{k}\cdot\vec{r}} u_{n\vec{k}}(\vec{r}), \tag{2.11}$$

where $u_{n\vec{k}}(\vec{r} + \vec{R}) = u_{n\vec{k}}(\vec{r})$ for all $\vec{R}$ in the Bravais lattice.[3]

The vector $\vec{k}$ in Bloch's theorem is called wave vector or quasimomentum. Bloch's theorem was earlier proved by Floquet in a one-dimensional case, where it is sometimes called Floquet's theorem [19]. But here the term Floquet's theorem will be referring to the one utilizing the time translational symmetries.

Considering the aforementioned, the discrete time translational symmetries suggest contriving a Bloch's theorem analogue in time. Indeed such a theorem exists. It should be noted that the proof of the theorem addressing the time translation, found in [14] and in section 2.2.2 for a finite-dimensional Hilbert space, is slightly more intricate than the proof of Bloch's theorem (in space), found in [19]. This is simply the consequence of time and position not being treated on an equal footing in standard quantum mechanics.

Floquet's theorem

Floquet's theorem in time, hereafter called Floquet's theorem, states: Suppose a Hamiltonian $\widehat{H}(t)$ is periodic in time with the period T (2.1). And suppose the appropriate Hilbert space for the system is finite.[4] Then the solutions to the Schrödinger equation

$$i\frac{\partial}{\partial t}\left|\psi(t)\right\rangle = \widehat{H}(t)\left|\psi(t)\right\rangle \tag{2.12}$$

[3] A (three-dimensional) Bravais lattice consists of all points with position vectors $\vec{R}$ of the form $\vec{R} = n_1\vec{a}_1 + n_2\vec{a}_2 + n_3\vec{a}_3$, where $\vec{a}_1$, $\vec{a}_2$, and $\vec{a}_3$ are fixed vectors not all in the same plane and $n_1, n_2, n_3 \in \mathbb{Z}$.

[4] There exist variants of Floquet's theorem in time for infinite Hilbert spaces. In this thesis only the variant of Floquet's theorem for finite Hilbert spaces is needed.

are linear combinations of vectors of the form (2.7)

$$\boxed{|\psi_\alpha(t)\rangle = e^{-i\varepsilon_\alpha t}\,|u_\alpha(t)\rangle},$$

where $|u_\alpha(t)\rangle$ is periodic in time t with the period $T = 2\pi/\omega$. The coefficients in the linear combinations are time-independent.

The states $|u_\alpha(t)\rangle$ are called Floquet modes and the values $\varepsilon_\alpha \in \mathbb{R}$ are called quasienergies [14]. The states $|\psi_\alpha(t)\rangle$ are called Floquet states [17].

Note that the states $|u_\alpha(0)\rangle$ evolved in time are the states $|\psi_\alpha(t)\rangle$. Generally speaking, $|u_\alpha(t)\rangle$ is a state parametrized by the parameter t, but not the evolution of the state $|u_\alpha(0)\rangle$ in time (except for Floquet states belonging to $\varepsilon_\alpha = 0$).

First Brillouin zone

The quasienergies ε_α are unique up to an addition of constants $n\omega$, $n \in \mathbb{Z}$. Clearly, if the pair $(|u_\alpha(t)\rangle, \varepsilon_\alpha)$ is the pair of Floquet mode and its quasienergy, the pair

$$(|u_{\alpha'}(t)\rangle = e^{in\omega t}\,|u_\alpha(t)\rangle, \varepsilon_{\alpha'} = \varepsilon_\alpha + n\omega), n \in \mathbb{Z} \tag{2.13}$$

also defines a solution to the Schrödinger equation (2.12). The solution defined by $(|u_{\alpha'}(t)\rangle, \varepsilon_{\alpha'})$ (2.13) is identical to the solution $(|u_\alpha(t)\rangle, \varepsilon_\alpha)$. Thus, we can consider only the quasienergies in the first Brillouin zone defined by $-\omega/2 < \varepsilon_\alpha \leq \omega/2$.

Floquet operator

It is expedient to denote

$$\boxed{\widehat{\mathcal{F}}[t_s] \stackrel{\text{def}}{=} \widehat{U}(T + t_s, t_s)}, \tag{2.14}$$

the evolution operator evolving a system for the duration of one period T from the time t_s. The operator $\widehat{\mathcal{F}}[t_s]$ is called the Floquet operator [7]. The starting time could be indicated next to the Floquet operator $\widehat{\mathcal{F}}$ in square brackets $[t_s]$.

Floquet Hamiltonian

A Hermitian operator $\widehat{G}$ is said to be Floquet Hamiltonian if there exists $t_s \in [0, T)$ and a Hermitian operator $\widehat{K}$ such that

$$\boxed{\widehat{\mathcal{F}}[t_s] = e^{-i\widehat{K}} e^{-i\widehat{G}T} e^{i\widehat{K}}}, \tag{2.15}$$

where the operator $\widehat{\mathcal{F}}[t_s]$ is the Floquet operator.

Generally, for any $t \in [0, T)$ the following relations hold

$$\widehat{U}(T + t, t)\,|\psi_\alpha(t)\rangle = |\psi_\alpha(t + T)\rangle = e^{-i\varepsilon_\alpha T} e^{-i\varepsilon_\alpha t}\,|u_\alpha(t)\rangle, \tag{2.16}$$

$$\widehat{\mathcal{F}}[t]\,|\psi_\alpha(t)\rangle = e^{-i\varepsilon_\alpha T}\,|\psi_\alpha(t)\rangle \tag{2.17}$$

so we easily see that eigenvalues of a Floquet Hamiltonian $\widehat{G}$ are quasienergies ε_α. Considering the first Brillouin zone only, we must add multiples of ω to eigenvalues of a Floquet Hamiltonian to yield the quasienergies in the first Brillouin zone.

In this thesis, we occasionally use the convention that the quasienergies ε_α with $\alpha = 1, 2, ..., d$ are the quasienergies mapped to the First Brillouin zone and ε_α with $\alpha = d+1, d+2, ...$ are general quasienergies (the dimension of the appropriate Hilbert space is d). If $\{\varepsilon_\alpha\}_{\alpha=d+1}^{2d}$ are the eigenvalues of a Floquet Hamiltonian, then there exist $\{m_\alpha\}_{\alpha=d+1}^{2d}, m_\alpha \in \mathbb{Z}$ such that $\{\varepsilon_\alpha + m_\alpha \cdot \omega\}_{\alpha=d+1}^{2d}$ are the quasienergies in the First Brillouin zone.[5]

Stroboscopic versus full description

Time-periodic systems are usually described in a stroboscopic way. It means that only the states at stroboscopic times $t = t_s + n \cdot T, n \in \mathbb{N}_0$ are of our interest. The starting time t_s is some fixed time we choose.

The full description of the time evolution is also possible and Floquet's theorem and a Floquet Hamiltonian are still important parts of the full description. But the description of the evolution for all times is more difficult than a mere stroboscopic description. More information regarding the full description is in subsection 2.2.3.

2.2.2 Proof of Floquet's theorem

We define the operator $\widehat{G}[0]$ in the following way

$$\widehat{U}(T,0) = e^{-i\widehat{G}[0]T}. \tag{2.18}$$

The meaning of the square brackets [0] in $\widehat{G}[0]$ will be elucidated in the next subsection and here is not important. The operator $\widehat{G}[0]$ is not defined uniquely and it suffices to consider just one of the operators satisfying equation (2.18).

We transcribe

$$\left[\widehat{U}(T,0)\right]^{m_2-m_1} = \overbrace{e^{+i\widehat{G}[0]\Delta t_2}\underbrace{e^{-i\widehat{G}[0]\Delta t_2}}_{\widehat{I}}e^{-i\widehat{G}[0]T(m_2-m_1)}\underbrace{e^{+i\widehat{G}[0]\Delta t_1}}_{\widehat{I}}e^{-i\widehat{G}[0]\Delta t_1}}^{e^{-i\widehat{G}[0](t_2-t_1)}} \tag{2.19}$$

and from (2.4) we get

$$\widehat{U}(t_2,t_1) = \widehat{U}(\Delta t_2,0)e^{+i\widehat{G}[0]\Delta t_2}e^{-i\widehat{G}[0](t_2-t_1)}e^{-i\widehat{G}[0]\Delta t_1}\widehat{U}^\dagger(\Delta t_1). \tag{2.20}$$

We define

$$\widehat{P}(t) \stackrel{\text{def}}{=} \widehat{U}(t,0)e^{+i\widehat{G}[0]t}. \quad \text{(fast motion operator)} \tag{2.21}$$

The operator $\widehat{P}(t)$ has the properties

$$\widehat{P}(t+T) = \underbrace{\widehat{U}(T+t,T)}_{\widehat{U}(t,0)}\ \underbrace{\widehat{U}(T,0)\overbrace{e^{+i\widehat{G}[0]T}}^{\widehat{U}^\dagger(T,0)}}_{\widehat{I}}e^{+i\widehat{G}[0]t} \tag{2.22}$$

$$= \widehat{P}(t), \tag{2.23}$$

$$\widehat{P}(t_{1,2}) = \widehat{P}(\Delta t_{1,2}). \tag{2.24}$$

[5] This must be true since the eigenvectors of the Floquet operator must yield a complete basis in the d-dimensional Hilbert space.

Substituting (2.21) into (2.20) and using (2.24) we get

$$\widehat{U}(t_2,t_1) = \widehat{P}(t_2)e^{-i\widehat{G}[0](t_2-t_1)}\widehat{P}^\dagger(t_1). \tag{2.25}$$

We suppose the appropriate Hilbert space to be finite, of the dimension d. The operator $\widehat{G}[0]$ is Hermitian since $\widehat{U}(T,0)$ is unitary. The operator $\widehat{G}[0]$ has eigenvalues[6] $\{\varepsilon_\alpha\}_{\alpha=d+1}^{2d}$

$$\widehat{G}[0]\left|w_\alpha\right\rangle = \varepsilon_\alpha\left|w_\alpha\right\rangle. \tag{2.26}$$

We define

$$\left|u_\alpha(t)\right\rangle \overset{\text{def}}{=} \widehat{P}(t)\left|w_\alpha\right\rangle, \quad \alpha = d+1,...,2d. \quad \text{(Floquet mode)} \tag{2.27}$$

And we also define

$$\left|\psi_\alpha(t)\right\rangle \overset{\text{def}}{=} e^{-i\varepsilon_\alpha t}\left|u_\alpha(t)\right\rangle, \quad \alpha = d+1,...,2d. \quad \text{(Floquet state)} \tag{2.28}$$

The following relations hold

$$\begin{aligned}
\widehat{U}(t_2,t_1)\left|\psi_\alpha(t_1)\right\rangle &= e^{-i\varepsilon_\alpha t_1}\widehat{U}(t_2,t_1)\left|u_\alpha(t_1)\right\rangle && (2.29)\\
&\overset{(2.27)}{=} e^{-i\varepsilon_\alpha t_1}\widehat{U}(t_2,t_1)\widehat{P}(t_1)\left|w_\alpha\right\rangle. && (2.30)\\
&\overset{(2.25)}{=} e^{-i\varepsilon_\alpha t_1}\widehat{P}(t_2)e^{-i\widehat{G}[0](t_2-t_1)}\left|w_\alpha\right\rangle && (2.31)\\
&\overset{(2.26)}{=} e^{-i\varepsilon_\alpha t_1}\widehat{P}(t_2)e^{-i\varepsilon_\alpha(t_2-t_1)}\left|w_\alpha\right\rangle && (2.32)\\
&\overset{(2.27,\ 2.28)}{=} \left|\psi_\alpha(t_2)\right\rangle. && (2.33)
\end{aligned}$$

From (2.33) it follows that a general state $\left|\psi(t)\right\rangle$ has the form[7]

$$\begin{aligned}
\left|\psi(t)\right\rangle &= \sum_{\alpha=d+1}^{2d}\beta_\alpha e^{-i\varepsilon_\alpha t}\left|u_\alpha(t)\right\rangle, \forall t\in\mathbb{R}, && (2.34)\\
\left|u_\alpha(t+T)\right\rangle &\overset{(2.27,\ 2.23)}{=} \left|u_\alpha(t)\right\rangle, \forall t\in\mathbb{R}, && (2.35)
\end{aligned}$$

where the coefficients $\beta_\alpha\in\mathbb{C}, \varepsilon_\alpha\in\mathbb{R}$ are time-independent, which is the content of Floquet's theorem. The proof was inspired by [18, 16, 14].

2.2.3 Another form of Floquet's theorem

Here we transform a time-dependent problem with periodic Hamiltonian into a time-independent problem with a new time-independent Hamiltonian using a specific form of similarity transformation. At the end we identify the result as another form of Floquet's theorem.

Instead of finding a differential equation for usual quantum states $\left|\psi(t)\right\rangle$, we demand the differential equation for new states defined by

$$\left|\phi(t)\right\rangle \overset{\text{def}}{=} e^{i\widehat{K}(t)}\left|\psi(t)\right\rangle, \tag{2.36}$$

[6] We use the indexes $\alpha = d+1, d+2, ..., 2d$. The indexes $\alpha = 1,...,d$ we reserve for ε_α napped to the interval $(-\omega/2, \omega/2]$.

[7] Since $\widehat{P}(t)$ is unitary, $\{\left|u_\alpha(t)\right\rangle\}_{\alpha=d+1}^{2d}$ spans the whole Hilbert space.

where we require the periodicity of the new operator $\widehat{K}(t)$, i.e.

$$\widehat{K}(t) = \widehat{K}(t+T). \tag{2.37}$$

We also require the operator $\widehat{K}(t)$ to be Hermitian. The operator $\widehat{K}(t)$ is called a kick operator. Using (2.36), we can easily transform between $|\phi(t)\rangle$ and $|\psi(t)\rangle$.

We apply $e^{i\widehat{K}(t)}$ to both sides of the Schrödinger equation (2.12) and add the term $i\left(\frac{\partial}{\partial t}e^{i\widehat{K}(t)}\right)|\psi(t)\rangle$ to its both sides and get

$$\begin{aligned} i\frac{\partial}{\partial t}\left(e^{i\widehat{K}(t)}|\psi(t)\rangle\right) &= e^{i\widehat{K}(t)}\widehat{H}(t)|\psi(t)\rangle + i\left(\frac{\partial}{\partial t}e^{i\widehat{K}(t)}\right)|\psi(t)\rangle \qquad (2.38)\\ &= e^{i\widehat{K}(t)}\widehat{H}(t)e^{-i\widehat{K}(t)}e^{i\widehat{K}(t)}|\psi(t)\rangle \\ &\quad + i\left(\frac{\partial}{\partial t}e^{i\widehat{K}(t)}\right)e^{-i\widehat{K}(t)}e^{i\widehat{K}(t)}|\psi(t)\rangle\,, \\ i\frac{\partial}{\partial t}|\phi(t)\rangle &= \left[e^{i\widehat{K}(t)}\widehat{H}(t)e^{-i\widehat{K}(t)} + i\left(\frac{\partial}{\partial t}e^{i\widehat{K}(t)}\right)e^{-i\widehat{K}(t)}\right]|\phi(t)\rangle\,. \qquad (2.39) \end{aligned}$$

We define a new Hamiltonian

$$\widehat{G} \stackrel{\text{def}}{=} e^{i\widehat{K}(t)}\widehat{H}(t)e^{-i\widehat{K}(t)} + i\left(\frac{\partial e^{i\widehat{K}(t)}}{\partial t}\right)e^{-i\widehat{K}(t)}. \tag{2.40}$$

Equation (2.39) reads

$$i\frac{\partial}{\partial t}|\phi(t)\rangle = \widehat{G}\,|\phi(t)\rangle\,. \tag{2.41}$$

In view of the previous explanation (see equation (2.25)) we require that there exists such an operator $\widehat{K}(t)$ that makes the new Hamiltonian $\widehat{G}$ time-independent. Nevertheless, it is important to note here that there is an ambiguity in the choice of a kick operator $\widehat{K}(t)$, and consequently the fast motion operator $\widehat{P}(t)$ and the operator $e^{-i\widehat{K}(t)}$ are not necessarily equal. From now on we suppose that the new Hamiltonian $\widehat{G}$ is time-independent. Then equation (2.41) dictates the evolution of $|\phi(t)\rangle$ in the form of a linear combination of

$$|\phi_\alpha(t)\rangle = e^{-i\varepsilon_\alpha t}|v_\alpha\rangle\,, \tag{2.42}$$

where $|v_\alpha\rangle$ are the eigenvectors of $\widehat{G}$. Transforming the solutions (2.42) back we find the solutions to the Schrödinger equation with the original Hamiltonian $\widehat{H}(t)$

$$|\psi_\alpha(t)\rangle = e^{-i\widehat{K}(t)}|\phi_\alpha(t)\rangle = e^{-i\varepsilon_\alpha t}e^{-i\widehat{K}(t)}|v_\alpha\rangle\,. \tag{2.43}$$

Comparing equation (2.7) with equation (2.43), we get Floquet modes

$$|u_\alpha(t)\rangle = e^{-i\widehat{K}(t)}|v_\alpha\rangle\,, \tag{2.44}$$

which must be time periodic since we require the time periodicity $\widehat{K}(t) = \widehat{K}(t+T)$ of the kick operator $\widehat{K}(t)$.

Under the assumption that $\widehat{G}$ is time-independent, we identify the result above as the already mentioned Floquet's theorem.[8] In section 2.2.2 we proved that at least one time-independent Hamiltonian $\widehat{G}$ exists. But the Hamiltonian discussed here can differ from the one constructed in section 2.2.2. Particularly equation (2.18) is not a necessary property of the new Hamiltonian $\widehat{G}$ and a redefinition of the initial time does not necessarily restore a similar statement about $\widehat{G}$. We also show how to construct such a Floquet Hamiltonian in section 2.3.

The evolution operator can be constructed as the transformation $e^{i\widehat{K}(t_1)}$, evolution by $\widehat{G}$ and the transformation back by $e^{-i\widehat{K}(t_2)}$ [15]. The evolution operator reads

$$\boxed{\widehat{U}(t_2,t_1) = e^{-i\widehat{K}(t_2)}e^{-i(t_2-t_1)\widehat{G}}e^{i\widehat{K}(t_1)}}. \tag{2.45}$$

Be careful when comparing the fast motion operator $\widehat{P}(t)$ with $e^{-i\widehat{K}(t)}$. For non-stroboscopic Floquet Hamiltonians (defined on page 20), they are not the same. In this thesis, we defined the fast motion operator only for stroboscopic Floquet Hamiltonians, but a sensible relation for non-stroboscopic Floquet Hamiltonians would be $\widehat{P}(t) = e^{-i\widehat{K}(t)}e^{+i\widehat{K}(0)}$ [16].[9]

From the above discussion, it is clear that (2.45) is another form of Floquet's theorem. We also identify the new time-independent Hamiltonian $\widehat{G}$ from equation (2.45) as the Floquet Hamiltonian $\widehat{G}$ already defined by equation (2.15).

We formulate the second form of Floquet's theorem: For the system described by a time-periodic Hamiltonian with the period T and for the system whose Hilbert space is finite, the evolution operator $\widehat{U}(t_2,t_1)$ has the form (2.45), where $\widehat{G}$ is Hermitian and time independent and where $\widehat{K}(t)$ is Hermitian and time-periodic with the period T [16].

At this place, we would like to point out the ambiguity in Floquet Hamiltonians and the dependence between the operators $\widehat{G}$ and $\widehat{K}(t)$. Having an arbitrary unitary operator $\widehat{S}$ we rewrite equation (2.45) the following way

$$\begin{aligned}
\widehat{U}(t_2,t_1) &= e^{-i\widehat{K}(t_2)}\widehat{S}\widehat{S}^\dagger e^{-i(t_2-t_1)\widehat{G}}\widehat{S}\widehat{S}^\dagger e^{i\widehat{K}(t_1)} && (2.46)\\
&= e^{-i\widehat{K}'(t_2)}e^{-i(t_2-t_1)\widehat{G}'}e^{i\widehat{K}'(t_1)}, && (2.47)\\
e^{-i\widehat{K}'(t)} &= e^{-i\widehat{K}(t_2)}\widehat{S} \text{ unitary } \implies \widehat{K}'(t) \text{ is Hermitian}, && (2.48)\\
\widehat{G}' &\stackrel{\text{def}}{=} \widehat{S}^\dagger\widehat{G}\widehat{S}. && (2.49)
\end{aligned}$$

From the above equations, we see that the Floquet Hamiltonian is not uniquely defined and there is a great ambiguity in the definition. The above equations as well show that the operators $\widehat{K}(t)$ and $\widehat{G}$ are not defined independently.

[8] It is assumed that $e^{i\widehat{K}}$ (and $e^{-i\widehat{K}}$) map the domain of $\widehat{H}(t)$ into the domain of $\widehat{G}$ and vice versa. This may not be true in general and should be further mathematically analysed. This problem vanishes in finite Hilbert spaces.

[9] Let us have a general Floquet Hamiltonian $\widehat{\mathcal{G}}$ for which the equation (2.45) holds and the (stroboscopic) Floquet Hamiltonian from section 2.2.2 $\widehat{G}[0]$. Considering the equation $\widehat{U}(T,0) = e^{-i\widehat{K}(0)}e^{-i\widehat{\mathcal{G}}T}e^{+i\widehat{K}(0)} = e^{-i\widehat{G}[0]T}$, we see that we can refine the definition of $\widehat{G}[0]$ to $\widehat{G}[0] \stackrel{\text{def}}{=} e^{-i\widehat{K}(0)}\widehat{\mathcal{G}}e^{+i\widehat{K}(0)}$. According to equation (2.21) $\widehat{P}(t) \stackrel{\text{def}}{=} \widehat{U}(t,0)e^{+i\widehat{G}[0]t} = e^{-i\widehat{K}(t)}e^{+i\widehat{\mathcal{G}}t}e^{+i\widehat{K}(0)}e^{-i\widehat{K}(0)}e^{-i\widehat{\mathcal{G}}t}e^{+i\widehat{K}(0)} = e^{-i\widehat{K}(t)}e^{+i\widehat{K}(0)}$.

In the above discussion, we considered an arbitrary time-independent unitary operator $\widehat{S}$. More general transformation with $\widehat{\mathcal{S}}(t)$ dependent on time

$$\begin{aligned} \widehat{U}(t_2,t_1) &= e^{-i\widehat{K}(t_2)}\widehat{\mathcal{S}}(t_2)\widehat{\mathcal{S}}^\dagger(t_2)e^{-i(t_2-t_1)\widehat{G}}\widehat{\mathcal{S}}(t_1)\widehat{\mathcal{S}}^\dagger(t_1)e^{i\widehat{K}(t_1)}, & (2.50)\\ e^{-i\widehat{K}''(t)} &= e^{-i\widehat{K}(t_2)}\widehat{\mathcal{S}}(t) & (2.51) \end{aligned}$$

is also possible, but then the new Floquet Hamiltonian

$$\widehat{G}'' \stackrel{\text{def}}{=} \frac{i}{t_2-t_1}\ln\left[\widehat{\mathcal{S}}^\dagger(t_2)e^{-i(t_2-t_1)\widehat{G}}\widehat{\mathcal{S}}(t_1)\right] \tag{2.52}$$

must be independent on t_1 and t_2. Also, the new kick operator $\widehat{K}''(t)$ must be time-periodic with the period T. A similar transformation we will see in equation (2.104).

2.2.4 More on formalism

Here we present some theorems and some mathematical objects, which could prove useful for an analysis of time-periodic systems. In this subsection, we suppose that the appropriate Hilbert space of the system that we describe is finite. The time period of the system (and of its Hamiltonian) is denoted by T.

Time translation invariance of evolution operator

The Schrödinger equation for the evolution operator

$$i\frac{\partial}{\partial t_2}\widehat{U}(t_2,t_1) = \widehat{H}(t_2)\widehat{U}(t_2,t_1) \tag{2.53}$$

with the condition

$$\widehat{U}(t_1,t_1) = \widehat{I} \tag{2.54}$$

defines the evolution operator $\widehat{U}(t_2,t_1)$.

Defining the operator

$$\widehat{L}(t_2,t_1) \stackrel{\text{def}}{=} \widehat{U}(t_2+nT,t_1+nT), \tag{2.55}$$

we have

$$\begin{aligned} i\frac{\partial}{\partial t_2}\widehat{U}(t_2+nT,t_1+nT) &= \widehat{H}(t_2+nT)\widehat{U}(t_2+nT,t_1+nT) & (2.56)\\ &= \widehat{H}(t_2)\widehat{U}(t_2+nT,t_1+nT) & (2.57)\\ i\frac{\partial}{\partial t_2}\widehat{L}(t_2,t_1) &= \widehat{H}(t_2)\widehat{L}(t_2,t_1) & (2.58)\\ \widehat{L}(t_1,t_1) &= \widehat{I}. & (2.59) \end{aligned}$$

Since $\widehat{L}(t_2,t_1)$ and $\widehat{U}(t_2,t_1)$ are the solutions to the same differential equation with the same initial condition, we get

$$\widehat{U}(t_2+nT,t_1+nT) = \widehat{U}(t_2,t_1), \forall n \in \mathbb{Z}. \tag{2.60}$$

Evidently, the evolution operator is not an operator depending only on a difference of initial and final time, but a weaker version of this time translational symmetry (2.60) holds.

It could be easily derived that the evolution operator factorizes as follows

$$\widehat{U}(t+T,0) = \widehat{U}(t,0)\widehat{U}(T,0). \tag{2.61}$$

Thus, from the knowledge of the operator $\widehat{U}(t',0)$ for $t' \in [0,T]$, we easily construct $\widehat{U}(t,0)$ for any $t \in \mathbb{R}$ [18, 14].

Fast motion operator

We choose any operator $\widehat{M}$ such that

$$\widehat{U}(T,0) = e^{-i\widehat{M}T}, \tag{2.62}$$

where $\widehat{M}$ is Hermitian and $\widehat{M}$ is also a Floquet Hamiltonian in the sense of our definition (2.15). Then we construct a useful operator

$$\widehat{P}(t) \stackrel{\text{def}}{=} \widehat{U}(t,0)e^{+i\widehat{M}t}, \tag{2.63}$$

which is periodic in time

$$\widehat{P}(t+T) = \widehat{P}(t). \tag{2.64}$$

The operator $\widehat{P}(t)$ is called a fast motion operator.

In finite Hilbert spaces the operator $\widehat{U}(T,0)$ possesses a complete set of eigenvectors $\{|w_\alpha\rangle\}_{\alpha=d+1}^{2d}$. Then the states

$$|u_\alpha(t)\rangle = \widehat{P}(t)\,|w_\alpha\rangle \tag{2.65}$$

are Floquet modes from equation (2.7) [14].

Stroboscopic Floquet Hamiltonian

In review [16] stroboscopic and non-stroboscopic Floquet Hamiltonians are distinguished. A Floquet Hamiltonian $\widehat{G}$ (from equation (2.15)) is stroboscopic if and only if there exists a time $t_s \in [0,T)$ such that

$$\boxed{\widehat{U}(t_s+T,t_s) = e^{-i\widehat{G}[t_s]T}}. \tag{2.66}$$

This means that the operator $e^{i\widehat{K}(t_s)}$ from equation (2.45) commutes with the operator $e^{-i\widehat{G}T}$. Otherwise the Floquet Hamiltonian $\widehat{G}$ is non-stroboscopic. For stroboscopic Floquet Hamiltonians, we indicate that they are tied to the time t_s by the square brackets $[t_s]$ next to a stroboscopic Floquet Hamiltonian. It is obvious that the operator $\widehat{M} = \widehat{G}'[0]$ from equation (2.62) is a stroboscopic Floquet Hamiltonian with $t_s = 0$. Stroboscopic Floquet Hamiltonians can be transformed using [16]

$$\widehat{G}[t_s] = \widehat{P}(t_s)\widehat{G}[0]\widehat{P}^\dagger(t_s), \tag{2.67}$$

where $\widehat{G}[0]$ is a stroboscopic Floquet Hamiltonian tied to the starting time $t_s = 0$, not necessarily the same as another operator of this kind $\widehat{M} = \widehat{G}'[0]$ that is used in the definition of a fast motion operator $\widehat{P}(t)$.

2.2.5 Time independent problem for Floquet modes

This is just a small digression in order to present an interesting concept. We construct an artificial system with an artificial Hamiltonian that facilitates work with Floquet modes $|u_\alpha(t)\rangle$ and quasienergies ε_α.

Basic formalism

By substituting $|\psi_\alpha(t)\rangle = e^{-i\varepsilon_\alpha t}\,|u_\alpha(t)\rangle$ (2.7) into the Schrödinger equation (2.12) we find that the Floquet modes $|u_\alpha(t')\rangle$ are the eigenvectors of the Hermitian operator[10]

$$\widehat{\mathcal{H}} \stackrel{\text{def}}{=} -i\frac{\partial}{\partial t'} + \widehat{H}(t'). \tag{2.68}$$

This concept is touched upon in [15] and elaborated in [17]. Let us find out the more precise formulation of the aforementioned statement.

Since we just want to illustrate the formalism, we suppose the appropriate Hilbert space for the system is $\mathbb{C}^d$. For the operator $\widehat{\mathcal{H}}$ the standard Hilbert space needs to be expanded. We present the new Hilbert space $\mathbb{C}^d \otimes \mathcal{T}'$, where $\mathcal{T}'$ is the Hilbert space of periodic functions with the period $T = 2\pi/\omega$. The basis in $\mathcal{T}'$ is

$$\phi_m(t') \stackrel{\text{def}}{=} (t'|m) = e^{im\omega t'}, m \in \mathbb{Z}. \tag{2.69}$$

The scalar product in the Hilbert space $\mathcal{T}'$ reads

$$(\phi_a|\phi_b) = \frac{1}{T}\int_0^T \phi_a(t')\phi_b(t')\mathrm{d}t' \tag{2.70}$$

It is easy to find that the basis $\{|m)\}_{m=-\infty}^{+\infty}$ of the Hilbert space $\mathcal{T}'$ is orthonormal and complete.

Now, identifying the standard procedure of composing systems and consequently their Hilbert spaces, we rewrite the operator $\widehat{\mathcal{H}}$ in a verbose manner

$$\widehat{\mathcal{H}} = \widehat{I}_{\mathbb{C}^d} \otimes \left(-i\frac{\partial}{\partial t'}\right) + \widehat{H}_0 \otimes \widehat{I}_{\mathcal{T}'} + \widehat{\mathcal{V}}(t'), \tag{2.71}$$

where $\widehat{I}_{\mathbb{C}^d}$ is the identity operator in the Hilbert space $\mathbb{C}^d$ and $\widehat{I}_{\mathcal{T}'}$ is the identity operator in the Hilbert space $\mathcal{T}'$. The periodic part of the Hamiltonian $\widehat{H}(t) = \widehat{H}_0(t) + \widehat{V}(t)$

$$\widehat{\mathcal{V}}(t') \stackrel{\text{def}}{=} \widehat{V}(\widehat{t'}) \tag{2.72}$$

now couples[11] the Hilbert spaces $\mathbb{C}^d$ and $\mathcal{T}'$.

We see that in the new Hilbert space $\mathcal{T}'$ the new observables $\widehat{t'}$ and $\widehat{p}_{t'}$ can be defined the following way

$$\widehat{t'}\phi(t') = t'\phi(t'), \tag{2.73}$$

$$\widehat{p}_{t'}\phi(t') = -i\frac{\partial}{\partial t'}\phi(t'), \tag{2.74}$$

[10] the operator $\widehat{\mathcal{H}}$ is in [15] called Floquet Hamiltonian. In review [16] and in this thesis the term Floquet Hamiltonian has different meaning.

[11] Usually $\mathcal{V}(t') = g(\widehat{t'}) \otimes \widehat{W}$, where $g(t')$ is a periodic function of t' with the period T and $\widehat{W}$ is an operator in $\mathbb{C}^d$.

which implies

$$\left[\widehat{t}', \widehat{p}_{t'}\right] \;=\; i\widehat{I}_{\mathcal{T}'}. \tag{2.75}$$

The scalar product in $\mathbb{C}^d$ we denote by $\langle\psi_1|\psi_2\rangle$. The scalar product in the composite Hilbert space $\mathbb{C}^d \otimes \mathcal{T}'$ reads

$$\langle\langle\Phi_1|\Phi_2\rangle\rangle = \frac{1}{T}\int_0^T \langle\Phi_1(t')|\Phi_2(t')\rangle \,\mathrm{d}t'. \tag{2.76}$$

Let $\alpha \in \{1, ..., d\}$ numbers the Floquet modes $\{|u_\alpha(t)\rangle\}_{\alpha=1}^d$ corresponding to the quasienergies in the first Brillouin zone $\varepsilon_\alpha \in (-\omega/2, \omega/2]$. Then all the eigenvectors of $\widehat{\mathcal{H}}$ are

$$|\Phi_{\alpha,m}\rangle\rangle = e^{im\omega t'}\,|u_\alpha(t')\rangle\,, m \in \mathbb{Z}, \alpha \in \{1, ..., d\}. \tag{2.77}$$

The fact that the states (2.77) are the eigenstates of $\widehat{\mathcal{H}}$ could be easily proved using Floquet's theorem (page 13). The fact that equation (2.77) describes all the eigenstates of $\widehat{\mathcal{H}}$ is a consequence of the completeness relation

$$\begin{aligned}\sum_{\alpha=1}^{d}\sum_{m=-\infty}^{+\infty} e^{-im\omega t_1'}\,|u_\alpha(t_1')\rangle\,\langle u_\alpha(t_2')|\,e^{im\omega t_2'} &= \widehat{I}_{\mathcal{C}^n}\otimes T\cdot\delta(t_1'-t_2') \\ &= \widehat{I}_{\mathbb{C}^d}\otimes\widehat{I}_{\mathcal{T}'}.\end{aligned} \tag{2.78}$$

We used the known expression for the delta function tray

$$\sum_{m=-\infty}^{+\infty}\delta\left(x - m\cdot\frac{2\pi}{\omega}\right) = \frac{\omega}{2\pi}\sum_{m=-\infty}^{+\infty} e^{im\omega x} \tag{2.79}$$

and that

$$t_1', t_2' \in [0, T) \implies t_1' - t_2' \in \left(-\frac{2\pi}{\omega}, \frac{2\pi}{\omega}\right). \tag{2.80}$$

This approach is expedient because we are working with a time-independent problem characterized by the time-independent Schrödinger equation

$$\begin{aligned}\widehat{\mathcal{H}}\,|\Phi_{\alpha,m}\rangle\rangle &= \varepsilon_{\alpha,m}\,|\Phi_{\alpha,m}\rangle\rangle &(2.81)\\ &= (\varepsilon_\alpha + m\omega)\,|\Phi_{\alpha,m}\rangle\rangle, \\ \varepsilon_{\alpha,0} &= \varepsilon_\alpha, \alpha \in \{1, ..., d\}. &(2.82)\end{aligned}$$

Various theorems from quantum mechanics are thus available to use.

Example—use of Hellmann-Feynman theorem

We illustrate the discussed formalism on an example from [17]. Let us for a while come back to the simple Hilbert space $\mathbb{C}^d$. Here $|\psi_\alpha(t)\rangle$ is a state in $\mathbb{C}^d$ from Floquet's theorem (Floquet state) and its time evolution is prescribed by $|\psi_\alpha(t)\rangle = e^{-i\varepsilon_\alpha t}\,|u_\alpha(t)\rangle$ (2.7). Let us define a one-period averaged energy of the Floquet state $|\psi_\alpha(t)\rangle$ the following way

$$\begin{aligned}\overline{H}_\alpha \overset{\text{def}}{=} &\quad \frac{1}{T}\int_0^T \langle\psi_\alpha(t)|\widehat{H}(t)|\psi_\alpha(t)\rangle\,\mathrm{d}t &(2.83)\\ = &\quad \frac{1}{T}\int_0^T \langle u_\alpha(t)|\,e^{+i\varepsilon_\alpha t}\widehat{H}(t)e^{-i\varepsilon_\alpha t}\,|u_\alpha(t)\rangle\,\mathrm{d}t \\ = &\quad \frac{1}{T}\int_0^T \langle u_\alpha(t)|\,\widehat{H}(t)\,|u_\alpha(t)\rangle\,\mathrm{d}t. &(2.84)\end{aligned}$$

Now we can safely return to the composite Hilbert space $\mathbb{C}^d \otimes \mathcal{T}'$ and interpret the expression (2.84) as a mean value of the observable $\widehat{\mathcal{H}} + i\partial_{t'} = \widehat{H}(\hat{t'})$ in the state $|\Phi_{\alpha,0}\rangle\rangle$. Thus

$$\overline{H}_\alpha = \langle\langle\Phi_{\alpha,0}| \widehat{\mathcal{H}} + i\frac{\partial}{\partial t'} |\Phi_{\alpha,0}\rangle\rangle \tag{2.85}$$

$$= \varepsilon_\alpha + i\langle\langle\Phi_{\alpha,0}| \frac{\partial}{\partial t'} |\Phi_{\alpha,0}\rangle\rangle. \tag{2.86}$$

Now we set

$$\tau' = \omega t'. \tag{2.87}$$

Thus

$$\widehat{\mathcal{H}}(\tau') = \widehat{H}(\tau') \otimes \hat{I}_{\mathcal{T}''} - i\left(\frac{\partial \tau'}{\partial t'}\right) \hat{I}_{\mathbb{C}^d} \otimes \frac{\partial}{\partial \tau'}$$

$$= \widehat{H}(\tau') \otimes \hat{I}_{\mathcal{T}''} - i\omega \hat{I}_{\mathbb{C}^d} \otimes \frac{\partial}{\partial \tau'}. \tag{2.88}$$

And we also get the operator equation

$$\frac{\partial \widehat{\mathcal{H}}(\omega, \tau')}{\partial \omega} = -i\hat{I}_{\mathbb{C}^d} \otimes \frac{\partial}{\partial \tau'} \tag{2.89}$$

$$= -i\frac{1}{\omega}\hat{I}_{\mathbb{C}^d} \otimes \frac{\partial}{\partial t'}. \tag{2.90}$$

Thus

$$\langle\langle\Phi_{\alpha,0}| \frac{\partial}{\partial t'} |\Phi_{\alpha,0}\rangle\rangle = i\omega\langle\langle\Phi_{\alpha,0}| \frac{\partial \widehat{\mathcal{H}}(\omega, \tau')}{\partial \omega} |\Phi_{\alpha,0}\rangle\rangle. \tag{2.91}$$

Now we invoke the Hellmann-Feynman theorem [20]:

Let $\widehat{\mathcal{H}}(\lambda)$ be a Hermitian operator which depends on a real parameter λ, and $|\Phi_\lambda\rangle\rangle$ a normalized eigenvector of $\widehat{\mathcal{H}}(\lambda)$ of eigenvalue $E(\lambda)$:

$$\widehat{\mathcal{H}}(\lambda) |\Phi_\lambda\rangle\rangle = E(\lambda) |\Phi_\lambda\rangle\rangle \tag{2.92}$$

$$\langle\langle\Phi_\lambda \,|\, \Phi_\lambda\rangle\rangle = 1 \tag{2.93}$$

The Hellmann-Feynman theorem then says

$$\frac{\mathrm{d}E(\lambda)}{\mathrm{d}\lambda} = \langle\langle\Phi_\lambda| \left(\frac{\mathrm{d}}{\mathrm{d}\lambda}\widehat{\mathcal{H}}(\lambda)\right) |\Phi_\lambda\rangle\rangle. \tag{2.94}$$

From (2.94) we see that

$$\langle\langle\Phi_{\alpha,0}| \frac{\partial \widehat{\mathcal{H}}(\omega, \tau')}{\partial \omega} |\Phi_{\alpha,0}\rangle\rangle = \frac{\mathrm{d}\varepsilon_{\alpha,0}}{\mathrm{d}\omega}. \tag{2.95}$$

Thus, from (2.86, 2.91, 2.95) we get[12]

$$\overline{H}_\alpha = \varepsilon_\alpha - \omega\frac{\partial \varepsilon_\alpha}{\partial \omega} \tag{2.96}$$

[12]We signify by the partial derivation that all the other parameters on which the Hamiltonian $\widehat{H}(t)$ depends are kept constant, i.e. we cancel their possible dependence on ω. From another point of view, we demand that $\widehat{H}(\tau')$ does not depend on ω.

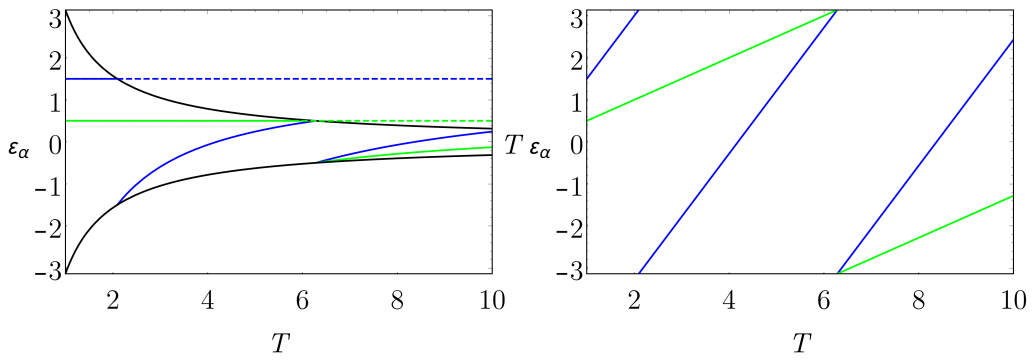

Figure 2.2: The quasienergies in the first Brillouin zone $\varepsilon_{1,2}$ (blue and green solid lines) for the system that is described by the Hamiltonian (1.1) with the parameters $\kappa = 1, p = 0.5$. The dependence on the length of the period. The dashed lines in the left plot represent the one-period averaged energies $\overline{H}_{1,2} = \kappa \pm p$ of the Floquet states. The eigenenergies of the Floquet Hamiltonian (quasienergies before mapping into the first Brillouin zone) are $\tilde{\varepsilon}_{1,2} = \kappa \pm p$ (1.14), i.e. not dependent on the time period T. The black lines in the left plot represent the boundaries of the first Brillouin zone $\pm\pi/T$.

It is easy to realise that for the eigenvalues

$$\varepsilon_{\alpha,m} \stackrel{\text{def}}{=} \varepsilon_\alpha + m\omega, \tag{2.97}$$

we get the equation similar to equation (2.96) and using $\omega = 2\pi/T$ we get

$$\overline{H}_\alpha = \varepsilon_{\alpha,m} + T\frac{\partial \varepsilon_{\alpha,m}}{\partial T}. \tag{2.98}$$

In figure 2.2 we show the dependence of the one-period average Floquet state energies $\overline{H}_\alpha$ and quasienergies in the first Brillouin zone ε_α on the length of the time period T for the simplistic example from section 1.1.

Time-dependent Schrödinger equation in composite Hilbert space

The stationary states of the time-independent Schrödinger equation $\widehat{\mathcal{H}}\,|\Phi_{\alpha,m}\rangle\rangle = \varepsilon_{\alpha,m}\,|\Psi_{\alpha,m}\rangle\rangle$ could be evolved in the standard manner

$$|\Phi_{\alpha,m}(t)\rangle\rangle = e^{-i\varepsilon_{\alpha,m}t}\,|\Phi_{\alpha,m}(0)\rangle\rangle \tag{2.99}$$

$$\langle t'\,|\,\Phi_{\alpha,m}(t)\rangle\rangle = e^{-i(\varepsilon_\alpha + m\omega)t}e^{im\omega t'}\,|u_\alpha(t')\rangle\,. \tag{2.100}$$

We see that by setting $t' = t$,

$$\langle t'\,|\,\Phi_{\alpha,m}(t)\rangle\rangle|_{t'=t} = e^{-i\varepsilon_\alpha t}\,|u_\alpha(t)\rangle\,, \tag{2.101}$$

$$= |\psi_\alpha(t)\rangle\,, \tag{2.102}$$

we get the Floquet states (2.7). From (2.100) we see again that the restriction to the quasienergies in the first Brillouin zone is justified.

2.2.6 Single-spin harmonically-driven system revisited

Now, having the knowledge of the Floquet theory, we are ready to return to the single-spin-$\frac{1}{2}$ harmonically-driven example (section 1.2) and to identify the elements of the theory in this example. This subsection is inspired by [16].

We already found out the form of the evolution operator (1.31). Although equation (1.31) resembles the second form of the Floquet theorem (2.45), the Hamiltonian $\widehat{H}_r$ (1.29) is *not* a Floquet Hamiltonian of the system with the period T since the unitary operator, providing the similarity transformation to the rotating basis,

$$e^{-i\omega t\widehat{S}_z} = \widehat{I}\cos\frac{\omega t}{2} - i\widehat{\sigma}_z\sin\frac{\omega t}{2} \tag{2.103}$$

is not T-periodic (but $2T$-periodic).

First Floquet Hamiltonian

We get an appropriate Floquet Hamiltonian, kick operator pair $(\widehat{G}^{\mathrm{I}}[0], \widehat{K}^{\mathrm{I}}(t))$ by simple mathematical trick—we transcribe equation (1.31) the following way

$$\begin{aligned}\widehat{U}(t_2,t_1) &= e^{-i\omega t_2\widehat{S}_z}e^{-i\frac{\omega t_2}{2}}e^{+i\frac{\omega t_2}{2}}e^{-i\widehat{H}_r(t_2-t_1)}e^{-i\frac{\omega t_1}{2}}e^{+i\frac{\omega t_1}{2}}e^{i\omega t_1\widehat{S}_z}\\ &= e^{-i\omega t_2\left(\widehat{S}_z+\frac{1}{2}\right)}e^{-i\left(\widehat{H}_r-\frac{\omega}{2}\right)(t_2-t_1)}e^{i\omega t_1\left(\widehat{S}_z+\frac{1}{2}\right)}.\end{aligned} \tag{2.104}$$

From equation (2.104), we easily identify the Floquet Hamiltonian, kick operator pair

$$\widehat{G}^{\mathrm{I}}[0] = \widehat{H}_r - \frac{\omega}{2}\widehat{I}, \tag{2.105}$$

$$\widehat{K}^{\mathrm{I}}(t) = \omega t\left(\widehat{S}_z + \frac{1}{2}\widehat{I}\right), t\in[0,T). \tag{2.106}$$

From the equation

$$e^{-i\omega t\left(\widehat{S}_z+\frac{1}{2}\right)} = \frac{1}{2}\left(e^{-i\omega t}-1\right)\widehat{\sigma}_z + \frac{1}{2}\left(e^{-i\omega t}+1\right)\widehat{I}, t\in\mathbb{R}, \tag{2.107}$$

we easily see that we could define the kick operator $\widehat{K}^{\mathrm{I}}(t)$, which is time-periodic with the time period T, by periodically extending its functional dependence on t in the interval $[0,T)$ (equation (2.106)). The Floquet Hamiltonian, kick operator pair $(\widehat{G}^{\mathrm{I}}[0], \widehat{K}^{\mathrm{I}}(t))$ constructed above has all the necessary properties that a pair of (stroboscopic) Floquet Hamiltonian and kick operator should have. Since for the starting time $t_s = 0$ the kick operator is equal to zero, the Floquet Hamiltonian is stroboscopic.

The eigenvalues of the rotational Hamiltonian $\widehat{H}_r$ are $\pm\epsilon_r$, where we defined

$$\epsilon_r \overset{\mathrm{def}}{=} \frac{1}{2}\sqrt{(\omega_0+\omega)^2+\omega_r^2}. \tag{2.108}$$

Consequently, the eigenvalues of the Floquet Hamiltonian $\widehat{G}^{\mathrm{I}}[0]$, i.e. the quasienergies, are

$$\varepsilon^{\mathrm{I}}_{\pm} = -\frac{\omega}{2}\pm\epsilon_r, \tag{2.109}$$

which follows from equation (2.105).

The choice of a Floquet Hamiltonian, kick operator pair is not unique and it could be expedient to choose the pair differently in order to yield some more convenient form of the operators constituting the pair. For the sake of education, we present two other such pairs. Before we do that, we note that the high-frequency limit of the eigenvalue $\varepsilon^{\mathrm{I}}_{-}$ diverges

$$\lim_{\omega\to+\infty}\varepsilon^{\mathrm{I}}_{-}=-\infty,\ \lim_{\omega\to+\infty}\varepsilon^{\mathrm{I}}_{+}=\frac{\omega_0}{2}. \tag{2.110}$$

We get rid of the divergence we mentioned by another choice of a Floquet Hamiltonian, kick operator pair.

Second Floquet Hamiltonian

The following two Floquet Hamiltonians were discussed in [16] and we introduce them without proof. Nevertheless, using equation (2.40), we could prove the validity of the Hamiltonians (we provide the appropriate exponentials of the kick operators). The proof is mechanical and could be facilitated by a computer, e.g. using the programming language Mathematica.

The single-spin harmonically-driven system (section 1.2) could be equivalently described by Floquet Hamiltonian

$$\widehat{G}^{\mathrm{II}}[0] \;=\; \left(1-\frac{\omega}{\sqrt{(\omega_0+\omega)^2+\omega_r^2}}\right)\widehat{H}_r. \tag{2.111}$$

We do not provide the exact form of the kick operator $\widehat{K}^{\mathrm{II}}(t)$ paired to the Floquet Hamiltonian $\widehat{G}^{\mathrm{II}}[0]$ but we provide its exponential that is used for the similarity transformation in (2.45)

$$\begin{aligned} e^{-i\widehat{K}^{\mathrm{II}}(t)} \;=\;& \widehat{I}-2\left(\cos^2\frac{\alpha}{2}\right)\left(\sin^2\frac{\omega t}{2}\right)\widehat{I}-i\frac{1}{2}\left(\sin\alpha\right)\left(\sin\omega t\right)\widehat{\sigma}_x \\ & -i\left(\sin\alpha\right)\left(\sin^2\frac{\omega t}{2}\right)\widehat{\sigma}_y-i\left(\cos^2\frac{\alpha}{2}\right)\left(\sin\omega t\right)\widehat{\sigma}_z, \end{aligned} \tag{2.112}$$

where we define the new parameter α the following way

$$\sin\alpha=-\frac{\omega_r}{\sqrt{(\omega_0+\omega)^2+\omega_r^2}},\ \ \cos\alpha=-\frac{\omega_0+\omega}{\sqrt{(\omega_0+\omega)^2+\omega_r^2}}. \tag{2.113}$$

Note that expressions (2.113) define the parameter α unambiguously.

Also note that since $\sin^2 x=(1-\cos 2x)/2$ and $\cos^2 x=(1+\cos 2x)/2$, the operator $\widehat{K}^{\mathrm{II}}(t)$ is T-periodic. For $t=0$ the similarity transformation (2.112) reduces to an identity matrix, thus the Floquet Hamiltonian $\widehat{G}^{\mathrm{II}}[0]$ is stroboscopic. The form of the exponential $e^{-i\widehat{K}^{\mathrm{II}}(t)}$ in equation (2.112) suggests the computation of the kick operator using the series

$$\ln(\widehat{I}-\widehat{X})=-\sum_{n=1}^{+\infty}\frac{1}{n}\widehat{X}^n. \tag{2.114}$$

Rather complicated expressions could be computed, e.g. using the programming language Mathematica.

The eigenvalues of the Floquet Hamiltonian $\widehat{G}^{\mathrm{II}}[0]$ are

$$\varepsilon^{\mathrm{II}}_{\pm} = \pm\left(\epsilon_r - \frac{\omega}{2}\right) = \pm\varepsilon^{\mathrm{I}}_{+} \tag{2.115}$$

and it is trivial to show that both eigenvalues (quasienergies) do not diverge since

$$\lim_{\omega\to+\infty}\varepsilon^{\mathrm{II}}_{\pm} = \pm\frac{\omega_0}{2}. \tag{2.116}$$

Third Floquet Hamiltonian

The third Floquet Hamiltonian we present is characterized by

$$\varepsilon^{\mathrm{III}}_{\uparrow} = \frac{\omega}{2} - \epsilon_r = \varepsilon^{\mathrm{II}}_{-} \tag{2.117}$$

$$\varepsilon^{\mathrm{III}}_{\downarrow} = -\varepsilon^{\mathrm{III}}_{\uparrow} = -\frac{\omega}{2} + \epsilon_r = \varepsilon^{\mathrm{II}}_{+} \tag{2.118}$$

$$\widehat{G}^{\mathrm{III}} = \left(\frac{\omega}{2} - \epsilon_r\right)\widehat{\sigma}_z = \varepsilon^{\mathrm{III}}_{\uparrow}\widehat{\sigma}_z \tag{2.119}$$

$$\widehat{K}^{\mathrm{III}}(t) = \frac{\alpha-\pi}{2}\left(-\widehat{\sigma}_x\sin\omega t + \widehat{\sigma}_y\cos\omega t\right) \tag{2.120}$$

$$e^{-i\widehat{K}^{\mathrm{III}}(t)} = \widehat{I}\sin\frac{\alpha}{2} - i\left(-\widehat{\sigma}_x\sin\omega t + \widehat{\sigma}_y\cos\omega t\right)\cos\frac{\alpha}{2}, \tag{2.121}$$

where the parameter α is defined by equation (2.113).

The third Floquet Hamiltonian has the same eigenvalues as the second one, but we conventionally present them in reversed order since it is more natural to present the 11 matrix element of the third Floquet Hamiltonian (2.119) first and the $\pm$ signs refer to the signs before ϵ_r. We also note that the form of the third Floquet Hamiltonian is exceptionally simple (2.119) and the eigenvectors are the well known z-direction spin-$\frac{1}{2}$ up and down states. Note also that the third Floquet Hamiltonian is non-stroboscopic since there is no t such that $e^{-i\widehat{K}^{\mathrm{III}}(t)}$ commutes with $e^{\widehat{G}^{\mathrm{III}}T}$.

Average energy in Floquet state

The one-period average energy in a Floquet state is defined by (2.83). We derived expression (2.98) that connects the quasienergies with the values of the one-period average energy in the respective Floquet state. From (2.98) (and $\omega = 2\pi/T$) we get

$$\overline{H}^{\mathrm{I}}_{\pm} = \varepsilon^{\mathrm{I}}_{\pm} - \omega\frac{\partial\varepsilon^{\mathrm{I}}_{\pm}}{\partial\omega} \tag{2.122}$$

$$= \pm\frac{1}{2}\frac{\omega\omega_0 + \omega_0^2 + \omega_r^2}{\sqrt{(\omega_0+\omega)^2 + \omega_r^2}}. \tag{2.123}$$

Clearly, the one-period average energy in the Floquet state could be computed using the pair of quasienergies $(\varepsilon^{\mathrm{I}}_{+}, \varepsilon^{\mathrm{I}}_{-})$ or the pair of quasienergies $(\varepsilon^{\mathrm{II}}_{+} = \varepsilon^{\mathrm{III}}_{\downarrow}, \varepsilon^{\mathrm{II}}_{-} = \varepsilon^{\mathrm{III}}_{\uparrow})$, i.e. we get

$$\overline{H}^{\mathrm{I}}_{+} = \overline{H}^{\mathrm{II}}_{+} = \overline{H}^{\mathrm{III}}_{\downarrow},\ \overline{H}^{\mathrm{I}}_{-} = \overline{H}^{\mathrm{II}}_{-} = \overline{H}^{\mathrm{III}}_{\uparrow}. \tag{2.124}$$

For the high-frequency limit we get the following values of the one-period average energies in the Floquet states

$$\lim_{\omega\to+\infty}\overline{H}^{\mathrm{I}}_{\pm} = \lim_{\omega\to+\infty}\overline{H}^{\mathrm{II}}_{\pm} = \lim_{\omega\to+\infty}\overline{H}^{\mathrm{III}}_{\downarrow\uparrow} = \pm\frac{\omega_0}{2}. \tag{2.125}$$

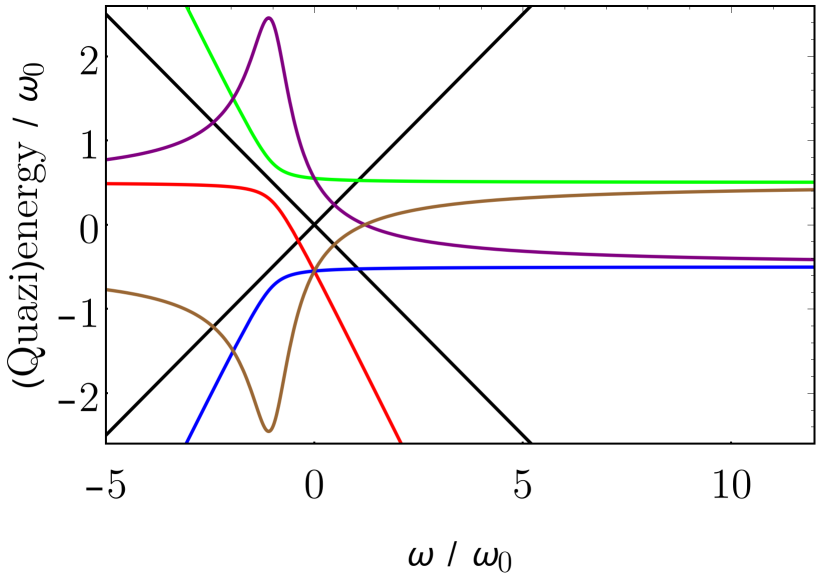

Figure 2.3: The dependencies of values $\varepsilon^{\mathrm{I}}_{-}$ (red), $\varepsilon^{\mathrm{II}}_{+}$ (green), $\varepsilon^{\mathrm{II}}_{-}$ (blue), $\overline{H}^{\mathrm{I}}_{\pm}$ (purple and brown) on ω for the parameters ω_r, ω_0 satisfying $\omega_r/\omega_0 = 0.46$. The black solid lines represent the boundaries of the first Brillouin zone.

Summary

We have seen that various Floquet Hamiltonians could be constructed. The first Hamiltonian was easily constructed, but its high-frequency limit is divergent. The second Floquet Hamiltonian has a good high-frequency limit and is stroboscopic. The third Floquet Hamiltonian has a good high-frequency limit and simple form but is non-stroboscopic. Although each Floquet Hamiltonian constructed here differs from the other ones, the one-period average energy in the Floquet state is not affected by the ambiguity in the definition of the Floquet Hamiltonian.

The topology of the problem—see figure 1.2—does not change if we change simultaneously the sign of ω and ω_0

$$\left.\begin{matrix}\omega\\ \omega_0\end{matrix}\right\} \to \begin{cases}-\omega\\ -\omega_0\end{cases}. \tag{2.126}$$

Note that the one-period average energy in a Floquet state (2.123) respects the symmetry (2.126) whereas the quasienergies $\varepsilon^{\mathrm{I}}_{\pm}, \varepsilon^{\mathrm{II}}_{\pm}, \varepsilon^{\mathrm{III}}_{\uparrow\downarrow}$ do not respect that symmetry. The first pair of quasienergies transforms the following way $\varepsilon^{\mathrm{I}}_{\pm} \to -\varepsilon^{\mathrm{I}}_{\mp}$. From the form of the quasienergies or from the equivalence of the problems when doing the symmetry transform (2.126) and the uniqueness of the quasienergies mapped to the first Brillouin zone (here we consider them as a set of real numbers with *no* order) we see that the quasienergies mapped to the first Brillouin zone respect the symmetry transform (2.126). The dependencies of values $\varepsilon^{\mathrm{I}}_{-}, \varepsilon^{\mathrm{II}}_{+}, \varepsilon^{\mathrm{II}}_{-}$ and $\overline{H}^{\mathrm{I}}_{\pm}$ on ω are plotted in figure 2.3.

2.3 Floquet Hamiltonian and kick operator expansion

Here we present the method for finding series for a Floquet Hamiltonian $\widehat{G}$ and a kick operator $\widehat{K}(t)$ described in [15]. This section is a continuation of the discussion in subsection 2.2.3. We divided the discussion into two parts since subsection 2.2.3 is much more general than the discussion in this section.

We will outline a procedure for finding the operators $\widehat{G}$ and $\widehat{K}(t)$ from equation (2.45) in the form of an expansion in powers of $1/\omega$. The pair $(\widehat{G}, \widehat{K}(t))$ we will construct here is one of the infinitely many different pairs $(\widehat{G}, \widehat{K}(t))$ satisfying equation (2.45).

We consider a Hamiltonian of a system which we describe in the form (2.2)

$$\widehat{H}(t) = \widehat{H}_0 + \widehat{V}_0 + \sum_{n=1}^{+\infty} \left(\widehat{V}_n e^{+in\omega t} + \widehat{V}_{-n} e^{-in\omega t} \right),$$

where $\widehat{V}_n^\dagger = \widehat{V}_{-n}$ because of Hermicity of $\widehat{H}(t)$.

It is convenient to transcribe equation (2.40),

$$\widehat{G} \stackrel{\text{def}}{=} e^{i\widehat{K}(t)} \widehat{H}(t) e^{-i\widehat{K}(t)} + i \left(\frac{\partial e^{i\widehat{K}(t)}}{\partial t} \right) e^{-i\widehat{K}(t)},$$

with $\tau \stackrel{\text{def}}{=} \omega t$. Then we have

$$\widehat{G} = e^{i\widehat{K}(\tau)} \widehat{H}(\tau) e^{-i\widehat{K}(\tau)} + i\omega \left(\frac{\partial e^{i\widehat{K}(\tau)}}{\partial \tau} \right) e^{-i\widehat{K}(\tau)}. \tag{2.127}$$

We consider the following expansions for $\widehat{G}$ and $\widehat{K}$

$$\widehat{G} = \sum_{n=0}^{\infty} \frac{1}{\omega^n} \widehat{G}_n, \tag{2.128}$$

$$\widehat{K}(\tau) = \sum_{n=1}^{\infty} \frac{1}{\omega^n} \widehat{K}_n(\tau). \tag{2.129}$$

Note that the sum for $\widehat{K}(\tau)$ begins with $n = 1$. If we do not denote the dependence of $\widehat{K}(\tau)$ on τ, we mean that $\widehat{K}$ or $\widehat{K}_n$ is evaluated at the rescaled time τ.

We will expand the first term on the right hand side of equation (2.127) using the expansion (1.19)

$$e^{i\widehat{K}} \widehat{H} e^{-i\widehat{K}} = \widehat{H} + i\left[\widehat{K}, \widehat{H}\right] - \frac{1}{2!}\left[\widehat{K}, \left[\widehat{K}, \widehat{H}\right]\right] - \frac{i}{3!}\left[\widehat{K}, \left[\widehat{K}, \left[\widehat{K}, \widehat{H}\right]\right]\right] + \ldots, \tag{2.130}$$

and the second term using the expansion

$$\left(\frac{\partial e^{i\widehat{K}}}{\partial \tau} \right) e^{-i\widehat{K}} = i\frac{\partial \widehat{K}}{\partial \tau} - \frac{1}{2!}\left[\widehat{K}, \frac{\partial \widehat{K}}{\partial \tau}\right] - \frac{i}{3!}\left[\widehat{K}, \left[\widehat{K}, \frac{\partial \widehat{K}}{\partial \tau}\right]\right] + \ldots, \tag{2.131}$$

which follows from (A.17) in appendix A.

The method consists of computing $\widehat{G}_n$ in terms of $\widehat{K}_1, \ldots, \widehat{K}_{n+1}$ and then setting $\widehat{K}_{n+1}$ so that $\widehat{G}_n$ is time independent.

Equating the terms directly proportional to ω^0, we get

$$\widehat{G}_0 = \widehat{H}_0 + \widehat{V}_0 + \sum_{n=1}^{\infty} \left(\widehat{V}_n e^{in\tau} + \widehat{V}_{-n} e^{-in\tau} \right) - \frac{\partial \widehat{K}_1}{\partial \tau}. \tag{2.132}$$

In order to cancel a time dependence of $\widehat{G}_0$, we set

$$\boxed{\widehat{K}_1 = \sum_{n=1}^{\infty} \frac{1}{in} \left(\widehat{V}_n e^{in\tau} - \widehat{V}_{-n} e^{-in\tau} \right)} \tag{2.133}$$

and thus

$$\boxed{\widehat{G}_0 = \widehat{H}_0 + \widehat{V}_0}. \tag{2.134}$$

Equating the terms directly proportional to ω^1, we get

$$\widehat{G}_1 = i \left[\widehat{K}_1, \widehat{H} \right] - \frac{\partial \widehat{K}_2}{\partial \tau} - \frac{i}{2} \left[\widehat{K}_1, \frac{\partial \widehat{K}_1}{\partial \tau} \right]. \tag{2.135}$$

Substituting (2.133) into (2.135), we get the time independent part of (2.135) $\widehat{G}_1 \equiv \overline{\widehat{G}}_1$

$$\boxed{\widehat{G}_1 = \sum_{n=1}^{\infty} \frac{1}{n} \left[\widehat{V}_n, \widehat{V}_{-n} \right]} \tag{2.136}$$

and the time dependent part of (2.135)

$$\begin{aligned} 0 = & \sum_{n=1}^{\infty} \frac{1}{n} \left(\left[\widehat{V}_n, \widehat{H}_0 + \widehat{V}_0 \right] e^{in\tau} + \text{H.c.} \right) \\ & + \frac{1}{2} \sum_{\substack{m,n=1 \\ m \neq n}}^{\infty} \frac{1}{n} \left(\left[\widehat{V}_n, \widehat{V}_m \right] e^{i(n+m)\tau} + \left[\widehat{V}_n, \widehat{V}_{-m} \right] e^{i(n-m)\tau} + \text{H.c.} \right) - \frac{\partial \widehat{K}_2}{\partial \tau}. \end{aligned} \tag{2.137}$$

We choose $\widehat{K}_2$ the following way

$$\boxed{\begin{aligned} \widehat{K}_2 = & \sum_{n=1}^{\infty} \frac{1}{in^2} \left[\widehat{V}_n, \widehat{H}_0 + \widehat{V}_0 \right] e^{in\tau} + \frac{1}{2} \sum_{\substack{m,n=1 \\ m \neq n}}^{\infty} \frac{1}{in(n+m)} \left[\widehat{V}_n, \widehat{V}_m \right] e^{i(n+m)\tau} \\ & + \frac{1}{2} \sum_{\substack{m,n=1 \\ m \neq n}}^{\infty} \frac{1}{in(n-m)} \left[\widehat{V}_n, \widehat{V}_{-m} \right] e^{i(n-m)\tau} + \text{H.c.} \end{aligned}} \tag{2.138}$$

Equating the terms directly proportional to ω^2, we get

$$\begin{aligned} \widehat{G}_2 = & i \left[\widehat{K}_2, \widehat{H} \right] - \frac{1}{2} \left[\widehat{K}_1, \left[\widehat{K}_1, \widehat{H} \right] \right] \\ & - \frac{\partial \widehat{K}_3}{\partial \tau} - \frac{i}{2} \left[\widehat{K}_1, \frac{\partial \widehat{K}_2}{\partial \tau} \right] - \frac{i}{2} \left[\widehat{K}_2, \frac{\partial \widehat{K}_1}{\partial \tau} \right] + \frac{1}{6} \left[\widehat{K}_1, \left[\widehat{K}_1, \frac{\partial \widehat{K}_1}{\partial \tau} \right] \right]. \end{aligned} \tag{2.139}$$

By similar arguments as above, we get

$$\boxed{\begin{aligned}\widehat{G}_2 =& \frac{1}{2}\sum_{n=1}^{\infty}\frac{1}{n^2}\left[\left[\widehat{V}_n, \widehat{H}_0+\widehat{V}_0\right], \widehat{V}_{-n}\right] - \frac{1}{3}\sum_{\substack{m,n=1\\ m\neq n}}^{\infty}\frac{1}{mn}\left[\widehat{V}_m, \left[\widehat{V}_{-n}, \widehat{V}_{n-m}\right]\right] \\ &+ \frac{1}{3}\sum_{m,n=1}^{\infty}\frac{1}{mn}\left[\widehat{V}_m, \left[\widehat{V}_n, \widehat{V}_{-m-n}\right]\right] + \text{H.c.}\end{aligned}} \tag{2.140}$$

In the aforementioned, it is shown that for high frequencies $\widehat{K}(t)$ could be chosen small, of the order of $1/\omega$. Then matrix elements of an observable $\widehat{O}$ could be calculated using the eigenvalues and eigenvectors of the Floquet Hamiltonian $\widehat{G}$

$$\begin{aligned}\langle\psi_\alpha(t)|\,\widehat{O}\,|\psi_\beta(t)\rangle &= \langle\phi_\alpha(t)|\,e^{i\widehat{K}(t)}\widehat{O}e^{-i\widehat{K}(t)}\,|\phi_\beta(t)\rangle &(2.141)\\ &= \langle\phi_\alpha(t)|\,\widehat{O}\,|\phi_\beta(t)\rangle + i\,\langle\phi_\alpha(t)|\left[\widehat{K}(t),\widehat{O}\right]|\phi_\beta(t)\rangle \\ &- \frac{1}{2}\,\langle\phi_\alpha(t)|\left[\widehat{K}(t),\left[\widehat{K}(t),\widehat{O}\right]\right]|\phi_\beta(t)\rangle + \ldots, &(2.142)\end{aligned}$$

where the states

$$|\phi_\alpha(t)\rangle = e^{+i\widehat{K}(t)}\,|\psi_\alpha(t)\rangle \tag{2.143}$$

are the eigenstates of the Floquet Hamiltonian $\widehat{G}$. The above equalities follow from (2.130) and (2.36).

2.4 Systems factorizing Floquet operator

Here we describe the method which derives an approximate form of a Floquet Hamiltonian using the Baker–Campbell–Hausdorff (BCH) formula. Generally speaking, when the Floquet operator, i.e. an evolution operator evolving a system for the duration of one period, could be expressed in the form of a product of exponentials, with known exponents, the BCH formula is expedient.

In this section we investigate the properties of stroboscopic Floquet Hamiltonians $\widehat{G}[t_s]$, their definition (2.66) is

$$\widehat{U}(t_s+T,t_s) = e^{-i\widehat{G}[t_s]T}.$$

2.4.1 General example of delta-driven system

For simplicity, we consider the delta-driven Hamiltonian

$$\widehat{H}(t) = \widehat{V}_P T\sum_{n=-\infty}^{\infty}\delta(t-nT) + \widehat{H}_0, \tag{2.144}$$

which describes a system driven by delta pulses. The Floquet operator for the Hamiltonian (2.144) could be written as

$$\boxed{\widehat{\mathcal{F}}[0] = e^{-i\widehat{V}_P T}e^{-i\widehat{H}_0 T}}. \tag{2.145}$$

From equation (2.145), we see that we describe the one-period evolution which begins just *after* the realisation of the delta function. At first, we evolve the system by the operator

$$e^{-i\widehat{H}_0 T}. \tag{2.146}$$

And then we evolve the system by the operator

$$e^{-i\widehat{V}_P T}, \tag{2.147}$$

which demonstrates the fact that the part of the Hamiltonian represented by the operator $\widehat{H}_0$ is negligible during an infinitesimal time interval which includes the realisation of a delta function.

The desired Floquet Hamiltonian $\widehat{G}$ can be constructed by satisfying the condition

$$\widehat{\mathcal{F}}[0] = e^{-i\widehat{G}T}. \tag{2.148}$$

In order to yield the Floquet Hamiltonian $\widehat{G}$, the standard BCH formula

$$\boxed{\ln(e^{\widehat{X}}e^{\widehat{Y}}) = \widehat{X} + \widehat{Y} + \frac{1}{2}\left[\widehat{X},\widehat{Y}\right] + \frac{1}{12}\left[\widehat{X}-\widehat{Y},\left[\widehat{X},\widehat{Y}\right]\right] + \dots} \tag{2.149}$$

could be used.

2.4.2 Special form of Baker–Campbell–Hausdorff formula

In a special case when $\widehat{V}_P$ depends linearly on the parameter p, i.e. the operator $\widehat{V}_P$ could be made small by lowering the parameter p, we apply the special form of the BCH formula (A.39) devised in appendix A

$$\boxed{-\ln\left(e^{-p\widehat{B}}e^{-\widehat{A}}\right) = \widehat{A} - p\frac{\mathrm{ad}_{\widehat{\mathrm{A}}}}{e^{\left(-\mathrm{ad}_{\widehat{\mathrm{A}}}\right)}-1}\widehat{B} + O(p^2)}, \tag{2.150}$$

where $\mathrm{ad}_{\widehat{\mathrm{X}}}\widehat{\mathrm{Y}} \stackrel{\mathrm{def}}{=} \left[\widehat{\mathrm{X}},\widehat{\mathrm{Y}}\right]$. The operator $\widehat{A}$ has to be small as well (which is a part of the requirements for the formula (A.39) to work).

We define the function of $\mathrm{ad}_{\widehat{\mathrm{A}}}$ by the Taylor series for the function $f(x)$

$$f(x) = \sum_{n=0}^{\infty} f_n \frac{x^n}{n!}. \tag{2.151}$$

The function f of the argument $\mathrm{ad}_{\widehat{\mathrm{A}}}$ is defined by

$$f\left(\mathrm{ad}_{\widehat{\mathrm{A}}}\right) \stackrel{\mathrm{def}}{=} \sum_{n=0}^{\infty} f_n \frac{1}{n!}\left(\mathrm{ad}_{\widehat{\mathrm{A}}}\right)^n. \tag{2.152}$$

The effect of the action of the nth power of $\mathrm{ad}_{\widehat{\mathrm{A}}}$ on an operator $\widehat{B}$ is straightforward, i.e.

$$\left(\mathrm{ad}_{\widehat{\mathrm{A}}}\right)^n \widehat{B} = \underbrace{\left[\widehat{A},\left[\widehat{A},\dots\left[\widehat{A},\widehat{B}\right]\right]\dots\right]_n}_{\text{n commutators}} \tag{2.153}$$

and $\left(\mathrm{ad}_{\widehat{\mathrm{A}}}\right)^0$ is defined to be an identity operator $\widehat{I}$.

2.4.3 Discussion about initial time choice

There is an ambiguity in the form of a Floquet Hamiltonian. We describe the ambiguity connected with the choice of a starting time regarding stroboscopic Floquet Hamiltonians. Stroboscopic Floquet Hamiltonians, for various initial times t_s, could be constructed using equations (2.67, 2.63)

$$\begin{aligned} \widehat{G}[t_s] &= \widehat{P}(t_s)\widehat{G}[0]\widehat{P}^{\dagger}(t_s), \\ \widehat{P}(t) &\stackrel{\text{def}}{=} \widehat{U}(t,0)e^{+i\widehat{G}'[0]t}, \end{aligned} \tag{2.154}$$

where $\widehat{G}[0]$ and $\widehat{G}'[0]$ are two, not necessarily the same, stroboscopic Floquet Hamiltonians tied to the starting time $t_s = 0$.

We stress that the ambiguity connected with the initial time choice is not the only ambiguity regarding stroboscopic Floquet Hamiltonians. Even a stroboscopic Floquet Hamiltonian tied to a starting time t_s is not uniquely defined. For example in our simplistic example from section 1.1 all the stroboscopic Floquet Hamiltonians in the matrix form

$$\left(\widehat{G}_s^{(m,n)}[0]\right) = \begin{pmatrix} \kappa + \frac{m+n}{T}\pi & p + \frac{m-n}{T}\pi \\ p + \frac{m-n}{T}\pi & \kappa + \frac{m+n}{T}\pi \end{pmatrix}, \forall m,n \in \mathbb{Z} \tag{2.155}$$

are possible stroboscopic Floquet Hamiltonians tied to the starting time $t_s = 0$.

Here we demonstrate the ambiguity connected with an initial time choice on a simple example from [4]. Consider the following Hamiltonian

$$\widehat{H}(t) = \begin{cases} \widehat{H}_0 + \widehat{V} & \text{if} \quad t \in [n \cdot T, T/2 + n \cdot T), n \in \mathbb{Z} \\ \widehat{H}_0 - \widehat{V} & \text{if} \quad t \in [T/2 + n \cdot T, T + n \cdot T), n \in \mathbb{Z}. \end{cases} \tag{2.156}$$

The Floquet operator tied to the starting time $t_s = 0$ factorizes the following way

$$\mathcal{F}[0] \stackrel{\text{def}}{=} \widehat{U}(T,0) = e^{-i\left(\widehat{H}_0 - \widehat{V}\right)\frac{T}{2}} e^{-i\left(\widehat{H}_0 + \widehat{V}\right)\frac{T}{2}}. \tag{2.157}$$

Using the definition of a stroboscopic Floquet Hamiltonian (2.66) and the standard BCH formula (2.149), we get the stroboscopic Floquet Hamiltonian

$$\begin{aligned} \widehat{G}[0]T &= \left(\widehat{H}_0 + \widehat{V}\right)\frac{T}{2} + \left(\widehat{H}_0 - \widehat{V}\right)\frac{T}{2} - i\frac{T^2}{8}\left[\widehat{H}_0 - \widehat{V}, \widehat{H}_0 + \widehat{V}\right] + O(T^3), \\ \widehat{G}[0] &= \widehat{H}_0 - i\frac{T}{4}\left[\widehat{H}_0, \widehat{V}\right] + O(T^2). \end{aligned} \tag{2.158}$$

Another stroboscopic Floquet Hamiltonian can be easily constructed by starting at the initial time $t_s = T/2$

$$\widehat{U}(t_s + T, t_s) = e^{-i\widehat{G}[T/2]T}, \tag{2.159}$$

$$\widehat{G}[T/2] = \widehat{H}_0 + i\frac{T}{4}\left[\widehat{H}_0, \widehat{V}\right] + O(T^2). \tag{2.160}$$

The whole term linear in T in equations (2.158, 2.160) could be eliminated by similarity transformation using equation (1.19)

$$\widehat{G}[0] = \widehat{S}^{\dagger}\widehat{H}_0\widehat{S} + O(T^2), \widehat{S} = e^{-i\frac{T}{4}\widehat{V}}. \tag{2.161}$$

Using the definition of a fast motion operator $\widehat{P}(t)$ (2.154) and the standard BCH formula (2.149), we calculate

$$\widehat{P}\left(\frac{T}{4}\right) \stackrel{\text{def}}{=} \widehat{U}\left(\frac{T}{4},0\right)e^{+i\widehat{G}[0]\frac{T}{4}} \tag{2.162}$$

$$= e^{-i\left(\widehat{H}_0+\widehat{V}\right)\frac{T}{4}}e^{+i\widehat{G}[0]\frac{T}{4}} \tag{2.163}$$

$$= e^{-i\frac{T}{4}\widehat{V}+\frac{T^2}{32}[H_0,V]+O(T^3)}. \tag{2.164}$$

From equations (2.161, 2.164) and equation (2.67) it is clear that

$$\widehat{G}\left[\frac{T}{4}\right] = \widehat{H}_0 + O\left(T^2\right). \tag{2.165}$$

Thus, we demonstrated that by choosing a particularly suitable starting time t_s, we could make the form of a stroboscopic Floquet Hamiltonian simpler.

2.5 Discussion about limit of small time period

In the previous parts of the thesis, we presented some methods for constructing an effective Hamiltonian—a series for a Floquet Hamiltonian. In most cases the series consist of the powers of the time period T. In subsection 2.4.1 we presented a Floquet operator (2.145)

$$\widehat{\mathcal{F}}[0] = e^{-i\widehat{V}_P T}e^{-i\widehat{H}_0 T}.$$

for systems described by the particular type of Hamiltonian (2.144). From the above form of the factorization of the Floquet operator, we see that if $||\widehat{V}_P T|| \ll 1$ and $||\widehat{H}_0 T|| \ll 1$, then the expansion using the standard BCH formula (2.149) converges. The discussion regarding the series for the kick operator $\widehat{K}(t)$ and the Floquet Hamiltonian $\widehat{G}$ constructed in section 2.3 is similar.

From the expansions (2.128, 2.129) and the forms of the terms $\widehat{G}_n$ and $\widehat{K}_n$ we see that it is natural to require the frequency to be high in comparison to all $\widehat{V}_n, n \in \mathbb{Z}$ and $\widehat{H}_0$, i.e.

$$T \ll \frac{1}{||\widehat{V}_n||}, n \in \mathbb{Z} \tag{2.166}$$

$$T \ll \frac{1}{||\widehat{H}_0||}. \tag{2.167}$$

Let us define

$$\delta \stackrel{\text{def}}{=} \max\left(\left\{||\widehat{V}_n||T, n \in \mathbb{Z}\right\} \cup \left\{||\widehat{H}_0||T\right\}\right). \tag{2.168}$$

The new parameter δ is a dimensionless quantity. The requirements (2.166, 2.167) tell us that $\delta \ll 1$. From the forms of the terms $\widehat{G}_n$ and $\widehat{K}_n(t)$ and their construction, we suppose that $\widehat{G}_n T^n = O(\delta^n)$ and $\widehat{K}_n(t)T^n = O(\delta^n)$ and we get the converging series (2.128, 2.129).

It is now interesting to look at how the fast motion operator—exhibiting fast changes of the wave function—behaves. The fast motion operator (2.21) scales the following way[13]

$$\begin{aligned}\widehat{P}(t) &\stackrel{\text{def}}{=} \widehat{U}(t,0)e^{+i\widehat{G}[0]t} \stackrel{(2.23)}{=} \widehat{P}(t+T) \\ &= \widehat{I}+O(\delta). \end{aligned} \tag{2.169}$$

The result above shows that in the limit (2.166, 2.167) the fast changes of the wavefunction[14] (2.27, 2.28, 2.34)

$$|\psi(t)\rangle = \sum_{\alpha=1}^{d} \beta_\alpha e^{-i\varepsilon_\alpha t}\widehat{P}(t)\,|w_\alpha\rangle \tag{2.170}$$

decrease as we decrease the length of the period T. For the times comparable to the time period T, i.e. $|-i\varepsilon_\alpha t| \ll 1$, the evolution operator approaches identity. Note that the exponent $-i\varepsilon_\alpha t$ can significantly deviate from the zero value by simply increasing the time t whereas equation (2.169) holds for all t since the operator $\widehat{P}(t)$ is T periodic.

Let us define $E_\alpha \stackrel{\text{def}}{=} \varepsilon_\alpha + O(\delta^l/T)$, where E_α represent eigenvalues of some effective Hamiltonian. From equation (2.170) we also see that we need to know the values $\varepsilon_\alpha T = O(\delta)$ with a discrepancy better than $O(\delta)$ since we do not consider the term $O(\delta t/T) = |-i\varepsilon_\alpha t|$ negligible, i.e. $l > 1$. Let us find the times when evolution is dominantly dictated by an effective Hamiltonian. Let us study the following corrections

$$\begin{aligned} e^{-iE_\alpha t} &= e^{-i\left[\varepsilon_\alpha T+O(\delta^l)\right]t/T} = e^{O(\delta^l t/T)}e^{-i\varepsilon_\alpha t} \\ &= (\widehat{I}+O(\delta^l t/T))e^{-i\varepsilon_\alpha t} && (2.171)\\ &= \widehat{I}+O(\delta t/T)+O(\delta^l t/T)+O(\delta^{l+1}t^2/T^2), && (2.172)\\ e^{-iE_\alpha t}\widehat{P}(t) &= \widehat{I}+O(\delta)+O(\delta t/T)+O(\delta^l t/T)+O(\delta^{l+1}t^2/T^2). && (2.173)\end{aligned}$$

If we want to get a non-negligible evolution, the following must hold

$$\begin{aligned}\delta &\ll \delta t/T, && (2.174)\\ t/T &\gg 1. && (2.175)\end{aligned}$$

The upper bound for the times considered could be inferred from equation (2.171) by considering $\delta^l t/T \ll 1$. We conclude that the evolution is dominantly dictated by an effective Hamiltonian for the times satisfying[15]

$$1 \ll t/T \ll 1/\delta^l. \tag{2.176}$$

[13]Note that $\widehat{U}(t,0) = e^{-i\widehat{K}(t)}e^{-i\widehat{G}t}e^{+i\widehat{K}(0)}$ where $\widehat{K}(t) = O(\delta)$, $\widehat{K}(0) = O(\delta)$ and $\widehat{G}t = O(\delta t/T)$. Thus, $\widehat{U}(t) = \widehat{I}+O(\delta)$ for $t \in [0,T]$.

[14]We consider the stroboscopic Floquet Hamiltonian $\widehat{G}[0]$ whose eigenvalues lie in the first Brillouin zone. The transition from a general stroboscopic Floquet Hamiltonian to the one with eigenvalues in the first Brillouin zone (by spectral decomposition and shifting the eigenvalues) preserves the required property (2.18).

[15]Since the perturbation connected with an uncertainty in ε_α represented by $O(\delta^l t/T)$ in equation (2.173) must by significantly lower than the correction to the time evolution $O(\delta t/T)$, we must require $l > 1$ (as we have already mentioned above).

We do not say that the times $t/T \approx 1$ are for our theory inaccessible. We can describe the short times by employing the action of the exponential of the kick operator $e^{-i\widehat{K}(t)}$. What we essentially say here is that the evolution of a quantum mechanical state is captured by an effective Hamiltonian with the uncertainty $O(\delta)$ in the time regime given by equation (2.176). The only possible fast changes in the state vector are of the order $O(\delta)$. The mathematics does not exclude a fast and minute trembling of the state vector.

Considering the above discussion, we see that in the high-frequency regime the Floquet Hamiltonian describes the most important features of the evolution and the fast changes in the state of the system become small. Generally speaking, the mathematical structure of the outlined expansions indicates that doing the expansions in the powers of the time period T in a wide range of problems yields sensible results.

3. Many-body qubit systems

In the previous chapter, we focused on the general theory describing quantum mechanical systems with a time-periodic Hamiltonian and the high-frequency limit of a wide range of these systems. In this chapter, we apply the theory and methods from the previous chapter to concrete models—delta-driven and harmonically-driven Lipkin–Meshkov–Glick model.

Throughout this chapter we measure time in the dimensionless units such that the period T is equal to one, i.e. $T = 1$. The expressions containing the variable T can be reached through dimensional analysis.

3.1 Lipkin–Meshkov–Glick model

The simple toy model called the Lipkin–Meshkov–Glick model (the Lipkin model for brevity), described in [21, 22, 23], serves as a playground for testing various hypotheses of theoretical physics. Here we briefly sketch its properties before we proceed to work with this model. The model is described by the Hamiltonian

$$\boxed{\widehat{H} = p\widehat{J}_x + \frac{\kappa}{2j}\widehat{J}_z^2}, \tag{3.1}$$

where p and κ are the parameters of the model. The total spin operator (or quasispin operator) $\widehat{J}_k$—the total spin of the composition of N individual spin-$\frac{1}{2}$ systems—is defined by

$$\boxed{\widehat{J}_k = \frac{1}{2}\sum_{i=1}^{N}\widehat{\sigma}_k^{(i)}}, \tag{3.2}$$

where i denotes the individual spin sites and $k \in \{x, y, z\}$. The operators $\widehat{\sigma}_k^{(i)}$ have the straightforward definition

$$\widehat{\sigma}_k^{(i)} = \underbrace{\widehat{I}\otimes ... \otimes \widehat{I}}_{i-1 \text{ identity operators}} \otimes \widehat{\sigma}_k \otimes \underbrace{\widehat{I}\otimes ... \otimes \widehat{I}}_{N-i \text{ identity operators}}, \tag{3.3}$$

where the direct product composes the individual spin sites. The operator $\widehat{\sigma}_k/2$ is the well known spin-$\frac{1}{2}$ angular momentum operator, where $\widehat{\sigma}_k$ is commonly represented by Pauli matrices.

Note that since

$$\widehat{J}_z^2 = \frac{1}{4}\sum_{i_1,i_2=1}^{N}\widehat{\sigma}_z^{(i_1)}\widehat{\sigma}_z^{(i_2)}, \tag{3.4}$$

the term $\frac{\kappa}{2j}\widehat{J}_z^2$ could be considered to be the term representing an interaction between the individual spin sites.

Restriction to Hilbert space of maximum $\widehat{J}^2$ eigenvectors

Firstly

$$\left[\widehat{J}^2, \widehat{H}\right] = 0, \tag{3.5}$$

thus the evolution of the system described by the Hamiltonian (3.1) conserves the quantum number j—the eigenvalues of $\widehat{J}^2$ are $j(j+1)$. We can consequently restrict ourselves to the Hilbert space of eigenvectors of $\widehat{J}^2$ with some fixed quantum number j. From the form of the Hamiltonian (3.1) we see that the only quantum numbers we are interested in are the quantum numbers j and m, whose definition we know from the general angular momentum problem [12]

$$\widehat{J}^2 \left|j, m, \{s\}\right\rangle = j(j+1) \left|j, m, \{s\}\right\rangle, \quad j = 0, \frac{1}{2}, 1, \frac{3}{2}, 2, \frac{5}{2}, ..., \frac{N}{2} \tag{3.6}$$

$$\widehat{J}_z \left|j, m, \{s\}\right\rangle = m \left|j, m, \{s\}\right\rangle, \; m = -j, -j+1, ..., j-1, j. \tag{3.7}$$

The symbol $\{s\}$ characterizes other quantum numbers we are not interested in. The operators $\widehat{\vec{J}} = (\widehat{J}_x, \widehat{J}_y, \widehat{J}_z)^T$ have really the properties of angular momentum operators since we are just adding the angular momentum states and operators.

But now we are not restricting ourselves to the angular momentum interpretation and describe the toy model that is rather general. The states and operators do not necessarily have the meaning of angular momentum, though the mathematical properties are the same. We are talking about a quasispin.

The minimum dimension of subspace preserving the quantum number j is $2j+1$. Consequently, the minimum dimension of the full Hilbert space $\mathcal{H}_{\text{Full}}$ is

$$\sum_{j=N/2-\lfloor N/2 \rfloor}^{N/2} (2j+1), \tag{3.8}$$

i.e. grows quadratically with N. We know the dimension of the full Hilbert space $\mathcal{H}_{\text{Full}}$ distinguishing each spin, it is 2^N, i.e. grows exponentially. The structure of the full Hilbert space $\mathcal{H}_{\text{Full}}$ is such that the eigenspaces with fixed j and with basis numbered by eigenvalues of $\widehat{J}_z$, i.e. with dimension $2j+1$, are used repeatedly in the construction of the full Hilbert space [22, 23]. Each such eigenspace with dimension $2j+1$ has some multiplicity—the number of its copies used when constricting $\mathcal{H}_{\text{Full}}$. The subspace of $\mathcal{H}_{\text{Full}}$ with maximal j, i.e. $j = N/2$, has multiplicity one, i.e. the dimension of the subspace is $2j+1$. It is the consequence of the eigenstate $\left|j = m = \frac{N}{2}\right\rangle$ having only one representation in the full Hilbert space of dimension 2^N—the vector representing the state in which all spins are possessing the state spin up $|\uparrow ... \uparrow\rangle \equiv |j = m = \frac{1}{2}\rangle$. As in other treatises considering the Lipkin model, we will restrict ourselves to the subspace of $\mathcal{H}_{\text{Full}}$ with the highest quantum number j possible, i.e. $j = N/2$.

For those who want a clear proof that the eigenspace with $j = N/2$ has the same dimension whether we consider the subspace of the full Hilbert space $\mathcal{H}_{\text{Full}}$ distinguishing each spin or whether we look at the space as the space with fixed $j = N/2$ and variable $m = -j, -j+1, ..., j-1, +j$, we try to clarify it. We define the well known ladder operators [12]

$$\widehat{J}_\pm \stackrel{\text{def}}{=} \widehat{J}_x \pm i\widehat{J}_y. \tag{3.9}$$

We also define the space

$$\mathcal{S}_{j_{max}} \stackrel{\text{def}}{=} \text{span}\left\{\left(\widehat{J}_-\right)^k |\uparrow ... \uparrow\rangle\right\}_{k=0}^{N}. \tag{3.10}$$

We state the following

$$\forall\,|\psi\rangle \in \mathcal{H}_{\text{Full}} : \widehat{\vec{J}}^{\,2}\,|\psi\rangle = \frac{N}{2}\left(\frac{N}{2}+1\right)|\psi\rangle \Rightarrow |\psi\rangle \in \mathcal{S}_{j_{max}}. \tag{3.11}$$

We prove the statement by contradiction—we suppose that

$$\exists\,|\psi''\rangle \in \mathcal{H}_{\text{Full}} : \widehat{\vec{J}}^{\,2}\,|\psi''\rangle = \frac{N}{2}\left(\frac{N}{2}+1\right)|\psi''\rangle \;\;\&\;\; |\psi''\rangle \notin \mathcal{S}_{j_{max}}.$$

The above mathematical statement is equivalent to the statement

$$\exists\,|\psi'\rangle \in \mathcal{H}_{\text{Full}} : \widehat{\vec{J}}^{\,2}\,|\psi'\rangle = \frac{N}{2}\left(\frac{N}{2}+1\right)|\psi'\rangle \;\;\&\;\forall\,|\psi\rangle \in \mathcal{S}_{j_{max}} : \langle\psi|\psi'\rangle = 0.$$

From the theory behind the angular momentum quantum systems, we know that

$$|\psi'\rangle = \sum_{m=-j}^{+j}\sum_{\{s\}} c(m,\{s\})\,|j,m,\{s\}\rangle\,, c(m,\{s\}) \in \mathbb{C}. \tag{3.12}$$

From equality (3.12), we infer that there exist some $k_0 \in \{0,...,N\}$ such that[1]

$$\left(\widehat{J}_+\right)^{k_0}|\psi'\rangle = c\,|\uparrow ... \uparrow\rangle\,, \tag{3.13}$$

where c is some non-zero complex number ($c \in \mathbb{C}, c \neq 0$). Let us choose

$$|\psi_0\rangle \stackrel{\text{def}}{=} \left(\widehat{J}_-\right)^{k_0}|\uparrow ... \uparrow\rangle \in \mathcal{S}_{j_{max}}.$$

Then

$$\begin{aligned}\langle\psi_0|\psi'\rangle &= \left(\left(\widehat{J}_-\right)^{k_0}|\uparrow ... \uparrow\rangle\,, |\psi'\rangle\right) \\ &= \langle\uparrow ... \uparrow|\left(\widehat{J}_+\right)^{k_0}|\psi'\rangle \\ &\stackrel{(3.13)}{=} c\,\langle\uparrow ... \uparrow|\uparrow ... \uparrow\rangle = c \neq 0,\end{aligned} \tag{3.14}$$

i.e. we get the contradiction. The notation $(\bullet,\bullet)$ in (3.14) means an ordinary scalar product.

Note that in equation (3.12) we considered a sum $\sum_{\{s\}}$. Having proved the statement (3.11) we know that the sum $\sum_{\{s\}}$ could be omitted. Apart from j and m, we do not need any additional quantum numbers $\{s\}$ in the case $j = N/2$.

From the structure of the space $\mathcal{S}_{j_{max}}$ (3.10) and the operator $\widehat{J}_-$ (3.9, 3.2)

$$\widehat{J}_- = \sum_{n=1}^{N}\underbrace{\widehat{I}\otimes ...\otimes\widehat{I}}_{n-1}\otimes\left(\frac{\widehat{\sigma}_x}{2} - i\frac{\widehat{\sigma}_y}{2}\right)\otimes\underbrace{\widehat{I}\otimes ...\otimes\widehat{I}}_{N-n},$$

we infer that the space $\mathcal{S}_{j_{max}}$ is the fully symmetrized part of $\mathcal{H}_{\text{Full}}$. It means that every permutation of the spin sites leaves a state of the system invariant if and only if the state belongs to $\mathcal{S}_{j_{max}}$.

[1]Note that $\widehat{J}_\mp\widehat{J}_\pm = \widehat{J}^2 - \widehat{J}_z^2 \mp \widehat{J}_z$. For $|\psi'_m\rangle \stackrel{\text{def}}{=} \sum_{\{s\}} c(m,\{s\})\,|j,m,\{s\}\rangle$ we get $\langle\psi'_m|\widehat{J}_\mp\widehat{J}_\pm|\psi'_m\rangle = [j(j+1) - m(m\pm 1)]\cdot||\,|\psi'_m\rangle\,||^2$. If $||\,|\psi'_m\rangle\,||^2 \neq 0 : \widehat{J}_+\,|\psi'_m\rangle = 0 \iff m = j$.

3.2 Delta-driven Lipkin model—kicked top system

The kicked top system is an archetypal system manifesting parametrically dependent chaos [24]. Best characterized by its Hamiltonian

$$\boxed{\widehat{H}(t) = \frac{\kappa}{2j}\widehat{J}_z^2 + p\widehat{J}_x T \sum_{n=-\infty}^{+\infty} \delta(t - n \cdot T)} \tag{3.15}$$

with the parameters κ and p it is simple enough for treatment and complex enough for investigating chaos. The operators $\widehat{J}_x, \widehat{J}_z$ are the quasispin operators discussed in section 3.1. From equation (3.1) we see that we could conceive of the kicked top model as a "delta-driven Lipkin model". As in the case of the Lipkin model we restrict ourselves to the case with the fixed quantum number j equal to its maximal value $j = N/2$. The dimension of the appropriate Hilbert space is $2j + 1$, which is a result of arguments similar to those in section 3.1.

Let us now invoke equation (2.2)

$$\widehat{H}(t) = \widehat{H}_0 + \widehat{V}_0 + \sum_{n=1}^{+\infty} \left(\widehat{V}_n e^{+in\omega t} + \widehat{V}_{-n} e^{-in\omega t} \right)$$

and identify

$$\begin{aligned} \widehat{H}_0 &= \frac{\kappa}{2j}\widehat{J}_z^2, \\ \widehat{V}_0 &= p\widehat{J}_x, \\ \widehat{V}_n &= p\widehat{J}_x, n \in \mathbb{Z}. \end{aligned} \tag{3.16}$$

We used (2.79)

$$\sum_{n=-\infty}^{+\infty} \delta\left(x - n \cdot \frac{2\pi}{\omega}\right) = \frac{\omega}{2\pi} \sum_{n=-\infty}^{+\infty} e^{in\omega x}.$$

Conceiving the simplest effective description we can get, a heuristic estimate could be

$$\widehat{H}_S = \frac{1}{T} \lim_{\varepsilon \to 0^+} \int_{0+\varepsilon}^{T+\varepsilon} \widehat{H}(t) \mathrm{d}t = \frac{\kappa}{2j}\widehat{J}_z^2 + p\widehat{J}_x = \widehat{H}_0 + \widehat{V}_0, \tag{3.17}$$

essentially the Lipkin Hamiltonian (3.1). But knowing the methodology from section 2.3 (equation (2.134)), we say that the Hamiltonian $\widehat{H}_S$ is a zero order expansion of the Floquet Hamiltonian. Thus $\widehat{H}_S = \widehat{G}_0$.

We remind that we use the units in which the period T is equal to one

$$T = \frac{2\pi}{\omega} = 1. \tag{3.18}$$

We formulated the above equations using the letter T for the time period. Since in our units $T = 1$, in the following we will omit the use of the letter T, knowing it could be retrieved by dimensional analysis.

For sufficiently small parameters (κ, p) the simple approximation yields a good approximation of quasienergy levels, i.e. the plots depicted in figure 3.1. The effective description (red dots) is compared with precise numerical results for periodically driven Hamiltonian (3.15) (black lines).

Since the operators needed are the $(2j+1) \times (2j+1)$ matrices, the precise quasienergies are easily yielded by finding the eigenvalues of the operator

$$e^{-i\kappa \widehat{J}_z^2/(2j)} e^{-ip\widehat{J}_x} = e^{-i(\text{Some stroboscopic Floquet Hamiltonian})}. \tag{3.19}$$

We get the precise quasienergies if we take the complex phases of the eigenvalues of (3.19) and multiply the phases by the factor minus one. The reason for such a procedure is that the expression (3.19) is equal to an exponential of $-i$ times some stroboscopic Floquet Hamiltonian. Eigenvalues of Floquet Hamiltonians are quasienergies. The computation of eigenvalues of (3.19) is facilitated by using the matrix expressions for the operators and replacing the operator exponentials with matrix exponentials.

3.2.1 Use of special form of BCH formula

Here we present the approach described in paper [7]. We continue the reasoning discussed in section 2.4. We repeat (2.150)

$$-\ln\left(e^{-p\widehat{B}} e^{-\widehat{A}}\right) = \widehat{A} - p\frac{\mathrm{ad}_{\widehat{A}}}{e^{\left(-\mathrm{ad}_{\widehat{A}}\right)} - 1}\widehat{B} + O(p^2)$$

and assign

$$\widehat{A} = i\frac{\kappa}{2j}\widehat{J}_z^2, \tag{3.20}$$

$$\widehat{B} = i\widehat{J}_x. \tag{3.21}$$

Bear in mind that $T = 1$.

It is required that

$$-\ln\left(e^{-p\widehat{B}} e^{-\widehat{A}}\right) = i\widehat{G}_{\mathrm{SBCH}}[0^+], \tag{3.22}$$

where $\widehat{G}_{\mathrm{SBCH}}[0^+]$ is the Floquet Hamiltonian we seek. For our choice of $\widehat{A}$ and $\widehat{B}$, we get (see section A.3 in appendix A)

$$\begin{aligned} \frac{\mathrm{ad}_{\widehat{A}}}{e^{\left(\mathrm{ad}_{\widehat{A}}\right)} - 1}\widehat{B} &= -\frac{1}{2}\widehat{J}_+ \frac{\frac{\kappa}{2j}(2\widehat{J}_z + 1)}{e^{\left[-i\frac{\kappa}{2j}(2\widehat{J}_z+1)\right]} - 1} \\ &\quad + \frac{1}{2}\frac{\frac{\kappa}{2j}(2\widehat{J}_z + 1)}{e^{\left[i\frac{\kappa}{2j}(2\widehat{J}_z+1)\right]} - 1}\widehat{J}_-. \end{aligned} \tag{3.23}$$

Thus

$$\boxed{\widehat{G}_{\mathrm{SBCH}}[0^+] \approx \frac{\kappa}{2j}\widehat{J}_z^2 + \frac{p}{2}\left\{-i\widehat{J}_+ \frac{\frac{\kappa}{2j}(2\widehat{J}_z+1)}{e^{\left[-i\frac{\kappa}{2j}(2\widehat{J}_z+1)\right]} - 1} + \mathrm{H.c.}\right\}}, \tag{3.24}$$

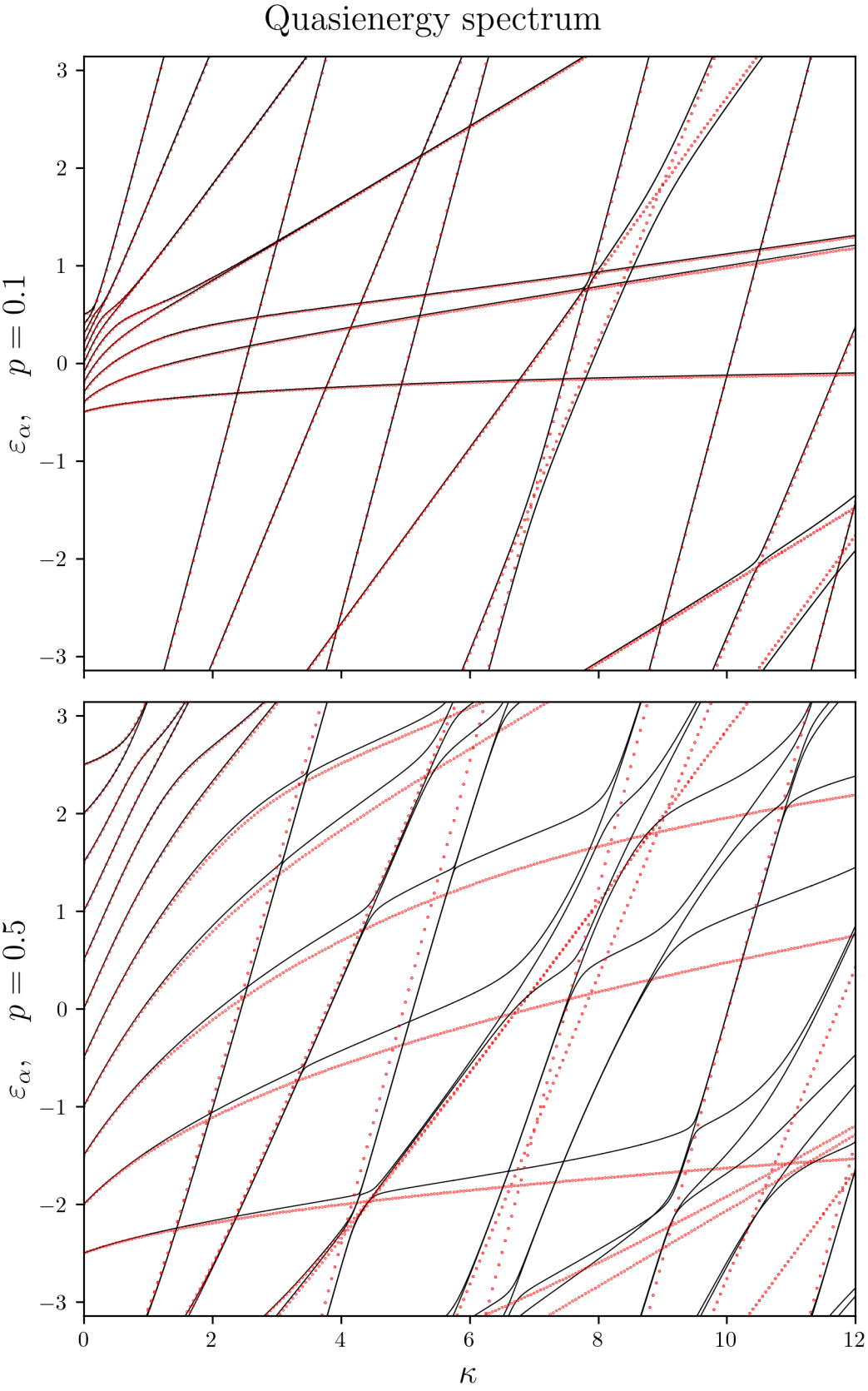

Figure 3.1: The eigenenergies of the effective Hamiltonian (3.17)—"average Hamiltonian"—mapped on the first Brillouin zone are plotted as red dots. For the comparison, the precise quasienergies for the kicked top system (3.15) are plotted as black solid lines. In this figure $j = 5$.

where $[0^+]$ signifies that $\widehat{G}_{\mathrm{SBCH}}[0^+]$ is a stroboscopic Floquet Hamiltonian tied to the initial time right after a kick—realisation of the time delta function. The quasienergies mapped to the first Brillouin zone are not affected by the choice of the time to which a stroboscopic Floquet Hamiltonian is tied.

The effective Hamiltonian is in the right hand side of relation (3.24). The eigenvalues of the effective Hamiltonian (3.24), approximating quasienergies, for various combinations of parameters (κ, p) are depicted in figure 3.2 and compared with precise numerical values of quasienergies.

We see that the effective description gives a good agreement for some range of parameters. For some range of parameters, e.g. $\kappa > 6, p = 0.1$, the effective description is insufficient. It is interesting that the complicated method presented here gives less satisfactory results than the simple method in the previous section approximating the Floquet Hamiltonian by $\widehat{H}_S = \widehat{G}_0$ (3.17), see figure 3.1.

3.2.2 Use of Floquet Hamiltonian and kick operator expansion

Next, and as far as we know the most successful method, seeks both the Floquet Hamiltonian and the kick operator and expresses them in the form of a series. We present the second-order expansion of the Floquet Hamiltonian and kick operator. We use the theory presented in section 2.3. This method is used for the kicked top model in paper [5]. As already mentioned

$$\widehat{G}_0 = \frac{\kappa}{2j}\widehat{J}_z^2 + p\widehat{J}_x, \tag{3.25}$$

where we used (3.16, 2.134, 2.133).

From (2.133) we see that

$$\widehat{K_1}(t) = 2p\widehat{J}_x \sum_{n=1}^{\infty} \frac{\sin(2\pi n t)}{n} \tag{3.26}$$

and from (2.136)

$$\widehat{G}_1 = \widehat{0}. \tag{3.27}$$

We repeat that $T = 1$ and the definition $\tau \stackrel{\mathrm{def}}{=} \omega t = 2\pi t$. There is a caveat when using the formula (3.26): for $x \in (0, 1)$ it holds

$$\sum_{n=1}^{\infty} \frac{\sin(2\pi n x)}{n} = \frac{\pi}{2} - \pi \cdot x \tag{3.28}$$

and for general x we can periodically extend the right hand side of equation (3.28). Thus

$$\lim_{x\to 0^-} \sum_{n=1}^{\infty} \frac{\sin(2\pi n x)}{n} = -\frac{\pi}{2}, \lim_{x\to 0^+} \sum_{n=1}^{\infty} \frac{\sin(2\pi n x)}{n} = \frac{\pi}{2}. \tag{3.29}$$

From (2.138), we get

$$\widehat{K_2} = \sum_{n=1}^{\infty} \frac{1}{in^2} \left[\widehat{V}_n, \widehat{H}_0 + \widehat{V}_0\right] \left(e^{in\tau} + e^{-in\tau}\right). \tag{3.30}$$

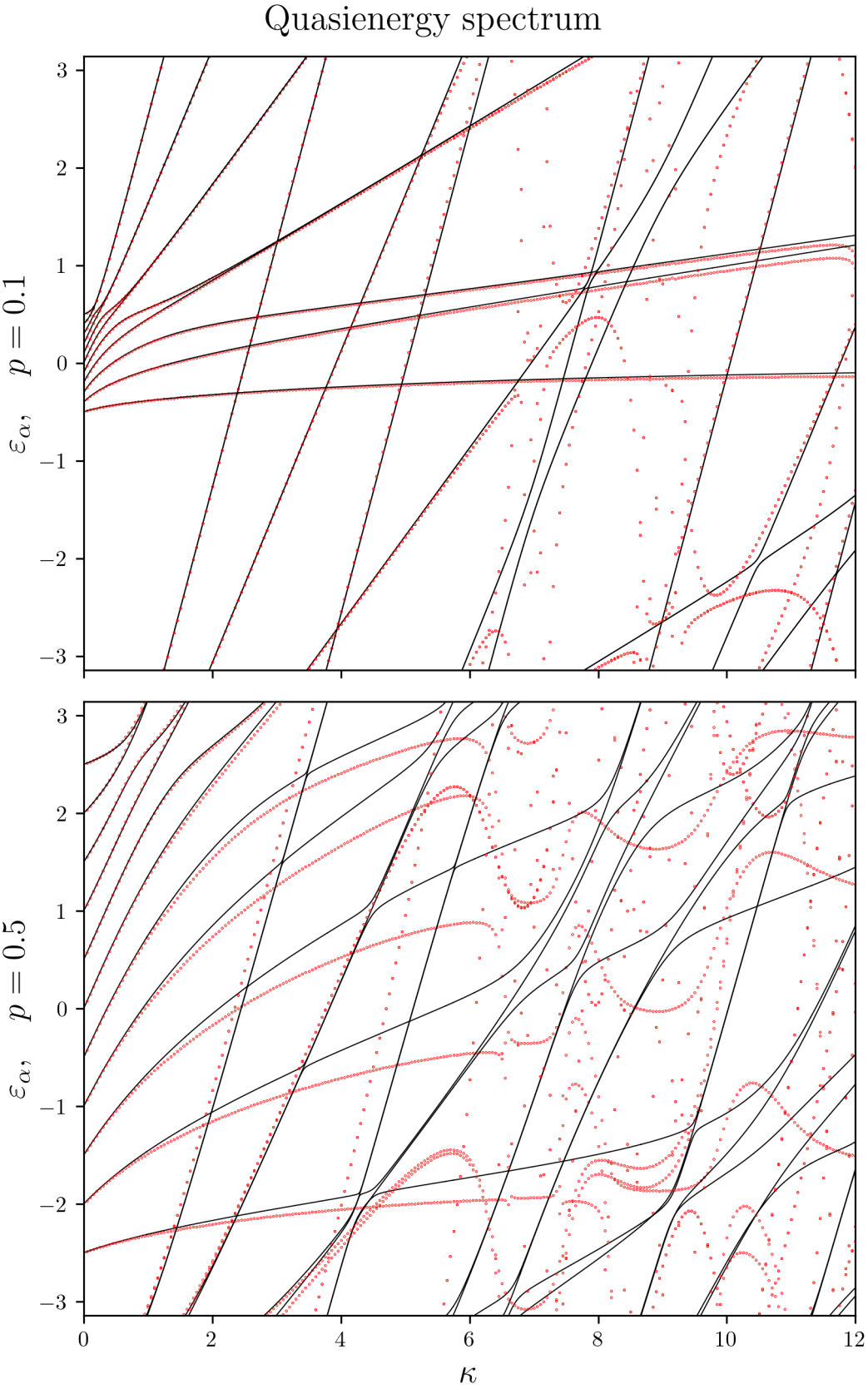

Figure 3.2: The eigenenergies of the effective Hamiltonian constructed using the special form of the BCH formula (3.24) mapped on the first Brillouin zone are plotted as red dots. For the comparison, the precise quasienergies for the kicked top system (3.15) are plotted as black solid lines. In this figure $j = 5$.

By computing the commutator

$$\begin{aligned}\left[\widehat{V}_n, \widehat{H}_0 + \widehat{V}_0\right] &= \left[\widehat{V}_n, \widehat{H}_0\right] && (3.31)\\ &= \frac{\kappa p}{2j}\left[\widehat{J}_x, \widehat{J}_z^2\right] && (3.32)\\ &= -i\frac{\kappa p}{2j}\left(\widehat{J}_y\widehat{J}_z + \widehat{J}_z\widehat{J}_y\right), && (3.33)\end{aligned}$$

we get

$$\widehat{K}_2 = -\frac{\kappa p}{j}\left(\widehat{J}_y\widehat{J}_z + \widehat{J}_z\widehat{J}_y\right)\cdot\sum_{n=1}^{\infty}\frac{\cos(2\pi n t)}{n^2}. \tag{3.34}$$

For $x \in (0,1)$ it holds[2]

$$\sum_{k=-\infty}^{+\infty}\frac{\cos(2\pi k x)}{k^2} = \pi^2\left(x - \frac{1}{2}\right)^2 - \frac{\pi^2}{12} \tag{3.35}$$

and for general $x \in \mathbb{R}$ we can periodically extend the right hand side of (3.35). We see that the sum on the left hand side of equation (3.35) is continuous for all $x \in \mathbb{R}$.

From equation (2.140), we write

$$\widehat{G}_2 = \sum_{n=1}^{\infty}\frac{1}{n^2}\left[\left[\widehat{V}_n, \widehat{H}_0 + \widehat{V}_0\right], \widehat{V}_{-n}\right]. \tag{3.36}$$

Using equations (3.31, 3.33), we get

$$\begin{aligned}\widehat{G}_2 &= -i\frac{\kappa p}{2j}\sum_{n=1}^{\infty}\frac{1}{n^2}\left[\widehat{J}_y\widehat{J}_z + \widehat{J}_z\widehat{J}_y, \widehat{V}_{-n}\right] && (3.37)\\ &= -i\frac{\kappa p^2}{2j}\sum_{n=1}^{\infty}\frac{1}{n^2}\left[\widehat{J}_y\widehat{J}_z + \widehat{J}_z\widehat{J}_y, \widehat{J}_x\right]. && (3.38)\end{aligned}$$

We compute the commutator separately

$$\begin{aligned}\left[\widehat{J}_y\widehat{J}_z + \widehat{J}_z\widehat{J}_y, \widehat{J}_x\right] &= \left[\widehat{J}_y\widehat{J}_z, \widehat{J}_x\right] + \left[\widehat{J}_z\widehat{J}_y, \widehat{J}_x\right]\\ &= \widehat{J}_y\left[\widehat{J}_z, \widehat{J}_x\right] + \left[\widehat{J}_y, \widehat{J}_x\right]\widehat{J}_z + \widehat{J}_z\left[\widehat{J}_y, \widehat{J}_x\right] + \left[\widehat{J}_z, \widehat{J}_x\right]\widehat{J}_y\\ &= 2i\widehat{J}_y^2 - 2i\widehat{J}_z^2. && (3.39)\end{aligned}$$

We use the known sum

$$\sum_{n=1}^{\infty}\frac{1}{n^2} = \frac{\pi^2}{6} \tag{3.40}$$

and get

$$\widehat{G}_2 = \frac{\pi^2\kappa p^2}{6j}\left(\widehat{J}_y^2 - \widehat{J}_z^2\right). \tag{3.41}$$

[2]The according relations for the Fourier transform are $a_k = \int_0^1 g(x)e^{-2\pi i k x}\mathrm{d}x$, $g(x) = \sum a_k e^{2\pi i k x}, k \in \mathbb{Z}$.

Using (3.26,3.34, 2.129), we get the second-order expansion of the kick operator

$$\widehat{K}_{E2}(t) = \frac{p\widehat{J}_x}{\pi}\sum_{n=1}^{\infty}\frac{\sin(2\pi nt)}{n} - \frac{\kappa p}{4\pi^2 j}\left(\widehat{J}_y\widehat{J}_z + \widehat{J}_z\widehat{J}_y\right)\cdot\sum_{n=1}^{\infty}\frac{\cos(2\pi nt)}{n^2}. \tag{3.42}$$

Setting the initial and final time right before the "kick"—participation of delta function—and using (3.29, 3.40), we get

$$\widehat{K}_{E2}(0^-) = \lim_{t\to 0^-}\widehat{K}_{E2}(t). \tag{3.43}$$

The second-order expansion of the kick operator (tied to the starting time "$t_s = 0^-$") reads

$$\boxed{\widehat{K}_{E2}(0^-) = -\frac{p\widehat{J}_x}{2} - \frac{\kappa p}{24j}\left(\widehat{J}_y\widehat{J}_z + \widehat{J}_z\widehat{J}_y\right)}. \tag{3.44}$$

When using (3.29), we have taken the limit approaching the time $t = 0$ from the left since we are describing the moment right before the kick.

Using (3.25, 3.27, 3.41, 2.128), we get the second-order expansion of the Floquet Hamiltonian

$$\boxed{\widehat{G}_{E2} = \frac{\kappa}{2j}\widehat{J}_z^2 + p\widehat{J}_x + \frac{\kappa p^2}{24j}\left(\widehat{J}_y^2 - \widehat{J}_z^2\right)}. \tag{3.45}$$

In figure 3.3 quasienergy spectrum for relevant parameters is computed using second-order effective Floquet Hamiltonian (3.45) (dotted red). For the comparison, the precise quasienergy spectrum is also plotted (black lines).

Figures 3.1, 3.2 and 3.3 present how faithfully the various methods approximate the quasienergies and consequently the Floquet Hamiltonians. The method presented in this section gives the most satisfactory results for the parameters considered.

3.2.3 Classical limit

The kicked top system was also studied in its classical form [24, 25]. We perform the classical limit for the quantum kicked top Hamiltonian (3.15) in the following way: We rescale the quantum quasispin operators

$$\widehat{X} = \frac{\widehat{J}_x}{j}, \quad \widehat{Y} = \frac{\widehat{J}_y}{j}, \quad \widehat{Z} = \frac{\widehat{J}_z}{j} \tag{3.46}$$

and identify the limits

$$\lim_{j\to\infty}\frac{\widehat{J}_x}{j} = X, \quad \lim_{j\to\infty}\frac{\widehat{J}_y}{j} = Y, \quad \lim_{j\to\infty}\frac{\widehat{J}_z}{j} = Z, \tag{3.47}$$

$$\lim_{j\to\infty}\frac{\widehat{H}(t)}{j} = H(t). \tag{3.48}$$

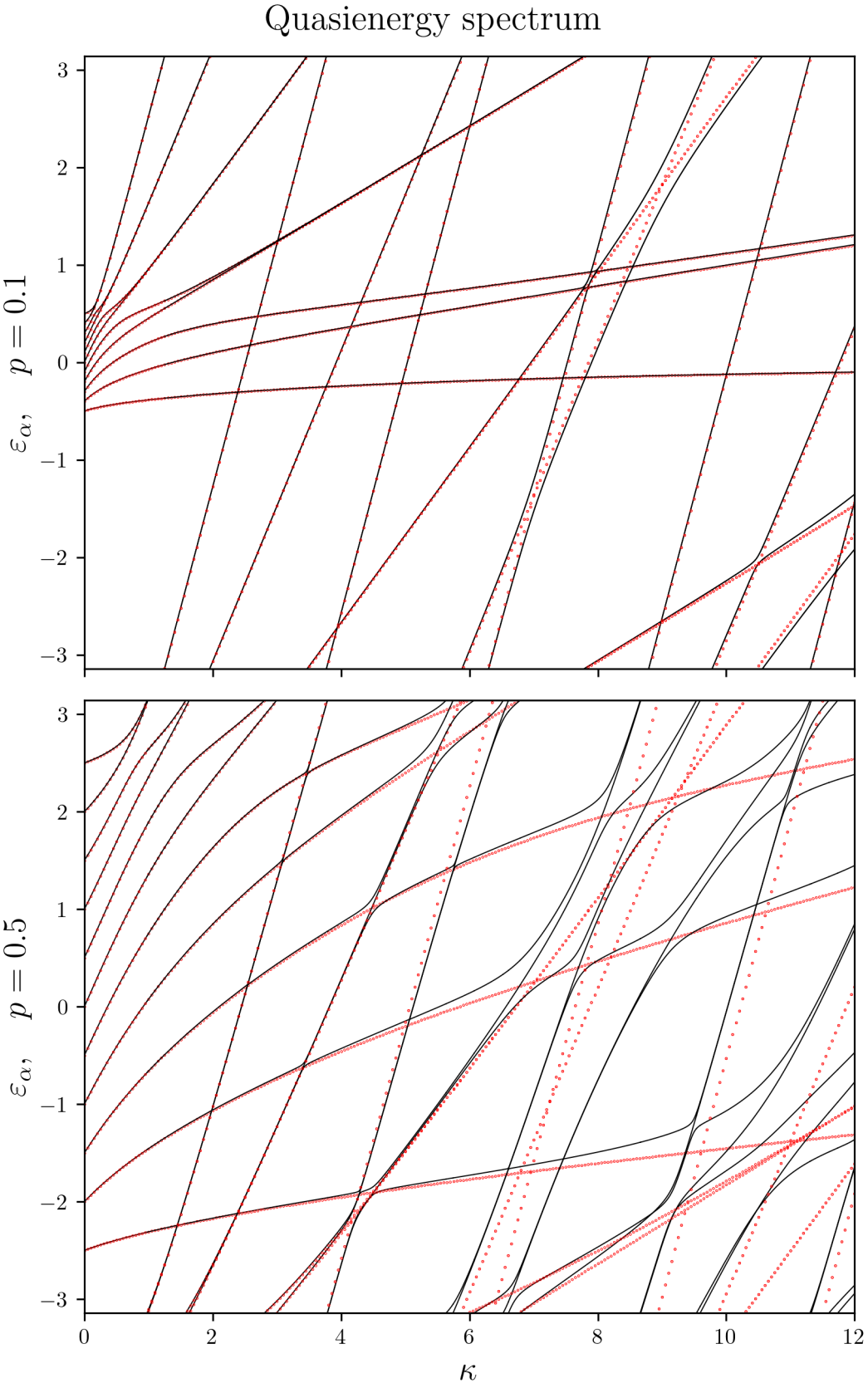

Figure 3.3: The eigenenergies of the second-order effective Hamiltonian (3.45) mapped on the first Brillouin zone are plotted as red dots. For the comparison, the precise quasienergies for the kicked top system (3.15) are plotted as black solid lines. In this figure $j = 5$.

On the right hand side of equations (3.47, 3.48) are the classical variables. The Hamiltonian for the classical kicked top[3] reads

$$\boxed{H(t) = \frac{\kappa}{2} Z^2 + pX \sum_{n=-\infty}^{+\infty} \delta(t-n)}. \tag{3.49}$$

We keep the period equal to one $T = 1$.

The evolution from time immediately before the kick—realization of delta function—to the time immediately before the next kick could be computed by mapping

$$\begin{aligned} X\left(n+\frac{1}{2}\right) &= X(n), \\ Y\left(n+\frac{1}{2}\right) &= Y(n)\cos p - Z(n)\sin p, \\ Z\left(n+\frac{1}{2}\right) &= Y(n)\sin p + Z(n)\cos p, \end{aligned} \tag{3.50}$$

$$\begin{aligned} X(n+1) &= X(n)\cos\left[\kappa Z\left(n+\frac{1}{2}\right)\right] - Y\left(n+\frac{1}{2}\right)\sin\left[\kappa Z\left(n+\frac{1}{2}\right)\right], \\ Y(n+1) &= X(n)\sin\left[\kappa Z\left(n+\frac{1}{2}\right)\right] + Y\left(n+\frac{1}{2}\right)\cos\left[\kappa Z\left(n+\frac{1}{2}\right)\right], \\ Z(n+1) &= Z\left(n+\frac{1}{2}\right), \end{aligned} \tag{3.51}$$

where we define the angular momentum immediately before the nth kick (realization of delta function)

$$\vec{R}(n) \stackrel{\text{def}}{=} (X(n), Y(n), Z(n))^T \tag{3.52}$$

and the angular momentum immediately after the nth kick

$$\vec{R}\left(n+\frac{1}{2}\right) \stackrel{\text{def}}{=} \left(X\left(n+\frac{1}{2}\right), Y\left(n+\frac{1}{2}\right), Z\left(n+\frac{1}{2}\right)\right)^T. \tag{3.53}$$

Derivation of equations (3.50, 3.51) is presented in the appendix B.

From equations (3.50, 3.51) we clearly see that we stay on a sphere $|\vec{R}| = const.$ when evolving from an arbitrary state $\vec{R}_0$. In the following we will always choose $|\vec{R}| = 1$. The conservation of $|\vec{R}|$ is also a consequence of

$$\left\{|\vec{R}|^2, \vec{R}\right\} = 0, \tag{3.54}$$

$$\left\{|\vec{R}|^2, H(t)\right\} = 0 \tag{3.55}$$

and known equation (B.7), where $\{\bullet, \bullet\}$ is the Poisson bracket.

The mapping $\vec{R}(n) \to \vec{R}(n+1/2)$ is a precession around the X axis linearly proportional to the parameter p.

The mapping $\vec{R}(n+1/2) \to \vec{R}(n+1)$ is a nonlinear precession around the Z axis—i.e. a precession the angular velocity of which depends on the value of the Z coordinate and on the value of the parameter κ. For its opposite sign on hemispheres $Z > 0$ and $Z < 0$, we sometimes call it "twisting" or "torsion". An example of an evolution of the classical kicked top on the Bloch sphere is depicted in figure 3.4.

[3]In the literature more complicated formulas for classical kicked top can be found. Generally speaking, formulas comprised of polynomials of (J_x, J_y, J_z) and familiar tray of delta kicks.

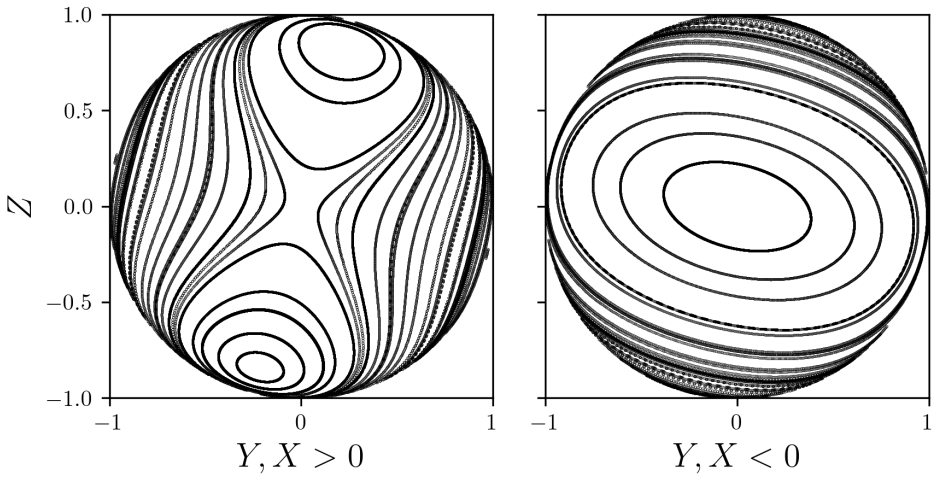

Figure 3.4: The evolution of the classical kicked top on the Bloch sphere using the parameters $\kappa = 1.0, p = 0.5$.

3.2.4 Classical limit of effective description

Contours of the effective Floquet Hamiltonian

We perform the classical limit of the second-order effective Floquet Hamiltonian (3.45) in the same way we did the classical limit for the quantum kicked top Hamiltonian. We rescale the $\widehat{\vec{J}}$ in accordance with equations (3.46). The classical effective Hamiltonian reads $H_{CE2} = \lim_{j\to\infty} \widehat{G}_{E2}/j$,

$$\boxed{H_{CE2} = \frac{\kappa}{2}Z^2 + pX + \frac{\kappa p^2}{24}\left(Y^2 - Z^2\right)}. \tag{3.56}$$

If we consider the evolution generated by the Hamiltonian H_{CE2}, we find that the Hamiltonian H_{CE2} is itself a constant of motion (which could be proved using (B.7)). The trajectories governed by H_{CE2} on the surface of the Bloch sphere are contours of constant H_{CE2}. Such contours are plotted in figure 3.5. The critical points (local maxima, minima and saddle points) for function (3.56) are discussed in appendix C.

For the parameters $\kappa = 1.0, p = 0.5$ we get one minimum in

$$\vec{R}_m = (-1, 0, 0)^T, \tag{3.57}$$
$$H_{CE2}\left(\vec{R}_m\right) = -p, \tag{3.58}$$

one saddle point in

$$\vec{R}_s = (1, 0, 0)^T, \tag{3.59}$$
$$H_{CE2}\left(\vec{R}_s\right) = p \tag{3.60}$$

and two maxima (case II) b) in appendix C)

$$\vec{R}_{M1,2} = \left(\frac{24}{47}, 0, \pm\frac{\sqrt{1633}}{47}\right)^T, \tag{3.61}$$
$$\vec{R}_{M1,2} \approx (0.511, 0, \pm 0.860)^T, \tag{3.62}$$
$$H_{CE2}\left(\vec{R}_{M1,2}\right) = \frac{2785}{4512} \approx 0.617. \tag{3.63}$$

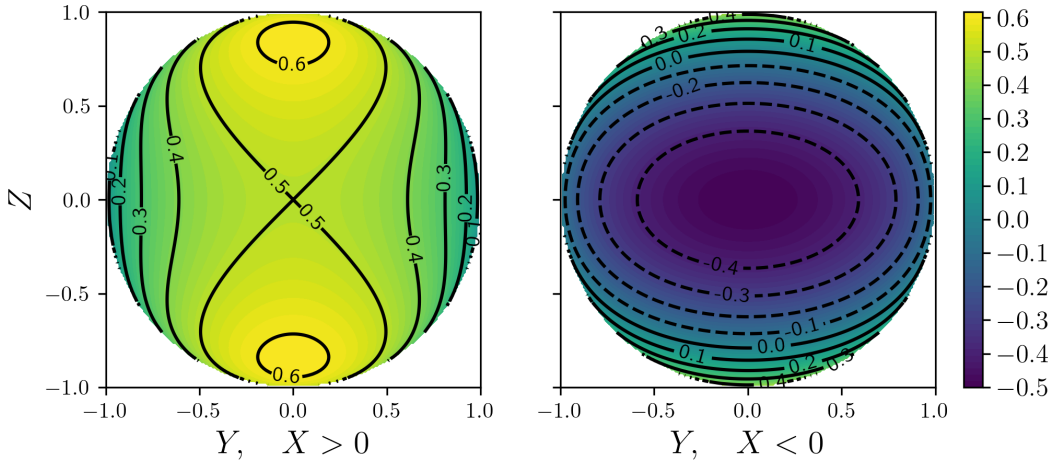

Figure 3.5: Contours for $H_{CE2} = \text{const.}$ as trajectories implied by the Hamiltonian (3.56). Here we use the parameters $\kappa = 1.0, p = 0.5$.

A glance at figures 3.4 and 3.5 tells us that the trajectories governed by (3.56) are significantly different from the precise results for the classical kicked top evolution. The main reason for the qualitative difference between figures 3.4 and 3.5 is that we did not include the action of the unitary transformation $e^{+i\widehat{K}}$ in our effective description. Some discrepancy is of course due to only second-order expansion of the Floquet Hamiltonian.

Trajectories from effective description

The classical effective Hamiltonian (3.56) generates itself some trajectories on the Bloch sphere. These trajectories are identical to the contours depicted in figure 3.5. Before we remedy these trajectories to closer fit their exact counterparts, we present the according equations of motion generated by the classical effective Hamiltonian (3.56)

$$\begin{aligned} \frac{\mathrm{d}X}{\mathrm{d}t} &= \left(-\kappa + \frac{\kappa p^2}{6}\right) YZ, \\ \frac{\mathrm{d}Y}{\mathrm{d}t} &= -pZ + \left(\kappa - \frac{\kappa p^2}{12}\right) XZ, \\ \frac{\mathrm{d}Z}{\mathrm{d}t} &= pY - \frac{\kappa p^2}{12} XY. \end{aligned} \tag{3.64}$$

The aforementioned equations of motion could be derived using equation (B.7).

In order to find the classical counterpart of quantum evolution, we return our focus to equation (2.45). The evolution using equation (2.45) is depicted in figure 3.6. We could conceive the evolution from the time t_1 and state $|\psi(t_1)\rangle$ to the time t_2 as a series of transformations done by unitary operators as follows

$$|\psi(t_1)\rangle \xrightarrow{e^{i\widehat{K}}} e^{i\widehat{K}} |\psi(t_1)\rangle \xrightarrow{e^{-i\widehat{G}(t_2-t_1)}} e^{-i\widehat{G}(t_2-t_1)} e^{i\widehat{K}} |\psi(t_1)\rangle \xrightarrow{e^{-i\widehat{K}}} |\psi(t_2)\rangle\,. \tag{3.65}$$

Now we use the trick—the action of the operator $e^{i\widehat{K}}$ will be in the classical limit changed to the evolution according to the classical limit of an auxiliary time-

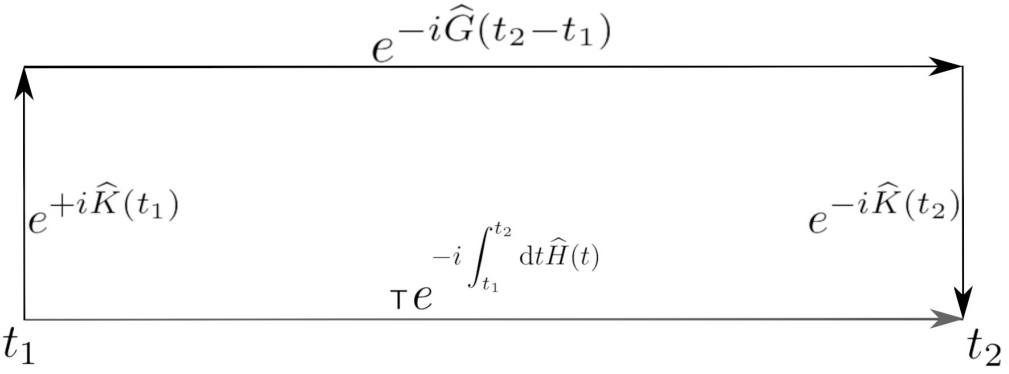

Figure 3.6: A schematic description of the evolution of the state of the system $|\psi(t_1)\rangle$ at the time t_1 to the state of the system $|\psi(t_2)\rangle$ at the time t_2 using equation (2.45). The grey arrow underneath represents a generic way of evolution using time ordering operator T and exponential of time integral of time-dependent Hamiltonian.

independent Hamiltonian for the transformation at the time t. The quantum time independent auxiliary Hamiltonian tied to the time t is

$$\widehat{H}_A[t] \stackrel{\text{def}}{=} -\widehat{K}(t) \tag{3.66}$$

and its classical limit is

$$H_A[t] \stackrel{\text{def}}{=} \lim_{j\to\infty} \frac{\widehat{H}_A[t]}{j}. \tag{3.67}$$

From equation (3.44) and performing the limit (3.67) with substitutions (3.46) we get

$$\boxed{H_A[0^-] = \frac{pX}{2} + \frac{\kappa p}{12} YZ}. \tag{3.68}$$

Having the Hamiltonians H_A and H_{CE2} (3.68, 3.56), we replace the performance of the time-dependent Hamiltonian (3.49)

$$\vec{R}(t_1) \xrightarrow{H(t)} \vec{R}(t_2) \tag{3.69}$$

with the three evolutions implied by the time-independent Hamiltonians

$$\vec{R}(t_1) \xrightarrow[\Delta t=1]{H_A[t_1]} \vec{R}_{A1} \xrightarrow[\Delta t=t_2-t_1]{H_{CE2}} \vec{R}_{A2} \xrightarrow[\Delta t=1]{-H_A[t_2]} \vec{R}(t_2). \tag{3.70}$$

Since we need only the vectors $\vec{R}(t)$ at the times

$$t = n \cdot T, n \in \mathbb{Z}, \tag{3.71}$$

it suffices to know the auxiliary Hamiltonian only at the time $t = 0^-$. Note that the auxiliary Hamiltonian $H_A[t]$ is periodic in t with the period[4] T. Note that even

[4]We use the variable T for instructiveness but we still conceive $T = 1$.

though the auxiliary Hamiltonian $H_A[t]$ is a function of time, once it is considered a Hamiltonian, it represents a time-*independent* Hamiltonian. Evolution dictated by the auxiliary Hamiltonian $H_A[0^-]$ (3.68) is determined by the equations

$$\begin{aligned}\frac{\mathrm{d}X}{\mathrm{d}t} &= \frac{\kappa p}{12}\left(-Y^2+Z^2\right),\\ \frac{\mathrm{d}Y}{\mathrm{d}t} &= -\frac{p}{2}Z+\frac{\kappa p}{12}XY,\\ \frac{\mathrm{d}Z}{\mathrm{d}t} &= \frac{p}{2}Y-\frac{\kappa p}{12}XZ\end{aligned} \tag{3.72}$$

easily derived by relation (B.7). The equations of evolution for the Hamiltonian $-H_A[T] = -H_A[0^-]$ are equations (3.72) with the right hand sides multiplied by the factor (-1).

Having equations (3.64, 3.72), we could perform the evolution of the initial state $\vec{R}_0$ by scheme (3.70). The according evolutions using effective description just described and precise evolutions (by equations (3.50, 3.51)) are depicted and compared in figures 3.7 and 3.8. For sufficiently small parameters (κ, p) we get a good agreement between the effective and the precise description. The integration of equations (3.64, 3.72) was done using the Python function `odeint` from the package `scipy.integrate`.

Similar curves are discussed in paper [5], but the effect of the kick operator was not taken into account in the paper. The kick operator (3.44) presented in [5] does not include the term reflecting the discontinuity of (3.42) and instead of taking the limit (3.29), the discontinuous term is considered to be zero.

3.2.5 Wigner function & classical effective description

The classical effective stroboscopic plots—the red curves in figures 3.7 and 3.8—have a character of integrable trajectories. This regular character is preserved even in the areas where the precise classical evolution is chaotic, e.g. in the lower plots in figure 3.8. We try to show that the effective trajectories can tell us something in addition to the information yield from the chaotic precise trajectories.

In paper [26] the effect of chaotic structure on the classical, quantum and semiclassical evolution was discussed. The use of effective trajectories instead of precise chaotic ones was proved useful in the subsequent paper [27], where the standard BCH formula was used for the construction of an effective Hamiltonian. In the paper [27] the semiclassical evolution based on classical effective trajectories and the semiclassical evolution based on precise classical trajectories were compared. The papers [26, 27] use the system in phase space of position and momentum and the Hamiltonian of the form (2.144), where the constant term is a free one spinless particle Hamiltonian and the sum of delta functions is multiplied by purely potential term.

In this subsection, we compare the quantum evolution, the classical precise evolution and classical effective stroboscopic plots for the kicked top system. We visualize the quantum states by the angular momentum Wigner distribution described in appendix D. The Wigner distribution was computed using the already

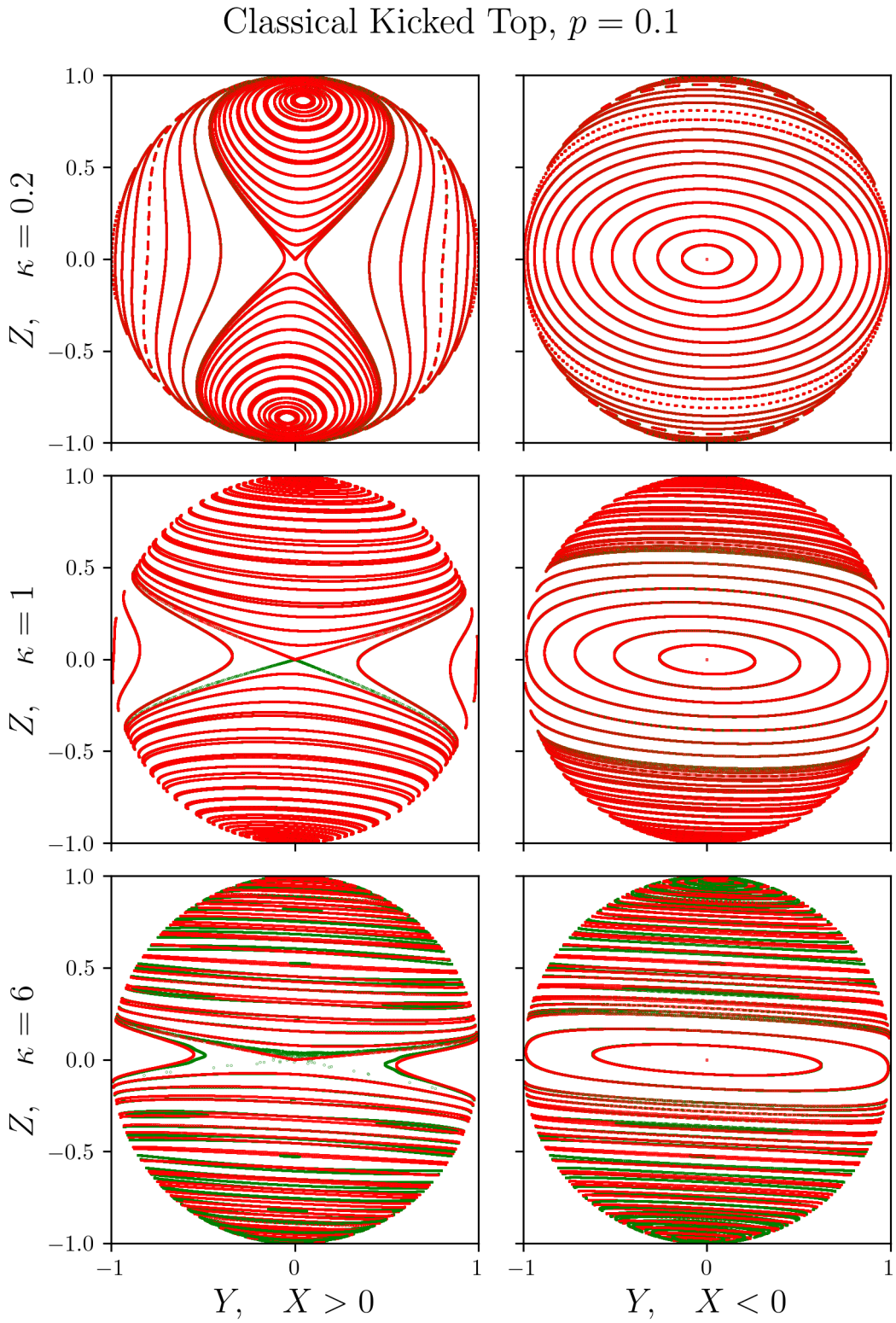

Figure 3.7: A stroboscopic plot of the classical evolution of the kicked top system for the parameter $p = 1$ and various parameters $\kappa \in \{0.2, 1, 6\}$. The precise evolution using equations (3.50, 3.51) is in green. The effective evolution using equations (3.64, 3.72) is in red.

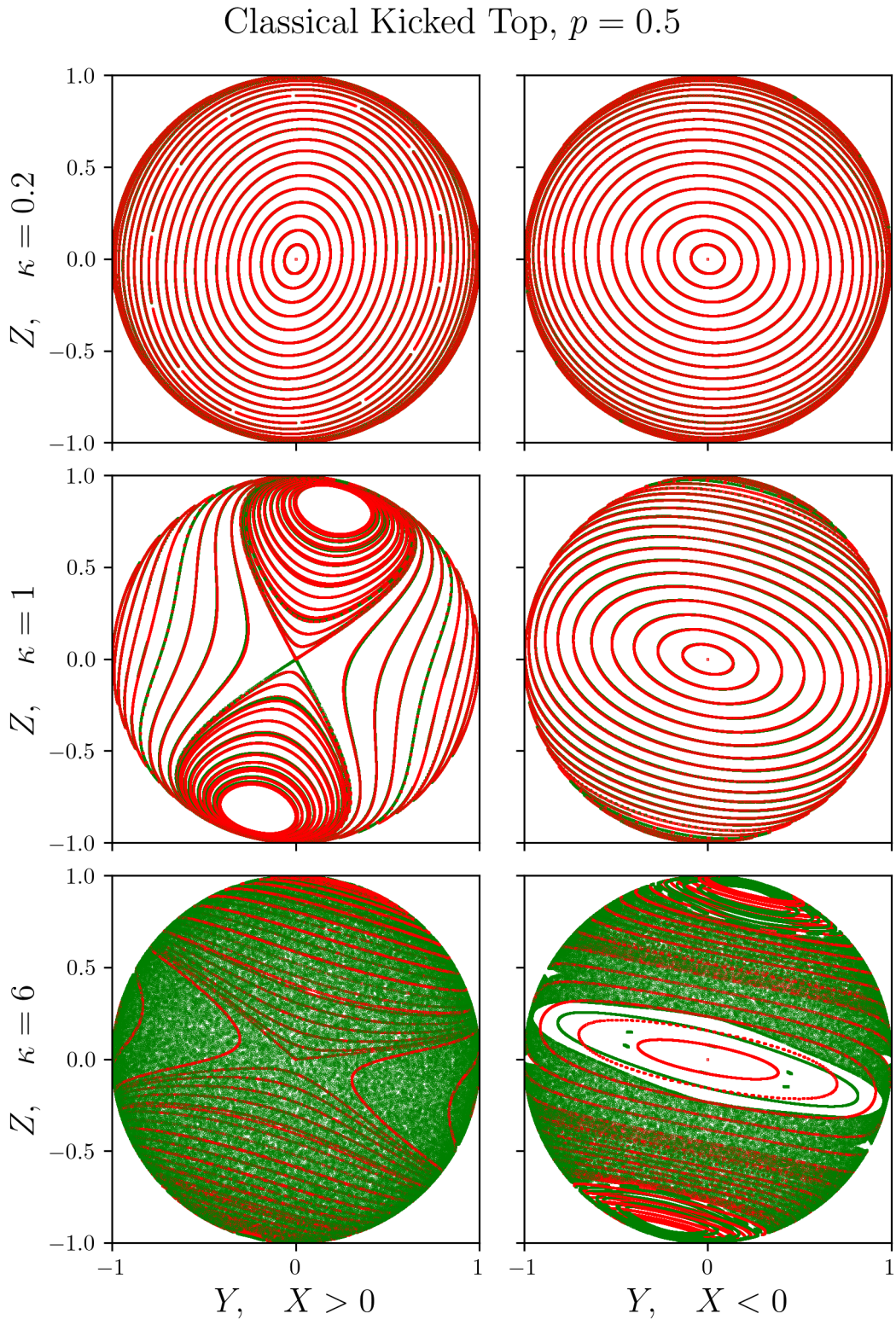

Figure 3.8: A stroboscopic plot of the classical evolution of the kicked top system for the parameter $p = 0.5$ and various parameters $\kappa \in \{0.2, 1, 6\}$. The precise evolution using equations (3.50, 3.51) is in green. The effective evolution using equations (3.64, 3.72) is in red.

existing code[5] from the package `QuantumOptics` of the programming language Julia [29]. We were also inspired by web page [28] where the use of the package `QuantumOptics` was discussed in connection with the kicked top system.

Regular case

We begin with an example where the evolution is regular and the effective stroboscopic trajectories do not significantly differ from the precise ones. We consider the example of regular (not chaotic) evolution plotted in the upper plots in figure 3.7, i.e. the kicked top system with the parameters $\kappa = 0.2, p = 0.1$. Since the effective stroboscopic trajectories do not significantly differ from the precise ones, we compare the evolution of the quantum case with the precise stroboscopic classical trajectories. We use the quantum system with the quantum number $j = 5$. The quantum states are represented by the angular momentum Wigner distribution described in appendix D, which is suitable for a system with a quasispin. The Wigner distributions for the initial state and the states propagated in time are plotted in figures 3.9 and 3.10. The initial state is the coherent spin state (D.33) centred in the position $\theta = \frac{\pi}{2}$ rad, $\phi = \frac{\pi}{2}$ rad. The coherent spin states are described in appendix D. In figures 3.9 and 3.10 we also plot the stroboscopic plot of the precise classical trajectories, which is placed on the colour contour plots of Wigner distributions for comparison. The right plots of figures 3.9 and 3.10 depict the precise classical evolution of the 79 355 points initially homogeneously distributed in the area where the Wigner distribution is greater than half of its maximum value. This area is characterized by the angular radius $\Delta\theta \approx 0.378$ rad. As we can see, the classical stroboscopic plot (in black) suggests how the initial coherent spin state will evolve.

The lower left plot in figure 3.10 resembles the initial state. This effect we identify as an effect of the Poincaré recurrence [30], the plots representing the times shortly before the time $t = 511$ are in figure D.11 in appendix D.

Chaotic case

For the demonstration of the chaotic case, we chose the parameters $\kappa = 3$ and $p = 0.7$. Figure 3.11 demonstrates that the effective Hamiltonian (3.45) still accurately approximates the quasienergies. The stroboscopic plot of the classical effective (in red) and classical precise (in green) evolution is in figure 3.12. The upper and lower part of the figure represent the same stroboscopic plot but use different ways of visualization of the plot. The red curves of the stroboscopic plots in figure 3.12 are used in figures 3.13 and 3.14 where they are plotted as black solid lines. Figures 3.13 and 3.14 also show the Wigner distribution for the quantum version of the kicked top system with the quantum number $j = 10$. The initial state is the coherent spin state centred in the position $\theta = \frac{\pi}{2}$ rad, $\phi = 0.9$ rad. The right plots in figures 3.13 and 3.14 represent precise classical evolution (in green) on the background of the classical effective stroboscopic plot (in black). For the precise classical evolution (in green) we used 79 847 points initially homogeneously distributed in the area where the Wigner distribution has its value greater than

[5] Although we used the code from [28], we checked its validity using our own code in Python and changed the normalisation of the Wigner function so that it follows the definitions presented in appendix D.

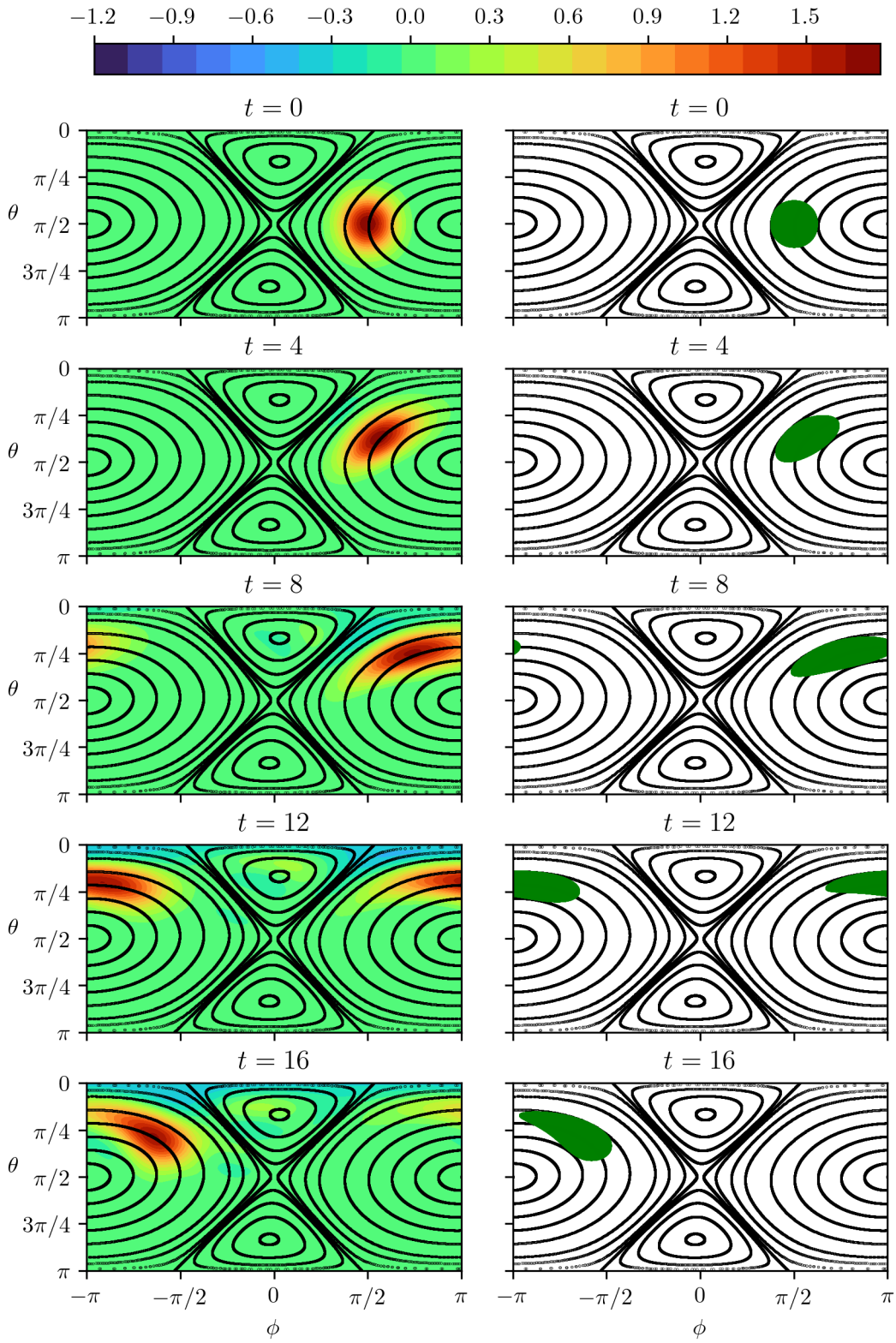

Figure 3.9: The evolution of the kicked top system. The stroboscopic plot of precise classical regular (not chaotic) trajectories is plotted as black solid lines. The precise classical evolution (3.50, 3.51) of the classical points at times t is plotted in green in the right column. The angular momentum Wigner function is plotted as a colour contour plot in the left column. We used the parameters $\kappa = 0.2, p = 0.1, j = 5$.

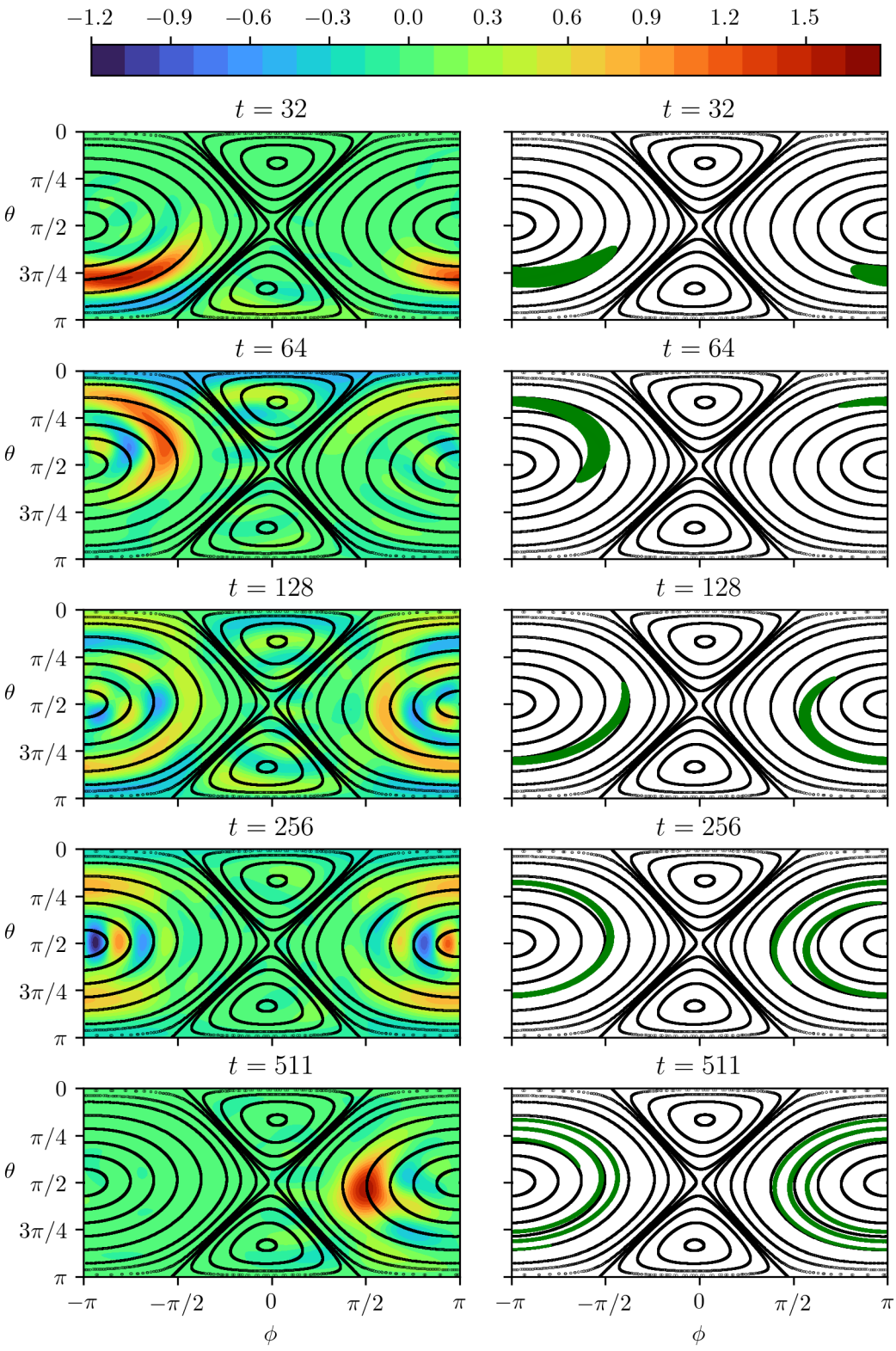

Figure 3.10: A continuation of figure 3.9. At the time $t = 511$ the system gets close to the initial state, i.e. we observe the effect of the Poincaré recurrence.

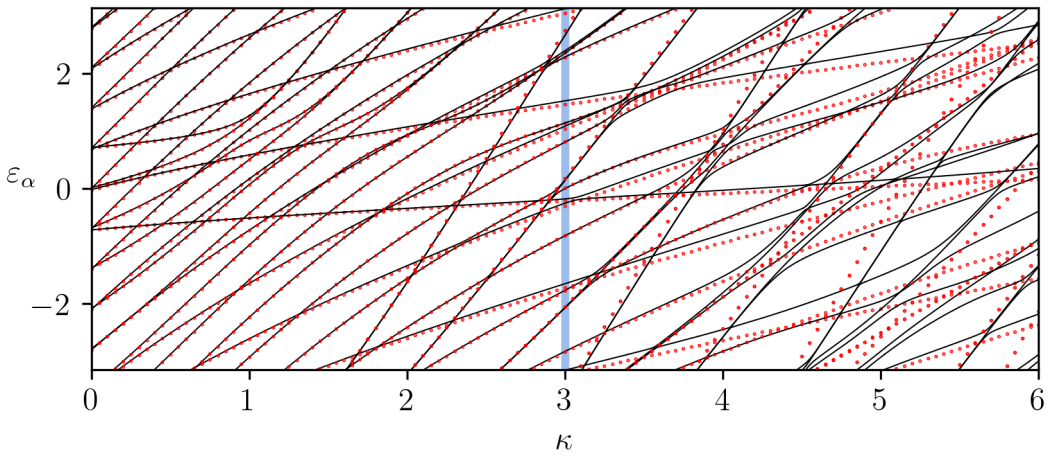

Figure 3.11: The eigenenergies of the second-order effective Hamiltonian (3.45) mapped on the first Brillouin zone are plotted as red dots. For the comparison, the precise quasienergies for the kicked top system (3.15) are plotted as black solid lines. In this figure $p = 0.7, j = 10$. The blue line in the figure represents the value $\kappa = 3$ used in figures 3.12 and 3.13.

half of its maximum. The area has a circular shape with the angular radius $\Delta\theta \approx 0.265$ rad.

Note that both the evolution of the quantum state of the system (colour contours) and the precise classical evolution of the system (in green) at the early stages of evolution evolve approximately in accordance with the classical effective trajectories.

From the lower right plot in figure 3.10, it could seem that the spreading of the classical points in figure 3.10 is similar to the spreading we see in the lower right plot in figure 3.14 (though much slower). The two instances are different since in the case of figure 3.10 the points of the precise evolution stay in the area with borders characterized by black curves. This is illustrated in figure 3.15 where the points for the time $t = 3000$ are plotted.

3.2.6 Kicked top and kicked rotor

Having worked with the kicked top system, it is worth mentioning another similar system manifesting chaotic motion—the kicked rotor [31, 25, 24].

Kicked rotor

The kicked rotor system is a simple model widely used for investigating chaos. We could conceive the kicked rotor as a system of a particle confined to a single circular trajectory. The particle thus has the position characterized by an angle $\varphi \in [0, 2\pi)$ and the angular momentum $p \in (-\infty, +\infty)$. In addition, we periodically switch on for infinitesimal duration the homogeneous potential field antiparallel to the x-axis. Such a system is depicted in figure 3.16.

The main characteristic of the kicked rotor system is its Hamiltonian. Its

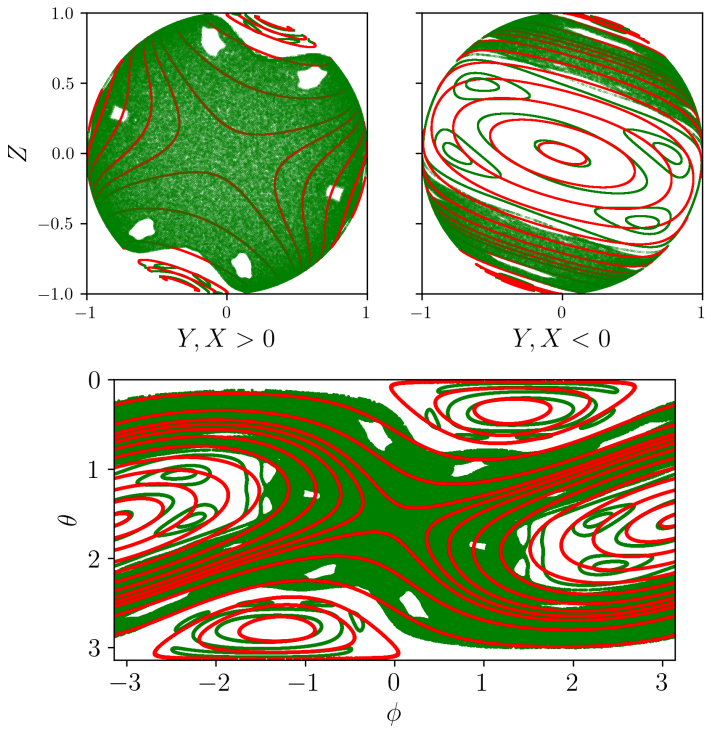

Figure 3.12: A stroboscopic plot of the classical evolution of the kicked top for the parameters $\kappa = 3, p = 0.7$. We show two equivalent visualisations (upper part versus lower part of the figure) of the stroboscopic evolution on the Bloch sphere. The precise evolution using equations (3.50, 3.51) is in green. The effective evolution using equations (3.64, 3.72) is in red.

quantum mechanical form reads

$$\boxed{\widehat{H}_R(t) = \frac{\widehat{p}^2}{2I} + k\cos(\widehat{\varphi}) \sum_{n=-\infty}^{+\infty} \delta(t-n)}, \tag{3.73}$$

where (I, k) are the parameters of the system, $\widehat{p}$ represents angular momentum and $\widehat{\varphi}$ represents an angle assigned to the particle and measured from the x-axis. The following commutation relation holds

$$[\widehat{\varphi}, \widehat{p}] = i\hbar. \tag{3.74}$$

Thus p and φ are canonical variables.

The system is best described stroboscopically. In order to yield such a description let us invoke the Heisenberg picture

$$|\psi_H\rangle \stackrel{\text{def}}{=} |\psi(t_0)\rangle = \text{const.}, \tag{3.75}$$

$$\widehat{A}_H(t) \stackrel{\text{def}}{=} \widehat{U}^\dagger(t, t_0)\widehat{A}\widehat{U}(t, t_0), \tag{3.76}$$

where $\widehat{A}$ is some observable in the Schrödinger picture and $\widehat{A}_H$ is its counterpart in the Heisenberg picture. Let us denote

$$(\widehat{\varphi}_H(n), \widehat{p}_H(n)) \tag{3.77}$$

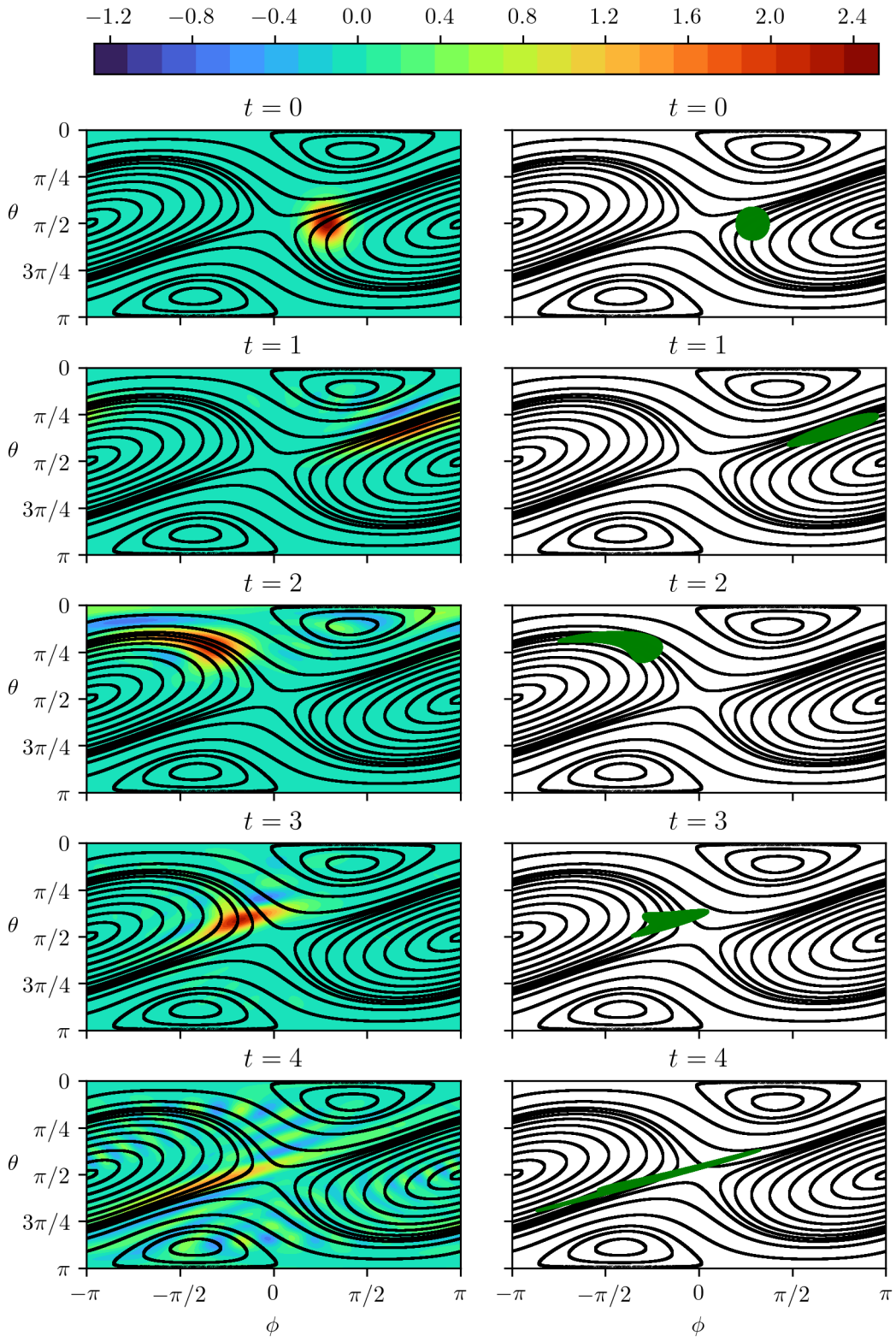

Figure 3.13: The evolution of the kicked top system. The quantum state at the time t is represented by the angular momentum Wigner distribution—the colour contours of the left plot (more about the distribution in appendix D). The green area in the right plots represents precise evolution using equations (3.50, 3.51). The black solid lines in the background of every plot represent the stroboscopic plot of the effective evolution computed by equations (3.64, 3.72), see figure 3.12. The parameters of the system are $\kappa = 3, p = 0.7, j = 10$.

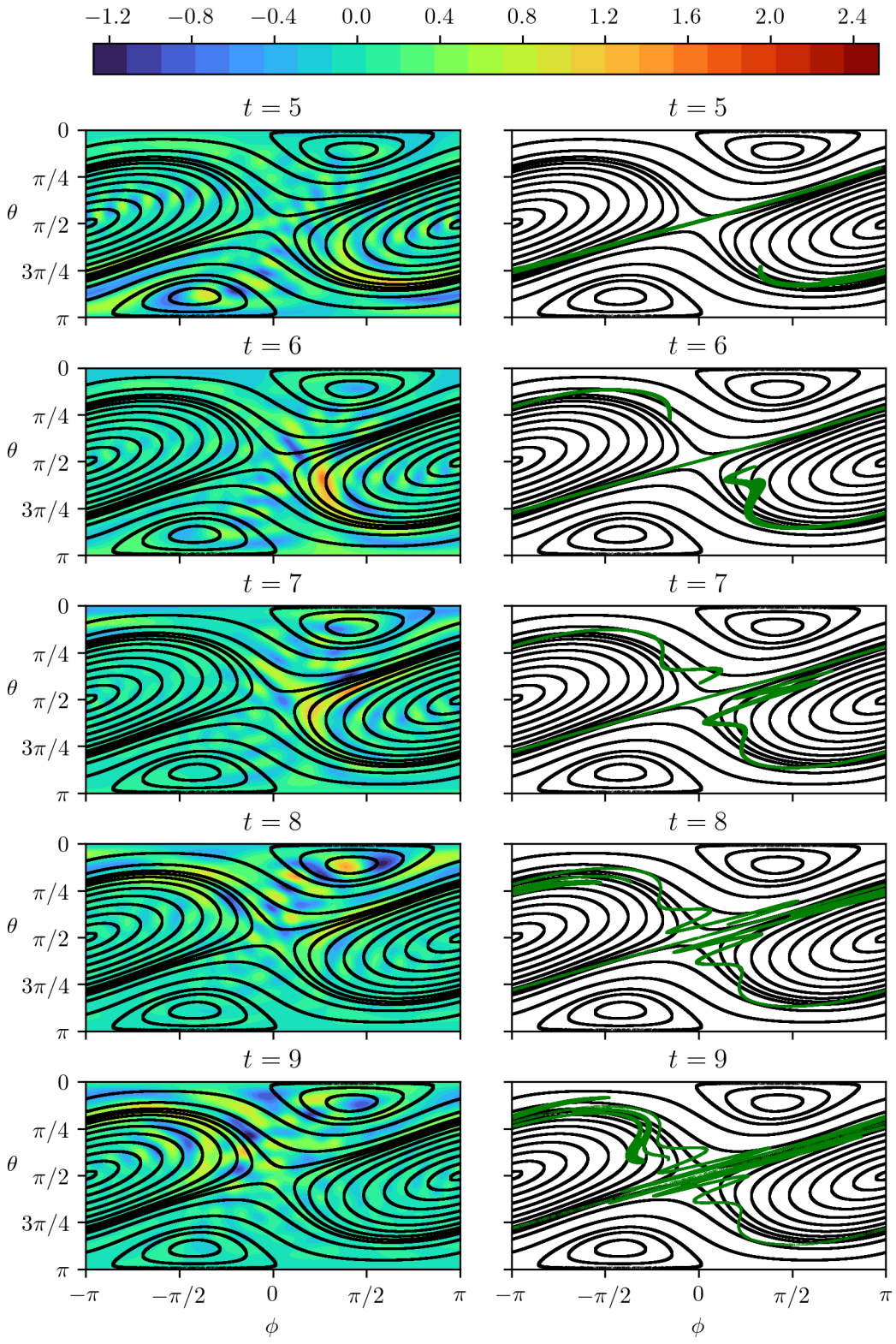

Figure 3.14: A continuation of figure 3.13.

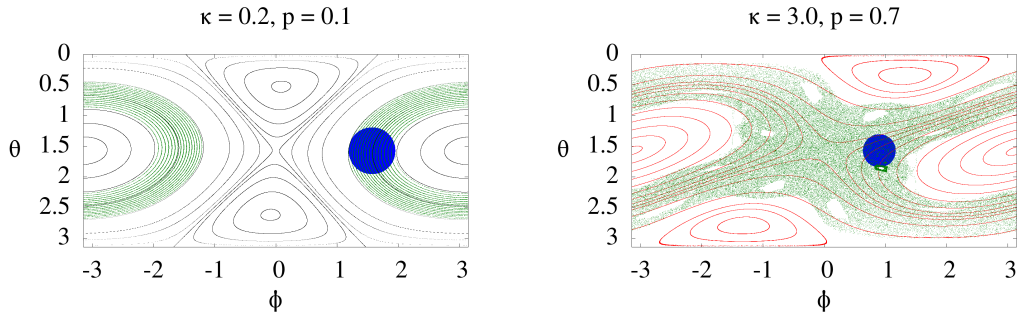

Figure 3.15: The precise classical points from figures 3.9 and 3.13 at the time $t = 3000$ are plotted in green. The initial points at the time $t = 0$ are plotted in blue. The stroboscopic classical precise plot for the case $\kappa = 0.2, p = 0.1$ is plotted in black (left plot). The stroboscopic classical effective plot for the case $\kappa = 3, p = 0.7$ is plotted in red (right plot).

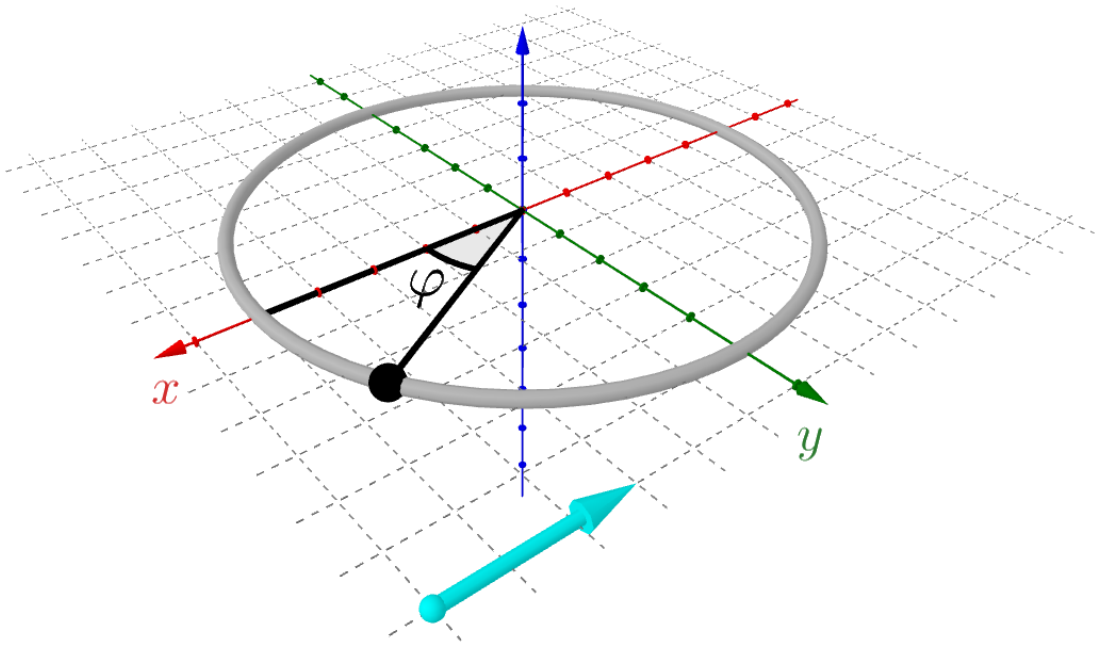

Figure 3.16: Kicked rotor system could be conceived as a particle confined to a circle and propelled by delta pulses of a homogeneous field antiparallel to the x-axis. The direction of the field is indicated by the turquoise arrow in the figure.

the angle and angular momentum operators in the Heisenberg picture right before the nth "kick"—realization of the time delta function. Then the stroboscopic equations for evolution read [25]

$$\widehat{p}_H(n+1) = \widehat{p}_H(n) + k\sin\left(\widehat{\varphi}_H(n)\right), \tag{3.78}$$

$$\widehat{\varphi}_H(n+1) = \widehat{\varphi}_H(n) + \frac{\widehat{p}_H(n+1)}{I}. \tag{3.79}$$

Classical limit and Chirikov standard map

The classical kicked rotor system is described by Hamiltonian (3.73), where we replace the operators with the phase variables without hats. The same process (omitting the hats) done to the stroboscopic equations (3.78, 3.79) yields classical stroboscopic equations for classical evolution [25]. By rescaling the momentum and introducing a new parameter,

$$P = \frac{p}{I}, \tag{3.80}$$

$$K = \frac{k}{I}, \tag{3.81}$$

we get a system described by one parameter K. The map

$$P(n+1) = \mathrm{mod}\left(P(n) + K\sin\left(\varphi(n)\right), 2\pi\right), \tag{3.82}$$

$$\varphi(n+1) = \mathrm{mod}\left(\varphi(n) + P(n+1), 2\pi\right) \tag{3.83}$$

is widely known as the Chirikov standard map [32]. Note that we have taken the space coordinate and momentum pair (φ, P) modulo 2π. The Chirikov standard map is depicted in figure 3.17.

We define the function modulo $\mathrm{mod}(\bullet,\bullet) : \mathbb{R}\times\mathbb{R}^+ \to \mathbb{R}_0^+$ the following way

$$\mathrm{mod}(a,c) = z \Leftrightarrow a\in\mathbb{R}, c\in\mathbb{R}_0^+ \exists! z\in[0,c), k\in\mathbb{Z} : a = k\cdot c + z. \tag{3.84}$$

It is easy to realise

$$\mathrm{mod}(a+b,c) = \mathrm{mod}\left(\mathrm{mod}(a,c)+b,c\right). \tag{3.85}$$

And thus the classical stroboscopic map of the kicked rotor (equation (3.82) without modulo function and equation (3.83)) is a periodic extension of the Chirikov standard map in the p (or P) phase variable.

Classical kicked rotor as limit of kicked top

The kicked top and kicked rotor systems are two different systems differing in their properties. Both are useful when studying classical and quantum chaos. The obvious difference is the topology of the phase spaces. The phase space of kicked rotor is an infinitely long cylinder with canonical phase variables φ and p. When it comes to quantum kicked top, introducing new operators $\widehat{\phi}$ and $\widehat{p}$ in the following way

$$\widehat{J}_x = \sqrt{j(j+1) - \widehat{\mathcal{P}}^2}\cdot\cos\widehat{\phi}, \tag{3.86}$$

$$\widehat{J}_y = \sqrt{j(j+1) - \widehat{\mathcal{P}}^2}\cdot\sin\widehat{\phi}, \tag{3.87}$$

$$\widehat{J}_z = \widehat{\mathcal{P}}, \tag{3.88}$$

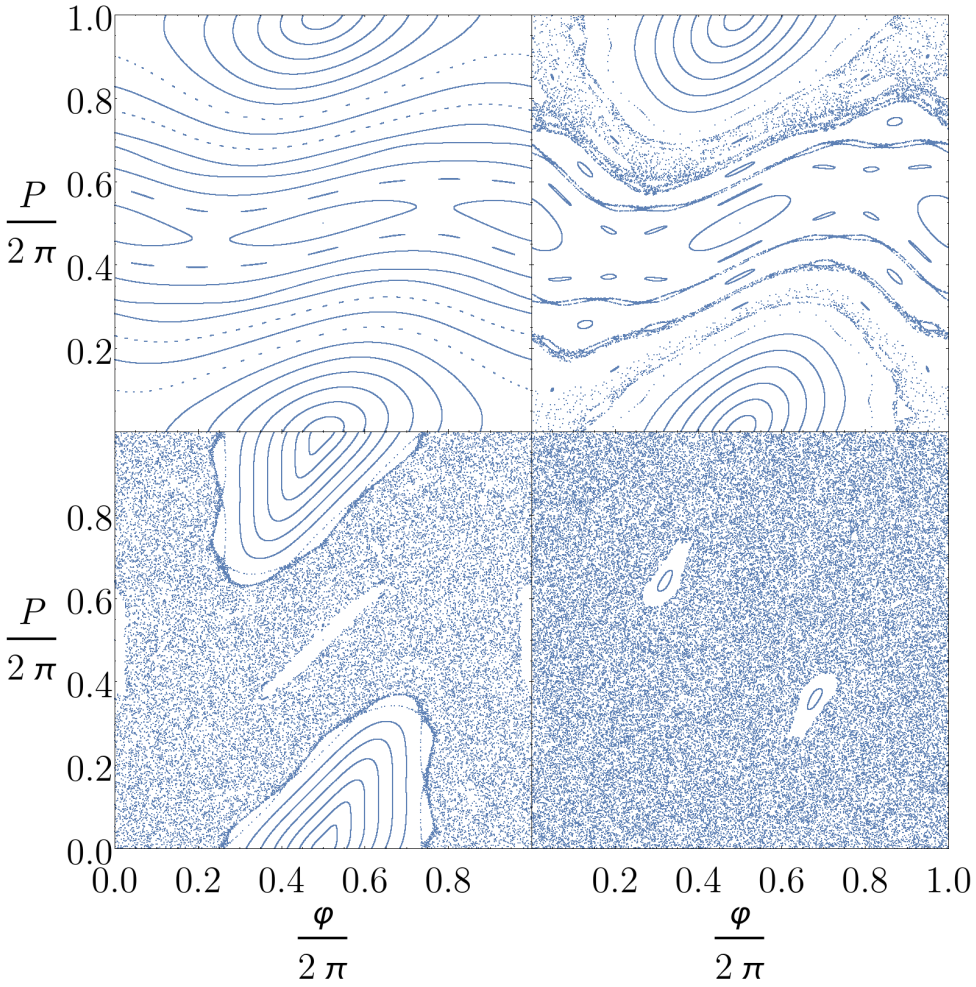

Figure 3.17: The Chirikov standard map for the four parameters $K = 0.5$—upper left, $K = 1$—upper right, $K = 2$—down left, $K = 5$—down right.

yields commutation relation [22, 25]

$$\left[\widehat{\phi}, \widehat{\mathcal{P}}\right] = i\widehat{I}, \tag{3.89}$$

where $\widehat{I}$ is an identity operator. Thus the variables ϕ, $\mathcal{P}$ are canonical phase variables and the phase space of the kicked top has the topology of a sphere.

We already did the classical limit of the kicked top in section 3.2.3. Now we would like to emphasise that the classical limit in section 3.2.3 is not a unique way of performing such a limit. But it is the way one would likely prefer. One reason for such a limit, where the parameters (κ, p) are kept constant, is that the thresholds for regularity–chaos transition are characterized by the parameters (κ, p) of the order of one.

In this section, we perform the classical limit of the quantum kicked top system in such a way that we arrive at the classical kicked rotor system. An intuitive way of doing it is to restrict the evolution of the kicked top system to a narrow equatorial waist band of the Bloch sphere. This equatorial waist band is then

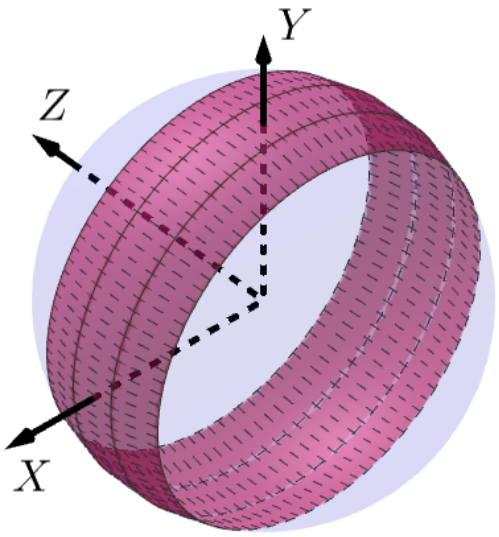

Figure 3.18: The Bloch sphere—the phase space of the kicked top system. The equatorial waist band considered when taking the classical limit is coloured in red. When the limit is applied the kicked top transforms into the kicked rotor.

identified with part of the infinitely long cylinder—the phase space of the kicked rotor system. Figure 3.18 illustrates the idea of the narrow equatorial waist band.

Now we present the technicalities of the limit. As j infinitely grows we rescale the parameters of the quantum kicked top in the following way

$$\kappa = \frac{j}{I'}, \tag{3.90}$$

$$p = \frac{k'}{j}, \tag{3.91}$$

where we introduced the new parameters (I', k') which are kept constant when performing the limit. And we describe the quantum kicked top Hamiltonian by the observables $\widehat{\phi}$ and $\widehat{\mathcal{P}}$, which were introduced by equations (3.86, 3.87, 3.88). The classical Hamiltonian after the limit is defined by

$$H_{\mathrm{CTR}} = \lim_{j\to\infty} \widehat{H}, \tag{3.92}$$

where $\widehat{H}$ is the kicked top Hamiltonian (3.15). We do not divide the quantum kicked top Hamiltonian by the quantum number j when doing the limit. The reason for not doing that is easily checked by transcribing the according equations with $\hbar$ which is throughout this thesis considered equal to one.

Since

$$\lim_{j\to\infty} \frac{\kappa}{2j} \widehat{J}_z^2 = \lim_{j\to\infty} \frac{1}{2I'} \widehat{\mathcal{P}}^2 = \frac{1}{2I'} \mathcal{P}^2 \tag{3.93}$$

and

$$\lim_{j\to\infty} p\widehat{J}_x = \lim_{j\to\infty} \frac{k'}{j} \widehat{J}_x = \lim_{j\to\infty} k' \sqrt{\frac{j(j+1)}{j^2} - \frac{\widehat{\mathcal{P}}^2}{j^2}} \cos\widehat{\phi} = k' \cos\phi, \tag{3.94}$$

the classical Hamiltonian yielded by the limit is

$$H_{\mathrm{CTR}} = \frac{1}{2I'}\mathcal{P}^2 + k'\cos\phi \sum_{n=-\infty}^{+\infty} \delta(t-n). \tag{3.95}$$

We get the same classical Hamiltonian as the classical Hamiltonian for the kicked rotor—equation (3.73) with observables turned into the classical variables by the omission of heads. After the classical limit of the quantum kicked top, we get the classical kicked rotor. This illustrates the non-uniqueness of quantization. So in some sense, we could consider the kicked top to be a quantized classical kicked rotor. But what we normally call the quantum kick rotor is different from the quantum kicked top. Note that there is principally no reason for the introduction of the operator

$$\sqrt{\frac{j(j+1)}{j^2} - \frac{\widehat{\mathcal{P}}^2}{j^2}} \tag{3.96}$$

that is equal to number one when the classical limit is done.

Quantum kicked rotor as semiclassical limit of kicked top

The quantum kicked rotor is described by its Hamiltonian (3.73) and by the range of its canonical phase variables, i.e. $\varphi \in [0, 2\pi)$ and $p \in (-\infty, +\infty)$. Thus, it is natural to impose the condition for wave functions[6] $\psi(\varphi) = \psi(\varphi + 2\pi)$. And it is also natural to introduce the following basis

$$\langle\varphi|m\rangle = \frac{1}{\sqrt{2\pi}} e^{i\varphi m}, m \in \mathbb{Z}. \tag{3.97}$$

The scalar product is

$$(\psi_1, \psi_2) = \int_0^{2\pi} \psi_1^*(\varphi)\psi_2(\varphi)\mathrm{d}\varphi. \tag{3.98}$$

It is easy to realise the following equalities hold

$$\widehat{p}\,|m\rangle = m\,|m\rangle\,, m \in \mathbb{Z}, \tag{3.99}$$

$$\widehat{\varphi}\,|\varphi\rangle = \varphi\,|\varphi\rangle\,, \varphi \in [0, 2\pi), \tag{3.100}$$

$$|\varphi\rangle = \frac{1}{\sqrt{2\pi}} \sum_{n=-\infty}^{+\infty} e^{-i\varphi n}\,|n\rangle\,, \tag{3.101}$$

$$|m\rangle = \frac{1}{\sqrt{2\pi}} \int_0^{2\pi} \mathrm{d}\varphi e^{i\varphi m}\,|\varphi\rangle\,. \tag{3.102}$$

Now we perform a semiclassical limit of the kicked top and show that we get the quantum kicked rotor system described above. We follow the procedure presented in [31].

Since equation (2.61) holds, the only important evolution operators are

$$\widehat{U}(t, 0^-) \tag{3.103}$$

[6] If we seek the quantum version of the Chirikov standard map, we may arrive at Hamiltonian (3.73), but $(\varphi, p) \in \mathbb{R}^2$. Then the quantum kicked rotor is characterized by the solutions for the quantum Chirikov standard map with quasimomentum $k = 0$ from Bloch's theorem (2.11).

for $t \in (0,1) \cup \{0^+\}$, where 0^- signifies that the initial time is right before the kick—realisation of the time delta function. The sign 0^+ signifies the time right after the kick.

For the quantum kicked rotor system the evolution operator reads

$$\begin{aligned} \widehat{U}_R(t,0^-) &= e^{-i\widehat{p}^2 t/(2I)} e^{-ik\cos(\widehat{\varphi})}, t \in (0,2\pi) && (3.104)\\ \widehat{U}_R(0^+,0^-) &= e^{-ik\cos(\widehat{\varphi})}, && (3.105)\\ \widehat{U}_R(0^-,0^-) &\equiv \widehat{I}, && (3.106) \end{aligned}$$

where $\widehat{I}$ is an identity operator.

For the quantum kicked top system the evolution operator, in new variables (3.90, 3.91), reads

$$\begin{aligned} \widehat{U}_T(t,0^-) &= e^{-i\widehat{\mathcal{P}}^2 t/(2I')} e^{-ik'\widehat{X}}, t \in (0,2\pi) && (3.107)\\ \widehat{U}_T(0^+,0^-) &= e^{-ik'\widehat{X}}, && (3.108)\\ \widehat{U}_T(0^-,0^-) &\equiv \widehat{I}. && (3.109) \end{aligned}$$

In the semi-classical limit we use rescaled variables

$$\begin{aligned} \widehat{X} &= \frac{\widehat{J}_x}{j}, && (3.110)\\ \widehat{Y} &= \frac{\widehat{J}_y}{j}, && (3.111)\\ \widehat{\mathcal{P}} &= \widehat{J}_z. && (3.112) \end{aligned}$$

The kicked top system is described by two quantum numbers j and m. It holds

$$\widehat{\mathcal{P}}\,|j,m\rangle = m\,|j,m\rangle\,, m \in \{-j,-j+1,...,0,1,...,j-1,j\}. \tag{3.113}$$

It is easily seen that when we perform the semi-classical limit

$$\frac{m}{j} \to 0 \tag{3.114}$$

the matrix elements of $\widehat{p}$ for the kicked rotor (3.99) and of $\widehat{\mathcal{P}}$ for the kicked top (3.113) become identical. What we want to show now is that the matrix elements of $\cos\widehat{\varphi}$ and $\widehat{X}$ become identical when we perform the semi-classical limit (3.114).

It is common formalism in quantum mechanics to introduce the operators $\widehat{J}_\pm$ (3.9). And it is a quite known result that

$$\widehat{J}_\pm\,|j,m\rangle = \sqrt{(j\mp m)(j\pm m+1)}\,|j,m\pm 1\rangle\,. \tag{3.115}$$

Since $\widehat{J}_x = (\widehat{J}_+ + \widehat{J}_-)/2$, we get the matrix elements

$$\langle m|\widehat{X}|n\rangle = \frac{1}{2j}\left[\sqrt{(j-n)(j+n+1)}\delta_{m,n+1} + \sqrt{(j+n)(j-n+1)}\delta_{m,n-1}\right]. \tag{3.116}$$

Now let us find the matrix elements of $\cos(\widehat{\varphi})$:

$$\langle m|\cos(\widehat{\varphi})|n\rangle = \int_0^{2\pi}\int_0^{2\pi} \mathrm{d}\varphi\mathrm{d}\varphi' \langle m|\varphi\rangle \langle\varphi|\cos(\widehat{\varphi})|\varphi'\rangle \langle\varphi'|n\rangle . \tag{3.117}$$

Expressing

$$\langle\varphi|\cos(\widehat{\varphi})|\varphi'\rangle = \frac{1}{2}\delta(\varphi-\varphi')\left(e^{i\varphi}+e^{-i\varphi}\right) \tag{3.118}$$

and using (3.97), we get

$$2\langle m|\cos(\widehat{\varphi})|n\rangle = \int_0^{2\pi}\mathrm{d}\varphi e^{i(n-m+1)\varphi} + \int_0^{2\pi}\mathrm{d}\varphi e^{i(n-m-1)\varphi}, \tag{3.119}$$

$$\langle m|\cos(\widehat{\varphi})|n\rangle = \frac{1}{2}\left(\delta_{m,n+1}+\delta_{m,n-1}\right). \tag{3.120}$$

Doing the semi-classical limit (3.114) of the kicked top, the right hand sides of equations (3.116) and (3.120) become identical. Thus this semi-classical limit of the kicked top yields the quantum kicked rotor.

3.3 Harmonically-driven Lipkin model I

Now we consider the Hamiltonian

$$\boxed{\widehat{H}(t) = \frac{\kappa}{2j}\widehat{J}_z^2\cos(2\pi t) + p\widehat{J}_x}. \tag{3.121}$$

The Hamiltonian above is the Hamiltonian of the Lipkin model (3.1) where we multiplied the "interaction" term $\frac{\kappa}{2j}\widehat{J}_z^2$ by the function $\cos(2\pi t)$ so in this sense we consider a "harmonically-driven Lipkin model". In the following, we seek effective Hamiltonians of this model. We present two methods. Both of the methods successfully approximate quasienergies for low values of the parameters κ, p and consequently provide effective Hamiltonians that work well for these parameters.

3.3.1 Numerical integration of Schrödinger equation

In the following subsections, we construct the effective Hamiltonians. Its eigenvalues approximate quasienergies. For comparison, we compute the quasienergies by numerical integration of the equation

$$i\frac{\partial}{\partial t}\widehat{U}(t,0) = \widehat{H}(t)\widehat{U}(t,0), \widehat{U}(0,0) = \widehat{I}, \tag{3.122}$$

which yields the Floquet operator $\widehat{\mathcal{F}}[0] = \widehat{U}(1,0)$.

Having computed the Floquet operator, we get quasienergies from the complex arguments (multiplied by minus one) of the eigenvalues of the Floquet operator $\widehat{\mathcal{F}}[0] = \widehat{U}(1,0)$. The quasienergies computed this way[7] are plotted in figures 3.19 and 3.20.

[7]For the numerical integration, we used the Python package `scipy.integrate` and from there we chose the interface `ode` in which we chose the integrator `'zvode'` with the parameters `method = 'bdf', rtol = 10**(-5)`.

3.3.2 Use of interaction picture

Here we describe the method that uses the interaction picture and some approximations. This procedure is presented in paper [8].

We define

$$\widehat{U}_0(t) \stackrel{\text{def}}{=} e^{-i\frac{\kappa\sin(2\pi t)}{4\pi j}\widehat{J}_z^2}. \tag{3.123}$$

We also define the operator $\widehat{U}_I(t)$. It is such an operator that the following equation holds

$$\widehat{U}(t,0) = \widehat{U}_0(t)\widehat{U}_I(t), \tag{3.124}$$

where $\widehat{U}(t,0)$ is the standard evolution operator in the Schrödinger picture.

We express the following term

$$\begin{aligned}
i\frac{\partial\widehat{U}_I(t)}{\partial t} &= -\frac{\kappa\cos(2\pi t)}{2j}\widehat{J}_z^2\widehat{U}_0^\dagger(t)\widehat{U}(t,0) + \widehat{U}_0^\dagger(t)\left(i\frac{\partial\widehat{U}(t,0)}{\partial t}\right) && (3.125)\\
&= \widehat{U}_0^\dagger(t)\left[-\frac{\kappa\cos(2\pi t)}{2j}\widehat{J}_z^2\right]\widehat{U}(t,0) + \widehat{U}_0^\dagger(t)\widehat{H}(t)\widehat{U}(t,0) && (3.126)\\
&\stackrel{(3.121)}{=} \widehat{U}_0^\dagger(t)\left(p\widehat{J}_x\right)\widehat{U}_0(t)\widehat{U}_I(t). && (3.127)
\end{aligned}$$

The solution to differential equation (3.127) could be found in an analogous way we solve the ordinary time-dependent Schrödinger equation using the time ordering operator T, i.e.

$$\widehat{U}_I(t) = \mathsf{T}e^{-ip\int_0^t \widehat{U}_0^\dagger(t)\widehat{J}_x\widehat{U}_0(t)\mathrm{d}t}. \tag{3.128}$$

From the equalities (A.45, A.47), devised in appendix A, or from known properties of quasispin operators we get

$$\begin{aligned}
\widehat{J}_z^2\widehat{J}_+ &= \widehat{J}_+\left(\widehat{I} + 2\widehat{J}_z + \widehat{J}_z^2\right), && (3.129)\\
\widehat{J}_-\widehat{J}_z^2 &= \left(\widehat{I} + 2\widehat{J}_z + \widehat{J}_z^2\right)\widehat{J}_-, && (3.130)\\
\widehat{U}_0^\dagger(t)\widehat{J}_+\widehat{U}_0(t) &\stackrel{(3.129)}{=} \widehat{J}_+ e^{+i\frac{\kappa\sin(2\pi t)}{4\pi j}(\widehat{I}+2\widehat{J}_z)}e^{+i\frac{\kappa\sin(2\pi t)}{4\pi j}\widehat{J}_z^2}\widehat{U}_0(t) && (3.131)\\
&= \widehat{J}_+ e^{+i\frac{\kappa\sin(2\pi t)}{4\pi j}(\widehat{I}+2\widehat{J}_z)}, && (3.132)\\
\widehat{U}_0^\dagger(t)\widehat{J}_-\widehat{U}_0(t) &\stackrel{(3.130)}{=} \widehat{U}_0^\dagger(t)e^{-i\frac{\kappa\sin(2\pi t)}{4\pi j}\widehat{J}_z^2}e^{-i\frac{\kappa\sin(2\pi t)}{4\pi j}(\widehat{I}+2\widehat{J}_z)}\widehat{J}_- && (3.133)\\
&= e^{-i\frac{\kappa\sin(2\pi t)}{4\pi j}(\widehat{I}+2\widehat{J}_z)}\widehat{J}_-, && (3.134)\\
\widehat{U}_0^\dagger(t)\widehat{J}_x\widehat{U}_0(t) &\stackrel{(3.9)}{=} \frac{1}{2}\widehat{J}_+ e^{+i\frac{\kappa\sin(2\pi t)}{4\pi j}(\widehat{I}+2\widehat{J}_z)} + \text{H.c.} && (3.135)
\end{aligned}$$

Now we express the Floquet operator

$$\widehat{\mathcal{F}}[0] \stackrel{(T=1)}{=} \widehat{U}(1) \stackrel{(3.124)}{=} \widehat{U}_0(1)\widehat{U}_I(1) \stackrel{(3.123)}{=} \widehat{U}_I(1). \tag{3.136}$$

Let us seek the approximation of the stroboscopic Floquet Hamiltonian tied to the initial time $t = 0$. Let us denote the Floquet Hamiltonian $\widehat{G}[0]$. The following relations hold

$$\widehat{\mathcal{F}}[0] = e^{-i\widehat{G}[0]} \approx \widehat{I} - i\widehat{G}[0]. \tag{3.137}$$

For low p we get

$$\widehat{\mathcal{F}}[0] \overset{(3.136)}{=} \widehat{U}_I(1) \overset{(3.128)}{\approx} \widehat{I} - ip\int_0^1 \widehat{U}_0^\dagger(t)\widehat{J}_x\widehat{U}_0(t)\mathrm{d}t \tag{3.138}$$

$$\overset{(3.140)}{\approx} \widehat{I} - ipI_E. \tag{3.139}$$

We define the integral

$$I_E \overset{\text{def}}{=} \int_0^1 \widehat{U}_0^\dagger(t)\widehat{J}_x\widehat{U}_0(t)\mathrm{d}t \tag{3.140}$$

$$\overset{(3.135)}{=} \frac{1}{2}\widehat{J}_+\int_0^1 e^{+i\frac{\kappa\sin(2\pi t)}{4\pi j}(\widehat{I}+2\widehat{J}_z)}\mathrm{d}t + \text{H.c.} \tag{3.141}$$

We transcribe the integral using the Jacobi–Anger identity [33]

$$e^{iz\cos(\tau)} = \sum_{n=-\infty}^{+\infty} i^n e^{in\tau}\mathcal{J}_n(z), \tag{3.142}$$

$$e^{iz\cos(\tau-\pi/2)} = e^{iz\sin(\tau)} = \sum_{n=-\infty}^{+\infty} e^{in\tau}\mathcal{J}_n(z), \tag{3.143}$$

where $\mathcal{J}_n$ are the nth-order Bessel functions, i.e.

$$I_E = \frac{1}{2}\widehat{J}_+\mathcal{J}_0\left[\frac{\kappa}{4\pi j}(\widehat{I}+2\widehat{J}_z)\right] + \text{H.c.} \tag{3.144}$$

Since

$$\widehat{G}[0] \overset{(3.137,\ 3.139)}{\approx} pI_E, \tag{3.145}$$

we have

$$\boxed{\widehat{G}[0] \approx \frac{p}{2}\widehat{J}_+\mathcal{J}_0\left[\frac{\kappa}{4\pi j}(\widehat{I}+2\widehat{J}_z)\right] + \text{H.c.}}, \tag{3.146}$$

where the right hand side of the equation above is the desired expression for the effective Hamiltonian.

Figure 3.19 depicts the quasienergies mapped to the first Brillouin zone for various parameters. In the figure, we compare the quasienergies approximated by the eigenvalues of the effective Hamiltonian above (3.146) with the quasienergies computed by the method described in subsection 3.3.1.

3.3.3 Use of Floquet Hamiltonian and kick operator expansion

Here we apply the method from section 2.3.We transcribe our Hamiltonian (3.121) into the form

$$\widehat{H}(t) = p\widehat{J}_x + \frac{\kappa}{4j}\widehat{J}_z^2\left(e^{2\pi it} + e^{-2\pi it}\right), \tag{3.147}$$

from which we identify (2.2)

$$\widehat{H}_0 + \widehat{V}_0 = p\widehat{J}_x, \tag{3.148}$$

$$\widehat{V}_1 = \widehat{V}_{-1} = \frac{\kappa}{4j}\widehat{J}_z^2. \tag{3.149}$$

From equation $\widehat{G}_0 = \widehat{H}_0 + \widehat{V}_0$ (2.134) we get

$$\widehat{G}_0 = p\widehat{J}_x \tag{3.150}$$

and from equation (2.133) and $\tau \stackrel{\text{def}}{=} \omega t = 2\pi t$ we get

$$\widehat{K}_1(t) = i\left(\widehat{V}_{-1}e^{-2\pi it} - \widehat{V}_1 e^{+2\pi it}\right) \tag{3.151}$$

$$= \frac{\kappa}{2j}\sin(2\pi t)\,\widehat{J}_z^2. \tag{3.152}$$

Equation (2.136) immediately gives

$$\widehat{G}_1 = 0. \tag{3.153}$$

In this case, when $\widehat{V}_1 = \widehat{V}_{-1}$ and the other operators $\widehat{V}_n, n > 1$ are equal to zero, equation (2.138) dictates

$$\widehat{K}_2(t) = -i\left[\widehat{V}_1, \widehat{H}_0 + \widehat{V}_0\right]e^{2\pi it} + i\left[\widehat{H}_0 + \widehat{V}_0, \widehat{V}_{-1}\right]e^{-2\pi it}. \tag{3.154}$$

We compute

$$\left[\widehat{V}_1, \widehat{H}_0 + \widehat{V}_0\right] = \frac{\kappa p}{4j}\left[\widehat{J}_z^2, \widehat{J}_x\right] \tag{3.155}$$

$$= \frac{i\kappa p}{4j}\left(\widehat{J}_y\widehat{J}_z + \widehat{J}_z\widehat{J}_y\right) \tag{3.156}$$

and by the Hermitian conjugation of (3.156) we get

$$\left[\widehat{H}_0 + \widehat{V}_0, \widehat{V}_{-1}\right] = -\frac{i\kappa p}{4j}\left(\widehat{J}_y\widehat{J}_z + \widehat{J}_z\widehat{J}_y\right). \tag{3.157}$$

From equations (3.154, 3.156, 3.157) we get

$$\widehat{K}_2(t) = \frac{\kappa p}{2j}\cos(2\pi t)\left(\widehat{J}_y\widehat{J}_z + \widehat{J}_z\widehat{J}_y\right). \tag{3.158}$$

Considering $\widehat{V}_1 = \widehat{V}_{-1}$, that the operators $\widehat{V}_n, n > 1$ are equal to zero and equation (2.140), we get

$$\widehat{G}_2 = \frac{1}{2}\left[\left[\widehat{V}_1, \widehat{H}_0 + \widehat{V}_0\right], \widehat{V}_{-1}\right] + \frac{1}{2}\left[\left[\widehat{V}_{-1}, \widehat{H}_0 + \widehat{V}_0\right], \widehat{V}_1\right] \tag{3.159}$$

$$= \left[\left[\widehat{V}_1, \widehat{H}_0 + \widehat{V}_0\right], \widehat{V}_1\right] \tag{3.160}$$

$$\stackrel{(3.156)}{=} \frac{ip\kappa^2}{16j^2}\left[\widehat{J}_y\widehat{J}_z + \widehat{J}_z\widehat{J}_y, \widehat{J}_z^2\right] \tag{3.161}$$

$$= -\frac{p\kappa^2}{16j^2}\left(\widehat{J}_x\widehat{J}_z^2 + 2\widehat{J}_z\widehat{J}_x\widehat{J}_z + \widehat{J}_z^2\widehat{J}_x\right). \tag{3.162}$$

Using equations (2.128, 3.150, 3.153, 3.162), we get the second-order expansion of the Floquet Hamiltonian

$$\boxed{\widehat{G} \approx p\widehat{J}_x - \frac{p\kappa^2}{64\pi^2 j^2}\left(\widehat{J}_x\widehat{J}_z^2 + 2\widehat{J}_z\widehat{J}_x\widehat{J}_z + \widehat{J}_z^2\widehat{J}_x\right)}. \tag{3.163}$$

Using equations (2.129, 3.152, 3.158), we get the second-order expansion of the kick operator

$$\boxed{\widehat{K}(t) \approx \frac{\kappa}{4\pi j}\sin(2\pi t)\,\widehat{J}_z^2 + \frac{\kappa p}{8\pi^2 j}\cos(2\pi t)\left(\widehat{J}_y\widehat{J}_z + \widehat{J}_z\widehat{J}_y\right)}. \tag{3.164}$$

The quasienergies approximated by the eigenvalues of the effective Hamiltonian (3.163) are plotted in figure 3.20 (after mapping them to the first Brillouin zone). In the figure, we also include the quasienergies yielded from the numerical integration of the Schrödinger equation (3.122) as described in subsection 3.3.1.

Comparing figures 3.19 and 3.20, we conclude that (in the chosen ranges of parameters) the method in section 3.3.2 yields better results than the method in this section. Note though, that the method in the present section is more universal, which is supported by its usefulness in finding effective Hamiltonians for all models in this chapter.

Note that since the effective Hamiltonians (3.163) and (3.146) are simple, the eigenvalues of the effective Hamiltonians depend linearly on p. The dependencies of the quasienergies approximated by the effective Hamiltonian on the parameter κ in the upper and lower plot in figure 3.20 are consequently related by scaling constant 3. This scaling is obscured by mapping to the first Brillouin zone. A similar scaling is in figure 3.19. Note though, that the method in subsection 3.3.1 does not show such simple dependence.

3.4 Harmonically-driven Lipkin model II

Another choice of harmonic driving is represented by the Hamiltonian

$$\boxed{\widehat{H}(t) = \frac{\kappa}{2j}\widehat{J}_z^2 + p\widehat{J}_x\cos(2\pi t)}. \tag{3.165}$$

We present this model since we want to provide the case where the delta driving, considered in the kicked top system, is substituted by harmonic driving. Also, the term $p\widehat{J}_x$ could represent the potential energy of the spins in some external field, which could be made time-dependent.

Here we construct the effective Hamiltonian by the method yielding a Floquet Hamiltonian and kick operator expansion, described in section 2.3. Using this method for the third time we straightforwardly infer the effective Hamiltonian and the second-order expansion of the kick operator.

From equation (2.2), we get

$$\widehat{H}_0 + \widehat{V}_0 = \frac{\kappa}{2j}\widehat{J}_z^2, \tag{3.166}$$

$$\widehat{V}_1 = \widehat{V}_{-1} = \frac{p\widehat{J}_x}{2}. \tag{3.167}$$

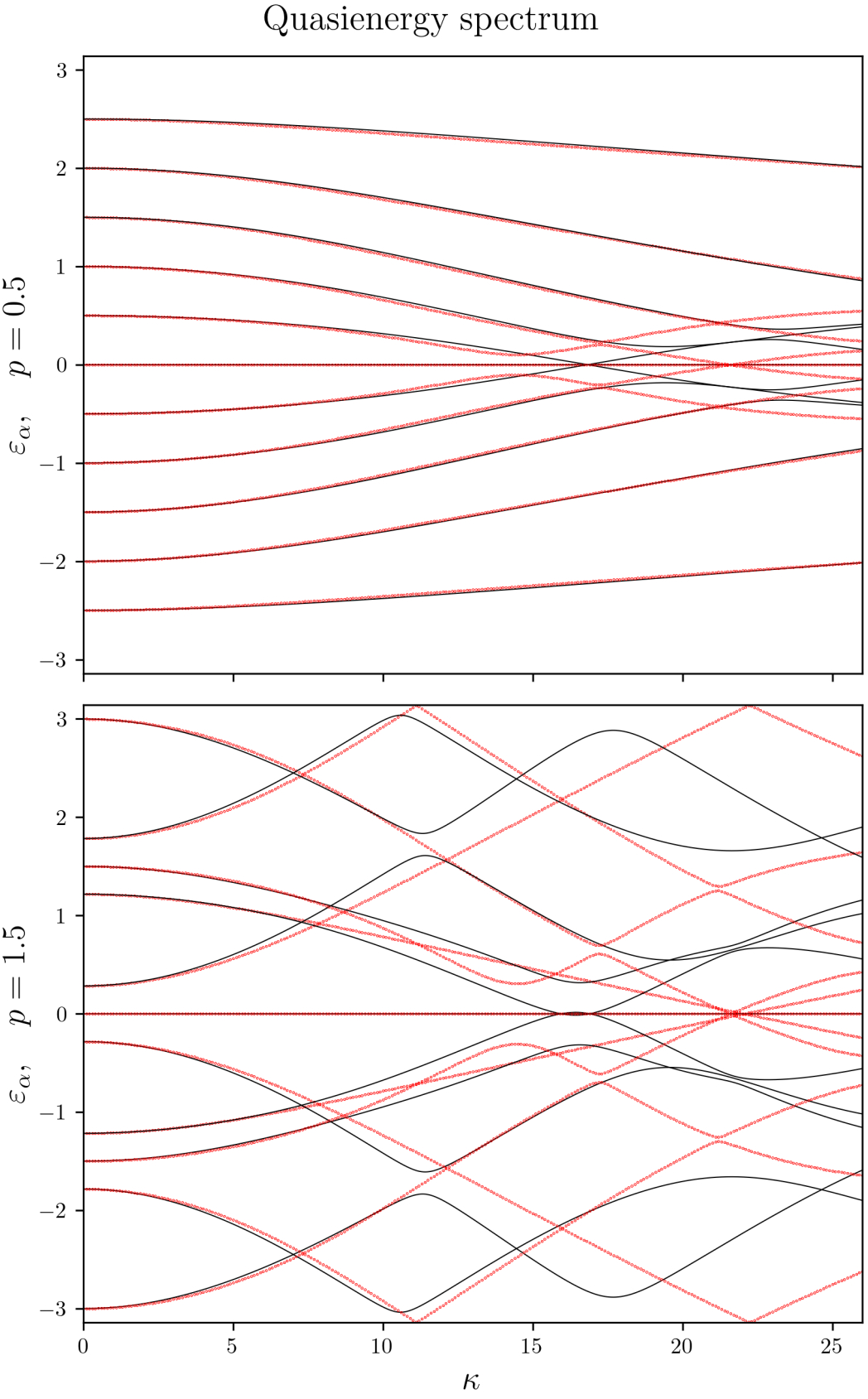

Figure 3.19: The eigenvalues of the effective Hamiltonian (3.146) mapped to the first Brillouin zone are plotted as red dots. The quasienergies obtained by numerically integrating the Schrödinger equation (3.122) are plotted as black lines. In this figure $j = 5$.

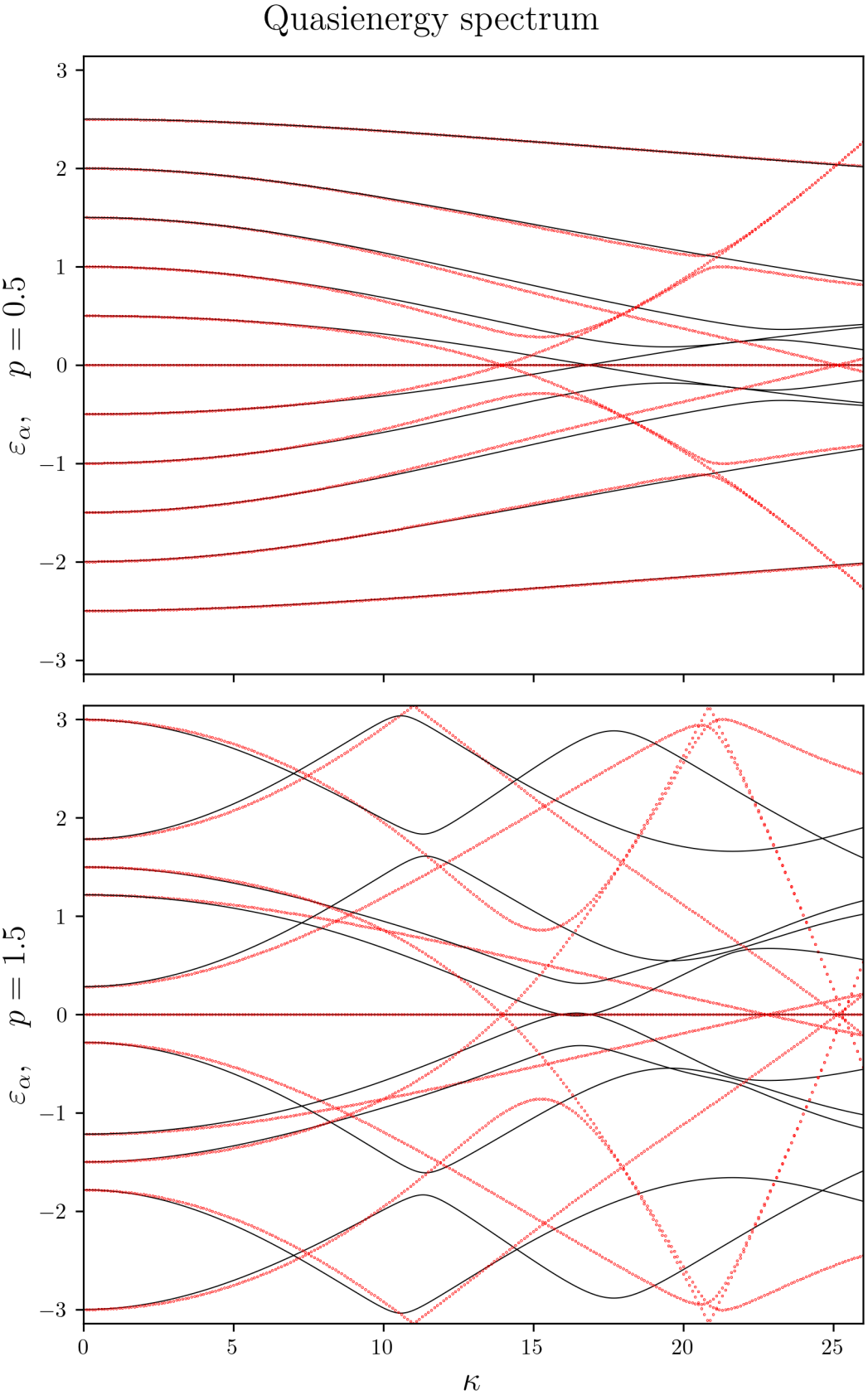

Figure 3.20: The eigenvalues of the effective Hamiltonian (3.163) mapped to the first Brillouin zone are plotted as red dots. The quasienergies obtained by numerically integrating the Schrödinger equation (3.122) are plotted as black lines. In this figure $j = 5$.

The next steps are similar to those in subsection 3.3.3.

$$\widehat{G}_0 \overset{(2.134)}{=} \frac{\kappa}{2j}\widehat{J}_z^2, \tag{3.168}$$

$$\widehat{K}_1(t) \overset{(2.133)}{=} -i\frac{p\widehat{J}_x}{2}\left(e^{2\pi it} - e^{-2\pi it}\right) \tag{3.169}$$

$$= p\widehat{J}_x \sin(2\pi t) \tag{3.170}$$

$$\widehat{G}_1 \overset{(2.136)}{=} 0. \tag{3.171}$$

We compute the term $\widehat{K}_2(t)$, from expansion (2.129), the following way

$$\widehat{K}_2(t) \overset{(2.138)}{=} -i\left[\widehat{V}_1, \widehat{H}_0 + \widehat{V}_0\right] e^{2\pi it} - i\left[\widehat{V}_{-1}, \widehat{H}_0 + \widehat{V}_0\right] e^{-2\pi it} \tag{3.172}$$

$$= -2i\cos(2\pi t)\left[\widehat{V}_1, \widehat{H}_0 + \widehat{V}_0\right] \tag{3.173}$$

$$\overset{(3.166,\ 3.167)}{=} -\frac{i\kappa p}{2j}\cos(2\pi t)\left[\widehat{J}_x, \widehat{J}_z^2\right] \tag{3.174}$$

$$\overset{(3.156)}{=} -\frac{\kappa p}{2j}\cos(2\pi t)\left(\widehat{J}_y\widehat{J}_z + \widehat{J}_z\widehat{J}_y\right). \tag{3.175}$$

Similarly, we compute the term $\widehat{G}_2$, from expansion (2.128), as follows

$$\widehat{G}_2 \overset{(2.140)}{=} \frac{1}{2}\left[\left[\widehat{V}_1, \widehat{H}_0 + \widehat{V}_0\right], \widehat{V}_{-1}\right] + \frac{1}{2}\left[\widehat{V}_1, \left[\widehat{H}_0 + \widehat{V}_0, \widehat{V}_{-1}\right]\right] \tag{3.176}$$

$$= \left[\left[\widehat{V}_1, \widehat{H}_0 + \widehat{V}_0\right], \widehat{V}_1\right] \tag{3.177}$$

$$\overset{(3.166,\ 3.167)}{=} \frac{\kappa p}{4j}\left[\left[\widehat{J}_x, \widehat{J}_z^2\right], \frac{p\widehat{J}_x}{2}\right] \tag{3.178}$$

$$= \frac{\kappa p^2}{4j}\left(\widehat{J}_y^2 - \widehat{J}_z^2\right). \tag{3.179}$$

Using equations (2.128, 3.168, 3.171, 3.179), we get the effective Hamiltonian

$$\boxed{\widehat{G} \approx \frac{\kappa}{2j}\widehat{J}_z^2 + \frac{\kappa p^2}{16\pi^2 j}\left(\widehat{J}_y^2 - \widehat{J}_z^2\right)}. \tag{3.180}$$

Similarly, from equations (2.129, 3.170, 3.175), we get the second-order expansion of the kick operator

$$\boxed{\widehat{K}(t) \approx \frac{p}{2\pi}\widehat{J}_x \sin(2\pi t) - \frac{\kappa p}{8\pi^2 j}\cos(2\pi t)\left(\widehat{J}_y\widehat{J}_z + \widehat{J}_z\widehat{J}_y\right)}. \tag{3.181}$$

The quasienergies approximated by the eigenvalues of the effective Hamiltonian (3.180) are (after mapping to the first Brillouin zone) plotted in figures 3.21 and 3.22. In these figures are also plotted the quasienergies yielded by numerical integration of equation $i\partial_t\widehat{U}(t,0) = \widehat{H}(t)\widehat{U}(t,0)$ and similar procedure as in section 3.3.1.

Note that since the effective Hamiltonian (3.180) linearly depends on the parameter κ, the quasienergies yielded from the effective Hamiltonian in figure 3.21 form straight lines. For the same reason, in figure 3.22 the curves yielded from the effective Hamiltonian in the upper and lower plot are connected by scaling factor $5 = 3.5/0.7$. This connection is less obvious due to mapping to the first Brillouin zone. The curves yielded by integrating the Schrödinger equation (2.53)—the black curves—do not have such simple properties.

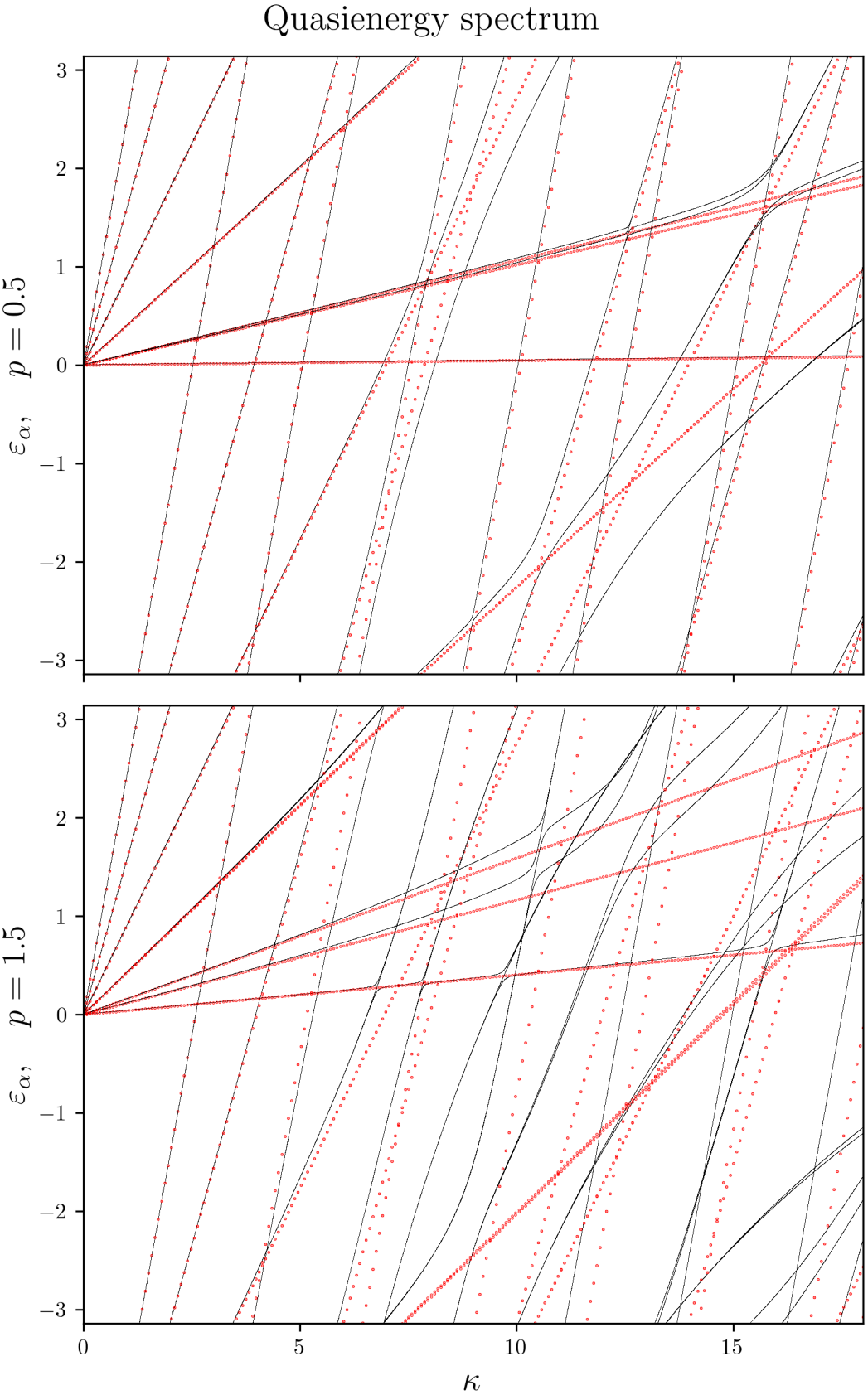

Figure 3.21: The eigenvalues of the effective Hamiltonian (3.180) mapped to the first Brillouin zone are plotted as red dots. The quasienergies obtained by numerically integrating the Schrödinger equation (2.53) are plotted as black lines. In this figure $j = 5$.

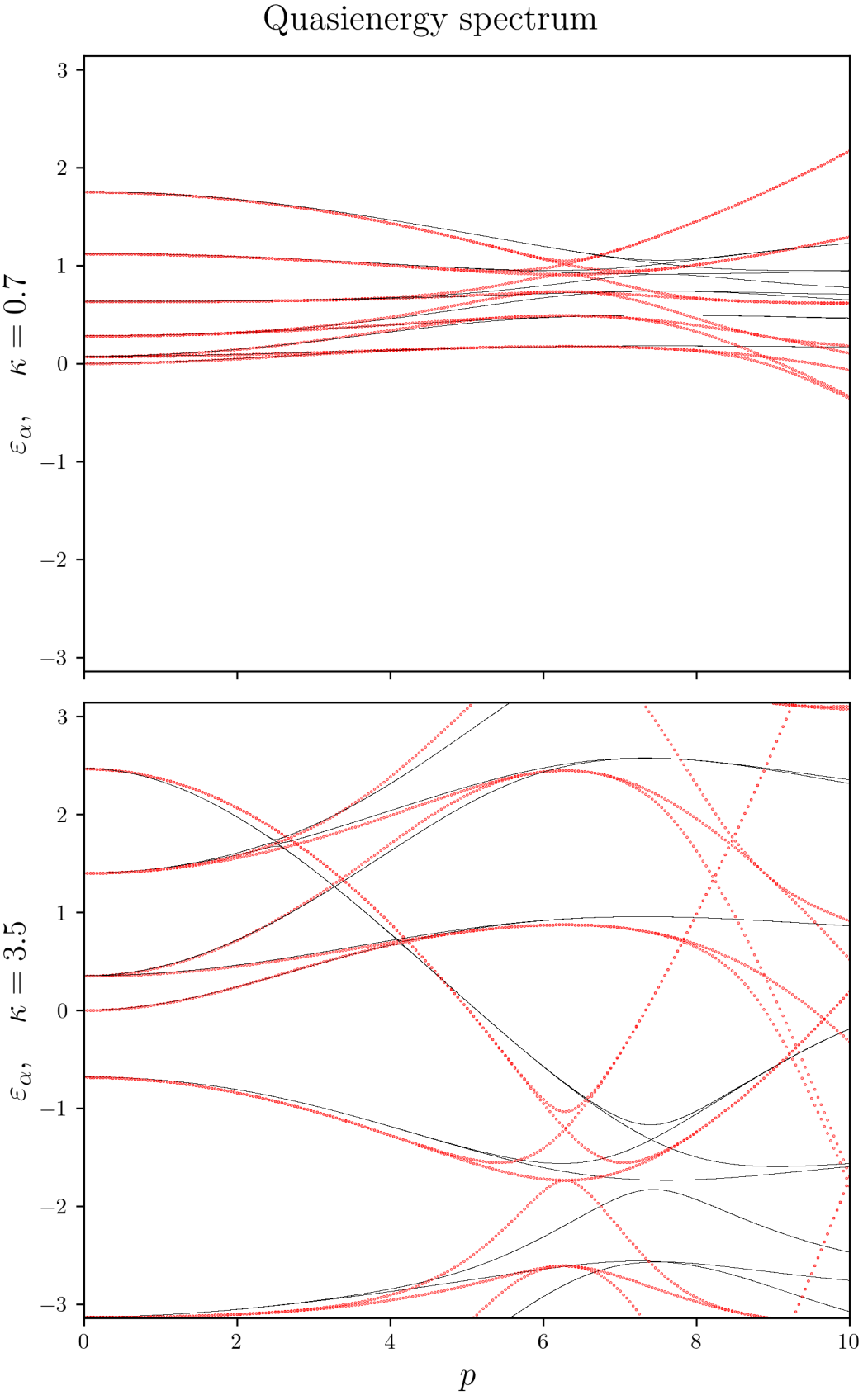

Figure 3.22: The eigenvalues of the effective Hamiltonian (3.180) mapped to the first Brillouin zone are plotted as red dots. The quasienergies obtained by numerically integrating the Schrödinger equation (2.53) are plotted as black lines. In this figure $j = 5$.

3.5 Comment on small time period

In section 2.5 we described the small time period limit by relations (2.166, 2.167). From the numerical simulations, particularly the figures of quasienergy spectra 3.1, 3.2, 3.3, 3.11, 3.19, 3.20, 3.21 and 3.22, we see that the effective Hamiltonians work well for the parameters which do not necessarily satisfy the requirements of equations (2.166, 2.167). Particularly, in the limiting case of high frequency $\omega/(2\pi) = 1$, the borders of the first Brillouin zone $\pm\pi$ are considered to be big numbers. Nevertheless, the eigenvalues of the effective Hamiltonians, which are in the limiting case (2.166, 2.167) small numbers, reach the border of the first Brillouin zone and still approximate accurately the precise quasienergies. But it is natural when testing physical models to test their limitations, particularly the ranges of parameters for which the models start to fail.

Considering all the effective Hamiltonians (3.17, 3.24, 3.45, 3.146, 3.163, 3.180) constructed in this thesis, the condition for converging Floquet Hamiltonian series is that the parameters κ and p are small.[8] We demonstrated this condition by the comparison between the quasienergies yielded using effective Hamiltonians and the quasienergies computed by other techniques. In the models studied the parameters κ and p give converging Floquet Hamiltonians not just for values[9] $\kappa \ll 1/j$ and $p \ll 1/j$, given by relations (2.166, 2.167), bud also for values $\kappa \approx 1$, $p \approx 1$ and $j = 5$.

The converging series for Floquet Hamiltonians does not mean that the fast changes are necessarily negligible. The fast changes are described by the operator $e^{-i\widehat{K}(t)}$ and generally could be significant (but they are not significant in the limiting case (2.166, 2.167), as was shown in section 2.5). Nevertheless, we saw that in the particular cases of the kicked top system with parameters $\kappa = 0.2, p = 0.1, j = 5$ (figure 3.9) and $\kappa = 3, p = 0.7, j = 10$ (figure 3.13) the evolution given by stroboscopic plots[10] told us a lot about the evolution of the systems without telling us anything about the fast part of the evolution.

[8] If we measure the parameters κ and p in energy units, then in SI units the values $\kappa T/\hbar$ and $pT/\hbar$ should be small.

[9] We estimate the norm of the angular momentum operators to be of the order of j.

[10] Constructing a stroboscopic plot, only a Floquet Hamiltonian and a kick operator $\widehat{K}(t_s)$ at a specific time t_s are needed, i.e. we do not need the full functional dependence of the kick operator.

Conclusion

The thesis comprises a pedagogical presentation of the theory and a study of the specific systems. To make the thesis more educational, we included the first chapter with simplistic examples that help the reader to understand the peculiarities of the theory. The thesis strives to be self-consistent and in doing so presents a couple of appendices.

Although appearing in the journals as a tailored method for a specific system, the Floquet theory is a universal theory describing quantum systems with time-dependent periodic Hamiltonians. The first part of the second chapter provides a general introduction to the Floquet theory with all its subtleties. Both forms of the central Floquet theorem are presented and their interconnection is manifested. Using simple examples and insight from the formalism described, we present the ambiguities in the formal objects that can arise. We have learned that the Floquet Hamiltonian unambiguously describes the quasienergy spectrum, even though Floquet Hamiltonians can have different sets of eigenvalues. With all the formal objects and concepts presented, the analysis of the systems is easier as is shown in the next parts of the thesis.

The second part of the second chapter is a detailed description of the methods for constructing the series for Floquet Hamiltonians. Apart from assuming that the systems are finite and subjected to fast driving, we aim to be as general as possible. Also, we expose the cases of systems whose theoretical treatment can be simplified and lay out how to handle these systems. At the end of the second chapter, we describe more precisely the limit of fast driving using the methods described earlier. We observe the division of the evolution into fast and slow parts and the scaling of the magnitude of fast changes with the length of the time period.

In the second chapter, we mostly compiled information from many sources. There are also a few works that aim at presenting the Floquet theory in a general way, as we do [16, 18]. Our discussion of formalism focuses on the elemental objects of the theory and variants and extensions of the formalism found in the literature. We illustrate the concepts on various examples, which were extracted from diverse sources.

One of the main outcomes of the thesis is the comparison between various methods for the construction of an effective Hamiltonian. This was done in the third chapter. While some of the examples were separately presented in the recent papers [5, 7, 8], this thesis puts them together, adds some new examples and compares the accuracy of the various methods. The method characterized by finding an effective Hamiltonian alongside constructing a kick operator has proved to be accurate and universal.

An important area of interest, which emerged in the third chapter, was the classical limit. The classical limit of the effective description is particularly interesting. As far as we know, there was done a little on this construct. The importance of the classical effective trajectories remains an unanswered question. Nevertheless, a recent paper presents that these trajectories are beneficial for quasiclassical evolution [27]. Although there has been some discussion over the classical limit of the effective Hamiltonian of the kicked top model [5], the classical

effective trajectories for the kicked top model constructed in this thesis (taking into account the action of the kick operator) are, to our knowledge, new result.

In connection with the kicked top system, we mentioned another famous system, the kicked rotor. Using infinite Hilbert space, the kicked rotor system represents an extension to the intended scope of the thesis. As was presented in the literature [24, 25] and in this thesis, these two systems have many common features and can be made identical by doing special limits. From this part, we can extend our thesis to address systems with infinite Hilbert spaces.

The first important possible extension of the thesis is, as was mentioned in the introduction, to study the analogues of quantum phase transitions in excited spectra based on the theory presented. We provided a good foundation on which a more specialized theory can be built. After reading this thesis the reader should be able to understand most of the insights found in the specialized papers, e.g. in [5, 7, 8]. The second important possible extension is a study of the classical effective trajectories mentioned above.

Appendices

A. Baker–Campbell–Hausdorff formula

Here several equalities connected with the BCH formula are discussed.

A.1 Integral form of BCH formula

We aim to devise a special form of the BCH formula for the special form of one of the two operators within the BCH formula. Here we prove the rather general integral form of the BCH formula from which we get the special form of the BCH formula as a special case. In our proof, we restrict ourselves to operators represented by $d \times d$ matrices. We will follow the proof presented in [34, 35].

Let $\boldsymbol{A}$ and $\boldsymbol{B}$ be arbitrary $d \times d$ complex matrices. We define the operator[1] $\mathrm{ad}_{\boldsymbol{A}}$ the following way

$$(\mathrm{ad}_{\boldsymbol{A}})(\boldsymbol{B}) \stackrel{\mathrm{def}}{=} [\boldsymbol{A}, \boldsymbol{B}] = \boldsymbol{A}\boldsymbol{B} - \boldsymbol{B}\boldsymbol{A}. \tag{A.1}$$

The function of $\mathrm{ad}_{\boldsymbol{A}}$ is defined using the Taylor series for that function. The powers of $\mathrm{ad}_{\boldsymbol{A}}$ have straightforward meaning

$$(\mathrm{ad}_{\boldsymbol{A}})^n \boldsymbol{B} = \underbrace{[\boldsymbol{A}, [\boldsymbol{A}, \ldots [\boldsymbol{A}, \boldsymbol{B}]] \ldots]_n}_{\text{n commutators}} \tag{A.2}$$

and $(\mathrm{ad}_{\boldsymbol{A}})^0$ is defined to be an identity matrix.

We define the norm of a matrix $\boldsymbol{A}$:

$$||\boldsymbol{A}|| = \sup_{||\vec{v}||} \frac{||\boldsymbol{A}\vec{v}||}{||\vec{v}||}, \tag{A.3}$$

where sup is an abbreviation for the supremum.

The integral form of the Baker–Campbell–Hausdorff formula states the following [34]:

For any two $d \times d$ matrices $\boldsymbol{A}$, $\boldsymbol{B}$ with sufficiently small norm (A.3), the matrix $\boldsymbol{C} = \ln(e^{\boldsymbol{A}} e^{\boldsymbol{B}})$ is uniquely defined and

$$\boxed{\boldsymbol{C} = \boldsymbol{B} + \int_0^1 g_{\mathrm{BCH}}\left(e^{t\,\mathrm{ad}_{\boldsymbol{A}}} e^{\mathrm{ad}_{\boldsymbol{B}}}\right) \boldsymbol{A}\mathrm{d}t}, \tag{A.4}$$

where

$$g_{\mathrm{BCH}}(z) = \frac{\ln z}{z - 1}. \tag{A.5}$$

Equation (A.4) is the integral form of the BCH formula to be proven below

Let us define a matrix function $\boldsymbol{Q}_\theta(\boldsymbol{M}_{\mathrm{any}})$ the following way

$$\boldsymbol{Q}_\theta(\boldsymbol{M}_{\mathrm{any}}) \stackrel{\mathrm{def}}{=} e^{\theta \boldsymbol{A}} \boldsymbol{M}_{\mathrm{any}} e^{-\theta \boldsymbol{A}}, \tag{A.6}$$

[1] By saying that $\mathrm{ad}_{\boldsymbol{A}}$ is an operator we mean that it takes a matrix and returns a matrix. It is simple to see that $\mathrm{ad}_{\boldsymbol{A}}$ is linear.

where $\boldsymbol{A}, \boldsymbol{M}_{\text{any}}$ are some arbitrary matrices.

By doing a derivative, we get

$$\frac{d}{d\theta}\boldsymbol{Q}_\theta(\boldsymbol{M}_{\text{any}}) = [\boldsymbol{A}, \boldsymbol{Q}_\theta(\boldsymbol{M}_{\text{any}})] = \text{ad}_{\boldsymbol{A}}\left(\boldsymbol{Q}_\theta(\boldsymbol{M}_{\text{any}})\right). \tag{A.7}$$

What we have is a differential equation. We know that for $\theta = 0$ we get $\boldsymbol{Q}_{\theta=0} = \boldsymbol{M}_{\text{any}}$, i.e. we know the initial condition for the solution of the differential equation (A.7). It is easy to check that the solution of the differential equation is

$$\begin{aligned} \boldsymbol{Q}_\theta(\boldsymbol{M}_{\text{any}}) &= e^{\theta \text{ad}_{\boldsymbol{A}}}(\boldsymbol{M}_{\text{any}}) & \text{(A.8)} \\ &= \boldsymbol{M}_{\text{any}} + \theta\,[\boldsymbol{A}, \boldsymbol{M}_{\text{any}}] + \frac{\theta^2}{2!}\,[\boldsymbol{A}, [\boldsymbol{A}, \boldsymbol{M}_{\text{any}}]] + ... & \text{(A.9)} \end{aligned}$$

By choosing $\theta = 1$ and from equalities (A.6, A.8) we get the equation

$$e^{\boldsymbol{A}}\boldsymbol{M}_{\text{any}}e^{-\boldsymbol{A}} = e^{\text{ad}_{\boldsymbol{A}}}\boldsymbol{M}_{\text{any}}. \tag{A.10}$$

The equation above will be used later during the proof.

We define another auxiliary matrix that is a function of two real arguments

$$\boldsymbol{M}_{\text{aux}}(s,t) \stackrel{\text{def}}{=} e^{s\boldsymbol{C}(t)}\frac{\partial}{\partial t}e^{-s\boldsymbol{C}(t)}, \tag{A.11}$$

where the t-dependent matrix $\boldsymbol{C}(t)$ will be defined later.

The following relation holds

$$\frac{\partial \boldsymbol{M}_{\text{aux}}(s,t)}{\partial s} = [\boldsymbol{C}(t), \boldsymbol{M}_{\text{aux}}(s,t)] - \frac{\partial \boldsymbol{C}(t)}{\partial t} = \text{ad}_{\boldsymbol{C}(t)}\boldsymbol{M}_{\text{aux}}(s,t) - \frac{\partial \boldsymbol{C}(t)}{\partial t}. \tag{A.12}$$

The solution of differential equation (A.12) is [35]

$$\boldsymbol{M}_{\text{aux}}(s,t) = e^{\text{ad}_{\boldsymbol{C}(t)}}\boldsymbol{M}_{\text{aux}}(0,t) - \int_0^s \text{d}r e^{(s-r)\text{ad}_{\boldsymbol{C}(t)}}\frac{\partial \boldsymbol{C}(t)}{\partial t}. \tag{A.13}$$

We realise that $\boldsymbol{M}_{\text{aux}}(0,t) = 0$, set $s = 1$ and transcribe equation (A.13) into

$$e^{\boldsymbol{C}(t)}\frac{\partial}{\partial t}e^{-\boldsymbol{C}(t)} = -f_{\text{aux}}(\text{ad}_{\boldsymbol{C}(t)})\frac{\partial \boldsymbol{C}(t)}{\partial t}, \tag{A.14}$$

where

$$f_{\text{aux}}(z) \stackrel{\text{def}}{=} \frac{e^z - 1}{z} = 1 + \frac{z}{2!} + \frac{z^2}{3!} + \frac{z^3}{4!} + \frac{z^4}{5!} + \frac{z^5}{6!} + O(z^6). \tag{A.15}$$

From the trivial equality

$$\frac{\partial}{\partial \tau}\left(e^{\boldsymbol{K}}e^{-\boldsymbol{K}}\right) = 0 = \left(\frac{\partial e^{\boldsymbol{K}}}{\partial \tau}\right)e^{-\boldsymbol{K}} + e^{\boldsymbol{K}}\left(\frac{\partial e^{-\boldsymbol{K}}}{\partial \tau}\right), \tag{A.16}$$

where $\boldsymbol{K}$ is an arbitrary matrix we get

$$\left(\frac{\partial}{\partial t}e^{\boldsymbol{K}(t)}\right)e^{-\boldsymbol{K}(t)} = f_{\text{aux}}(\text{ad}_{\boldsymbol{K}(t)})\frac{\partial \boldsymbol{K}(t)}{\partial t}, \tag{A.17}$$

which is also a useful equation.

Having devised the important equalities (A.10, A.14), we continue and use them. We define

$$\boldsymbol{C}(t) \stackrel{\text{def}}{=} \ln\left(e^{t\boldsymbol{A}}e^{\boldsymbol{B}}\right), \tag{A.18}$$

where the matrices $\boldsymbol{A}$ and $\boldsymbol{B}$ are the matrices from theorem (A.4). We remind that definition (A.18) works well only if the matrices $\boldsymbol{A}$ and $\boldsymbol{B}$ are sufficiently small (the norm is given by (A.3)).

The following relation holds

$$e^{\boldsymbol{C}(t)}\frac{\partial}{\partial t}e^{-\boldsymbol{C}(t)} = -\boldsymbol{A}. \tag{A.19}$$

Using (A.14) we get

$$\boldsymbol{A} = f_{\text{aux}}(\text{ad}_{\boldsymbol{C}(t)})\frac{\partial \boldsymbol{C}(t)}{\partial t}. \tag{A.20}$$

For an arbitrary matrix $\boldsymbol{M}_{\text{any}}$, we get

$$\begin{aligned} e^{\text{ad}_{\boldsymbol{C}}}\boldsymbol{M}_{\text{any}} &= e^{\boldsymbol{C}}\boldsymbol{M}_{\text{any}}e^{-\boldsymbol{C}} = e^{t\boldsymbol{A}}e^{\boldsymbol{B}}\boldsymbol{M}_{\text{any}}e^{-\boldsymbol{B}}e^{-t\boldsymbol{A}} && \text{(A.21)}\\ &= e^{t\,\text{ad}_{\boldsymbol{A}}}e^{\boldsymbol{B}}\boldsymbol{M}_{\text{any}}e^{-\boldsymbol{B}} && \text{(A.22)}\\ &= e^{t\,\text{ad}_{\boldsymbol{A}}}e^{\text{ad}_{\boldsymbol{B}}}\boldsymbol{M}_{\text{any}}, && \text{(A.23)} \end{aligned}$$

where we repeatedly used equation (A.10). From equation (A.23) we get

$$e^{\text{ad}_{\boldsymbol{C}}} = e^{t\,\text{ad}_{\boldsymbol{A}}}e^{\text{ad}_{\boldsymbol{B}}}. \tag{A.24}$$

For sufficiently small $\boldsymbol{A}$ and $\boldsymbol{B}$, the logarithm of the right hand side of (A.24) is defined and

$$\text{ad}_{\boldsymbol{C}} = \ln\left(e^{t\,\text{ad}_{\boldsymbol{A}}}e^{\text{ad}_{\boldsymbol{B}}}\right). \tag{A.25}$$

Noting that

$$f_{\text{aux}}(\ln(z))g_{\text{BCH}}(z) = 1, \tag{A.26}$$

we transcribe (A.25) the following way

$$\begin{aligned} f_{\text{aux}}\left(\text{ad}_{\boldsymbol{C}}\right) &= f_{\text{aux}}\left[\ln\left(e^{t\,\text{ad}_{\boldsymbol{A}}}e^{\text{ad}_{\boldsymbol{B}}}\right)\right] && \text{(A.27)}\\ &\stackrel{\text{(A.26)}}{=} \left[g_{\text{BCH}}\left(e^{t\,\text{ad}_{\boldsymbol{A}}}e^{\text{ad}_{\boldsymbol{B}}}\right)\right]^{-1}. && \text{(A.28)} \end{aligned}$$

Transcribing equation (A.20) using equation (A.28) we get

$$\begin{aligned} \boldsymbol{A} &= \left[g_{\text{BCH}}\left(e^{t\,\text{ad}_{\boldsymbol{A}}}e^{\text{ad}_{\boldsymbol{B}}}\right)\right]^{-1}\frac{\partial \boldsymbol{C}(t)}{\partial t}, && \text{(A.29)}\\ g_{\text{BCH}}\left(e^{t\,\text{ad}_{\boldsymbol{A}}}e^{\text{ad}_{\boldsymbol{B}}}\right)\boldsymbol{A} &= \frac{\partial \boldsymbol{C}(t)}{\partial t}. && \text{(A.30)} \end{aligned}$$

Integrating equation (A.30) from $t = 0$ to $t = 1$ and using definition (A.18), we get

$$\int_0^1 g_{\text{BCH}}\left(e^{t\,\text{ad}_{\boldsymbol{A}}}e^{\text{ad}_{\boldsymbol{B}}}\right)\boldsymbol{A}\text{d}t = \ln\left(e^{\boldsymbol{A}}e^{\boldsymbol{B}}\right) - \boldsymbol{B}, \tag{A.31}$$

which proves the integral form of the BCH formula (A.4).

A.2 Special form of BCH formula

Replacing

$$(\boldsymbol{A}, \boldsymbol{B}) \to (-\boldsymbol{B}, -\boldsymbol{A}), \tag{A.32}$$

we get the alternative form of the BCH formula

$$-\ln\left(e^{-\boldsymbol{B}}e^{-\boldsymbol{A}}\right) = \boldsymbol{A} + \int_0^1 g_{\mathrm{BCH}}\left(e^{-t\,\mathrm{ad}_{\boldsymbol{B}}}e^{-\mathrm{ad}_{\boldsymbol{A}}}\right)\boldsymbol{B}\mathrm{d}t. \tag{A.33}$$

Further replacement

$$\boldsymbol{B} \to p\boldsymbol{B}, \tag{A.34}$$

where p is considered to be a small parameter, gives

$$-\ln\left(e^{-p\boldsymbol{B}}e^{-\boldsymbol{A}}\right) = \boldsymbol{A} + p\int_0^1 g_{\mathrm{BCH}}\left(e^{-t\,\mathrm{ad}_{p\boldsymbol{B}}}e^{-\mathrm{ad}_{\boldsymbol{A}}}\right)\boldsymbol{B}\mathrm{d}t, \tag{A.35}$$

$$= \boldsymbol{A} + p\int_0^1 g_{\mathrm{BCH}}\left(e^{-tp\,\mathrm{ad}_{\boldsymbol{B}}}e^{-\mathrm{ad}_{\boldsymbol{A}}}\right)\boldsymbol{B}\mathrm{d}t, \tag{A.36}$$

where we used $\mathrm{ad}_{p\boldsymbol{B}} = p\,\mathrm{ad}_{\boldsymbol{B}}$.

By considering the parameter p to be small and approximating

$$e^{-tp\,\mathrm{ad}_{\boldsymbol{B}}} \approx \boldsymbol{I} + O(p), \tag{A.37}$$

where $\boldsymbol{I}$ is an identity matrix, we get

$$-\ln\left(e^{-p\boldsymbol{B}}e^{-\boldsymbol{A}}\right) = \boldsymbol{A} + p\,g_{\mathrm{BCH}}\left(e^{-\mathrm{ad}_{\boldsymbol{A}}}\right)\boldsymbol{B} + O(p^2). \tag{A.38}$$

The special form of the BCH formula reads

$$\boxed{-\ln\left(e^{-p\boldsymbol{B}}e^{-\boldsymbol{A}}\right) = \boldsymbol{A} - p\,\frac{\mathrm{ad}_{\boldsymbol{A}}}{e^{-\mathrm{ad}_{\boldsymbol{A}}} - 1}\boldsymbol{B} + O(p^2)}, \tag{A.39}$$

which in finite Hilbert spaces is equivalent to its operator form (2.150) used in this thesis. Since we consider finite Hilbert spaces, operators are represented by matrices. Note that since we used the integral form of the BCH formula (A.4), we require the matrix $\boldsymbol{A}$ to be sufficiently small.

A.3 Proof of identity (3.23) facilitating use of special BCH formula

Here we derive the identity (3.23)

$$\frac{\mathrm{ad}_{\widehat{A}}}{e^{\left(\mathrm{ad}_{\widehat{A}}\right)} - 1}\widehat{B} = -\frac{1}{2}\widehat{J}_+\frac{\frac{\kappa}{2j}(2\widehat{J}_z + 1)}{e^{\left[-i\frac{\kappa}{2j}(2\widehat{J}_z+1)\right]} - 1} + \frac{1}{2}\frac{\frac{\kappa}{2j}(2\widehat{J}_z + 1)}{e^{\left[i\frac{\kappa}{2j}(2\widehat{J}_z+1)\right]} - 1}\widehat{J}_-,$$

where (3.20, 3.21)

$$\begin{aligned}\widehat{A} &= i\frac{\kappa}{2j}\widehat{J}_z^2,\\ \widehat{B} &= i\widehat{J}_x.\end{aligned}$$

First we recall the well known formulas for quasispin operators

$$\left[\widehat{J}_\alpha, \widehat{J}_\beta\right] = i\varepsilon_{\alpha\beta\gamma}\widehat{J}_\gamma, \tag{A.40}$$

$$\left[\widehat{J}_z, \widehat{J}_+\right] = \widehat{J}_+, \tag{A.41}$$

$$\left[\widehat{J}_z, \widehat{J}_-\right] = -\widehat{J}_-. \tag{A.42}$$

We repeat the definition of the ladder operators (3.9)

$$\widehat{J}_\pm \stackrel{\text{def}}{=} \widehat{J}_x \pm i\widehat{J}_y$$

and express the operator $\widehat{B}$ using the ladder operators

$$\widehat{B} = i\widehat{J}_x = \frac{i}{2}(\widehat{J}_+ + \widehat{J}_-). \tag{A.43}$$

The following relations hold

$$\left[\widehat{J}_z^2, \widehat{J}_+\right] = \widehat{J}_z\left[\widehat{J}_z, \widehat{J}_+\right] + \left[\widehat{J}_z, \widehat{J}_+\right]\widehat{J}_z \tag{A.44}$$

$$= \widehat{J}_z\widehat{J}_+ + \widehat{J}_+\widehat{J}_z = 2\widehat{J}_+\widehat{J}_z + \widehat{J}_+ = \widehat{J}_+(2\widehat{J}_z + 1), \tag{A.45}$$

$$\left[\widehat{J}_z^2, \widehat{J}_-\right] = \widehat{J}_z\left[\widehat{J}_z, \widehat{J}_-\right] + \left[\widehat{J}_z, \widehat{J}_-\right]\widehat{J}_z \tag{A.46}$$

$$= -\widehat{J}_z\widehat{J}_- - \widehat{J}_-\widehat{J}_z = -2\widehat{J}_z\widehat{J}_- - \widehat{J}_- = -(2\widehat{J}_z + 1)\widehat{J}_-. \tag{A.47}$$

It is expedient to transcribe the term $\mathrm{ad}_{\widehat{A}}\widehat{B}$ using the $\widehat{J}_\bullet$ operators

$$\mathrm{ad}_{\widehat{A}}\widehat{B} = \left[i\frac{\kappa}{2j}\widehat{J}_z^2, \frac{i}{2}(\widehat{J}_+ + \widehat{J}_-)\right] \tag{A.48}$$

$$= -\frac{1}{2}\frac{\kappa}{2j}\left(\left[\widehat{J}_z^2, \widehat{J}_+\right] + \left[\widehat{J}_z^2, \widehat{J}_-\right]\right) \tag{A.49}$$

$$= -\frac{1}{2}\frac{\kappa}{2j}\left(\widehat{J}_+(2\widehat{J}_z + 1) - (2\widehat{J}_z + 1)\widehat{J}_-\right). \tag{A.50}$$

We also compute the double application of $\mathrm{ad}_{\widehat{A}}$ on $\widehat{B}$

$$\begin{aligned}\mathrm{ad}_{\widehat{A}}\left(\mathrm{ad}_{\widehat{A}}\widehat{B}\right) &= \left[\widehat{A}, \mathrm{ad}_{\widehat{A}}\widehat{B}\right]\\ &= \left[i\frac{\kappa}{2j}\widehat{J}_z^2, -\frac{1}{2}\frac{\kappa}{2j}\left(\widehat{J}_+(2\widehat{J}_z + 1) - (2\widehat{J}_z + 1)\widehat{J}_-\right)\right]\\ &= -\frac{i}{2}\left(\frac{\kappa}{2j}\right)^2\left(\left[\widehat{J}_z^2, \widehat{J}_+(2\widehat{J}_z + 1)\right] - \left[\widehat{J}_z^2, (2\widehat{J}_z + 1)\widehat{J}_-\right]\right)\\ &= -\frac{i}{2}\left(\frac{\kappa}{2j}\right)^2\left(\left[\widehat{J}_z^2, \widehat{J}_+\right](2\widehat{J}_z + 1) - (2\widehat{J}_z + 1)\left[\widehat{J}_z^2, \widehat{J}_-\right]\right)\\ &= -\frac{i}{2}\left(\frac{\kappa}{2j}\right)^2\left(\widehat{J}_+(2\widehat{J}_z + 1)^2 + (2\widehat{J}_z + 1)^2\widehat{J}_-\right).\end{aligned} \tag{A.51}$$

Considering the aforementioned we pose the conjecture

$$\left(\mathrm{ad}_{\widehat{A}}\right)^n \widehat{B} = -\frac{1}{2}(i)^{n-1}\left(\frac{\kappa}{2j}\right)^n \left(\widehat{J}_+(2\widehat{J}_z+1)^n + (-1)^n(2\widehat{J}_z+1)^n\widehat{J}_-\right). \quad \text{(A.52)}$$

We compute

$$\begin{aligned}
\mathrm{ad}_{\widehat{A}}\left(\left(\mathrm{ad}_{\widehat{A}}\right)^n \widehat{B}\right) = & \\
&= \left[i\frac{\kappa}{2j}\widehat{J}_z^2, -\frac{1}{2}(i)^{n-1}\left(\frac{\kappa}{2j}\right)^n \left(\widehat{J}_+(2\widehat{J}_z+1)^n + (-1)^n(2\widehat{J}_z+1)^n\widehat{J}_-\right)\right] \\
&= -\frac{(i)^{(n+1)-1}}{2}\left(\frac{\kappa}{2j}\right)^{(n+1)}\left(\left[\widehat{J}_z^2, \widehat{J}_+(2\widehat{J}_z+1)^n\right] + (-1)^n\left[\widehat{J}_z^2, (2\widehat{J}_z+1)^n\widehat{J}_-\right]\right) \\
&= -\frac{(i)^{(n+1)-1}}{2}\left(\frac{\kappa}{2j}\right)^{(n+1)}\left(\left[\widehat{J}_z^2, \widehat{J}_+\right](2\widehat{J}_z+1)^n + (-1)^n(2\widehat{J}_z+1)^n\left[\widehat{J}_z^2, \widehat{J}_-\right]\right).
\end{aligned}$$

Now according to equations (A.45) and (A.47) we get

$$\begin{aligned}
\mathrm{ad}_{\widehat{A}}\left(\left(\mathrm{ad}_{\widehat{A}}\right)^n \widehat{B}\right) = & \\
&= -\frac{1}{2}(i)^{(n+1)-1}\left(\frac{\kappa}{2j}\right)^{(n+1)} \left(\widehat{J}_+(2\widehat{J}_z+1)^{n+1} + (-1)^{n+1}(2\widehat{J}_z+1)^{n+1}\widehat{J}_-\right).
\end{aligned}$$

Thus the conjecture (A.52) is proven.

Now we use the expansion

$$\frac{z}{e^z-1} = \sum_{n=0}^{\infty} B_n\frac{z^n}{n!} = 1 - \frac{z}{2} + \frac{z^2}{12} - \frac{z^4}{720} + \frac{z^6}{30\,240} - \frac{z^8}{1\,209\,600} + O(z^{10}), \quad \text{(A.53)}$$

where B_n are the Bernoulli numbers [36]. And we transcribe

$$\begin{aligned}
\frac{\mathrm{ad}_{\widehat{A}}}{e^{\left(-\mathrm{ad}_{\widehat{A}}\right)}-1} &= -\frac{-\mathrm{ad}_{\widehat{A}}}{\exp\left(-\mathrm{ad}_{\widehat{A}}\right)-1} && \text{(A.54)} \\
&= -\sum_{n=0}^{\infty} B_n\frac{\left(-\mathrm{ad}_{\widehat{A}}\right)^n}{n!} = -\sum_{n=0}^{\infty} B_n\frac{(-1)^n}{n!}\left(\mathrm{ad}_{\widehat{A}}\right)^n. && \text{(A.55)}
\end{aligned}$$

Using the conjecture (A.52) we write

$$\begin{aligned}
\frac{\mathrm{ad}_{\widehat{A}}}{e^{\left(\mathrm{ad}_{\widehat{A}}\right)}-1}\widehat{B} = & \\
&= -\sum_{n=0}^{\infty} B_n\frac{(-1)^n}{n!}\left(-\frac{1}{2}\right)(i)^{n-1}\left(\frac{\kappa}{2j}\right)^n\left(\widehat{J}_+(2\widehat{J}_z+1)^n + (-1)^n(2\widehat{J}_z+1)^n\widehat{J}_-\right) \\
&= \left(-\frac{i}{2}\right)\sum_{n=0}^{\infty} B_n\frac{(-1)^n}{n!}(i)^n\left(\frac{\kappa}{2j}\right)^n\left(\widehat{J}_+(2\widehat{J}_z+1)^n + (-1)^n(2\widehat{J}_z+1)^n\widehat{J}_-\right) \\
&= -\frac{i}{2}\widehat{J}_+\sum_{n=0}^{\infty} B_n\frac{1}{n!}\left(-i\frac{\kappa}{2j}(2\widehat{J}_z+1)\right)^n - \frac{i}{2}\sum_{n=0}^{\infty} B_n\frac{1}{n!}\left(i\frac{\kappa}{2j}(2\widehat{J}_z+1)\right)^n\widehat{J}_- \\
&= -\frac{1}{2}\frac{\widehat{J}_+\frac{\kappa}{2j}(2\widehat{J}_z+1)}{\exp\left(-i\frac{\kappa}{2j}(2\widehat{J}_z+1)\right)-1} + \frac{1}{2}\frac{\frac{\kappa}{2j}(2\widehat{J}_z+1)\widehat{J}_-}{\exp\left(i\frac{\kappa}{2j}(2\widehat{J}_z+1)\right)-1}.
\end{aligned}$$

So the desired identity is proven.

B. Map for classical kicked top

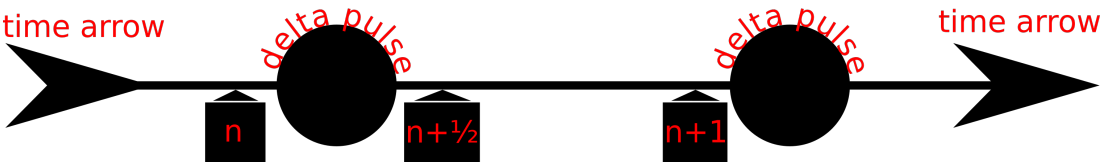

Figure B.1: A one period ($T = 1$) evolution from the moment immediately before a delta function performance (a "kick" or delta pulse) to the moment immediately before the next delta function performance. The evolution from the time t_n to the time t_{n+1} is divided into two steps. The first step is the evolution from immediately before the "kick" at t_n to immediately after the "kick" at $t_{n+1/2}$. The second step is the evolution from $t_{n+1/2}$ to immediately before the next "kick" at t_{n+1}.

Here we present the derivation of the classical map for the evolution of the kicked top system from immediately before an application of the delta function to immediately before the next application of the delta function.

First, we denote the time moments as follows

$$t_n = n - \Delta, n \in \mathbb{Z}, \tag{B.1}$$

$$t_{n+1/2} = n + \Delta, n \in \mathbb{Z}. \tag{B.2}$$

The labels of time moments defined by equations (B.1, B.2) are depicted in figure B.1. The time interval Δ is considered small (in comparison with $T = 1$).

As we know, the system is described by the kicked top Hamiltonian (3.15)

$$\widehat{H}(t) = \frac{\kappa}{2} Z^2 + pXT \sum_{n=-\infty}^{+\infty} \delta(t - n \cdot T).$$

We divide the time evolution from the time t_n to the time t_{n+1} into two steps. First, we evolve the system from the time t_n to the time $t_{n+1/2}$. During such evolution we consider the delta function part of the Hamiltonian (3.15) to be dominant. Thus the evolution is in practice governed by the Hamiltonian

$$H(p) = pX \sum_{n=-\infty}^{+\infty} \delta(t - n). \tag{B.3}$$

Since $t \in (t_n, t_{1+1/2}) \equiv (n - \Delta, n + \Delta)$, we have

$$H_n(p) = pX\delta(t - n). \tag{B.4}$$

In the following, we use the smallness of the auxiliary parameter Δ. We consider the delta function $\delta(x)$ to be well approximated by the "support function" $[1/(4\Delta)] \cdot (\mathrm{sign}(x + \Delta) - \mathrm{sign}(x - \Delta))$. Our approximation of the delta function is plotted in figure B.2.

The equation (B.4) is thus simplified and we have

$$H_n(p) = \frac{1}{2\Delta} pX. \tag{B.5}$$

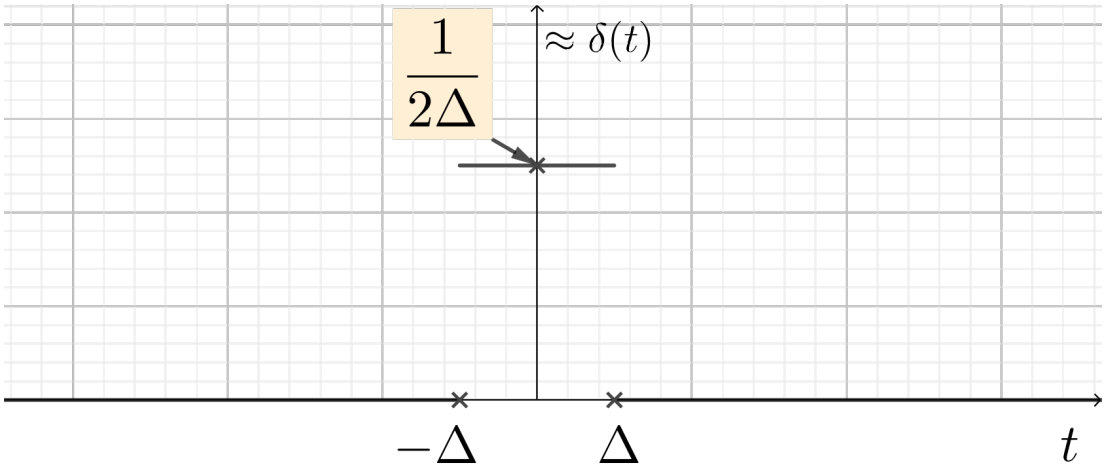

Figure B.2: An approximation of the delta function $\delta(t)$ using the small parameter Δ.

Now we use the known relation for angular momenta (or classical limit for commutator $[\hat{u}, \hat{v}] \to i\hbar\{u, v\}$)

$$\{X, Y\} = Z, \{Y, Z\} = X, \{Z, X\} = Y \tag{B.6}$$

and the known equation from classical mechanics

$$\frac{\mathrm{d}f}{\mathrm{d}t} = \{f, H\} + \frac{\partial f}{\partial t}, \tag{B.7}$$

where $\{\bullet, \bullet\}$ is the Poisson bracket. The function f is an arbitrary function of phase space coordinates and time. The function H is a Hamiltonian of a system. We substitute $f = J_k, k \in \{x, y, z\}$, $H = H_n(p)$ and we get

$$\frac{\mathrm{d}\vec{R}(t)}{\mathrm{d}t} = \frac{1}{2\Delta} \begin{pmatrix} 0 & 0 & 0 \\ 0 & 0 & -p \\ 0 & p & 0 \end{pmatrix} \vec{R}(t). \tag{B.8}$$

The solution is easy to get and easily verified by substitution. The solution reads

$$\vec{R}(t) = \exp\left(\begin{pmatrix} 0 & 0 & 0 \\ 0 & 0 & -p \\ 0 & p & 0 \end{pmatrix} \frac{t - t_n}{2\Delta} \right) \vec{R}(t_n). \tag{B.9}$$

Choosing $t = \Delta + n \equiv t_{n+1/2} = t_n + 2\Delta$ we get

$$\vec{R}\left(t_{n+1/2}\right) = \exp\left(\begin{pmatrix} 0 & 0 & 0 \\ 0 & 0 & -p \\ 0 & p & 0 \end{pmatrix} \right) \vec{R}\left(t_n\right) = \begin{pmatrix} 1 & 0 & 0 \\ 0 & \cos p & -\sin p \\ 0 & \sin p & \cos p \end{pmatrix} \vec{R}\left(t_n\right). \tag{B.10}$$

Now we can formally perform the limit $\Delta \to 0$. We devised equations (3.50).

In the second step, we evolve the system from the time $t_{n+1/2}$ to the time t_{n+1}. During this interval, the delta function could be considered zero. Thus the evolution is governed by the Hamiltonian

$$H(\kappa) = \frac{\kappa}{2} Z^2. \tag{B.11}$$

Using equation (B.7), we get

$$\frac{\mathrm{d}X}{\mathrm{d}t} = -\frac{\kappa}{2}\left\{X, Z^2\right\} = -\frac{\kappa}{2}\left(Z\left\{X, Z\right\} + \left\{X, Z\right\}Z\right) \tag{B.12}$$

$$= -\kappa Y Z, \tag{B.13}$$

$$\frac{\mathrm{d}Y}{\mathrm{d}t} = \kappa X Z, \tag{B.14}$$

$$\frac{\mathrm{d}Y}{\mathrm{d}t} = 0. \tag{B.15}$$

Using equation (B.15), we consider Z to be constant during the whole evolution from the time $t_{n+1/2}$ to the time t_{n+1}. Consequently, we get

$$\frac{\mathrm{d}\vec{R}(t)}{\mathrm{d}t} = \begin{pmatrix} 0 & -\kappa Z & 0 \\ \kappa Z & 0 & 0 \\ 0 & 0 & 0 \end{pmatrix} \vec{R}(t). \tag{B.16}$$

The solution of the above differential equation reads

$$\vec{R}(t) = \exp\left(\begin{pmatrix} 0 & -\kappa Z & 0 \\ \kappa Z & 0 & 0 \\ 0 & 0 & 0 \end{pmatrix}(t - t_{n+1/2})\right)\vec{R}\left(t_{n+1/2}\right). \tag{B.17}$$

Choosing $t = t_{n+1} = t_{n+1/2} + 1 - 2\Delta$ and considering the limit $\Delta \to 0$, we get

$$\vec{R}\,(n+1) = \exp\left(\begin{pmatrix} 0 & -\kappa Z & 0 \\ \kappa Z & 0 & 0 \\ 0 & 0 & 0 \end{pmatrix}\right)\vec{R}\left(n + \frac{1}{2}\right). \tag{B.18}$$

Computing the matrix exponential, we get equations (3.51)

$$\vec{R}\,(n+1) = \begin{pmatrix} \cos(\kappa Z) & -\sin(\kappa Z) & 0 \\ \sin(\kappa Z) & \cos(\kappa Z) & 0 \\ 0 & 0 & 1 \end{pmatrix}\vec{R}\left(1 + \frac{1}{2}\right). \tag{B.19}$$

C. Lagrange multipliers

Here we find the critical points of the function (3.56)

$$H_{CE2} = \frac{\kappa}{2}Z^2 + pX + \frac{\kappa p^2}{24}\left(Y^2 - Z^2\right) \tag{C.1}$$

depending on the parameters (κ, p).

The method of Lagrange multipliers uses the following theorem:

Let $U \subset \mathbb{R}^n$ is an open set. Let there is $\vec{a} = (a_1, ..., a_n) \in \mathbb{R}^n$. Let there are functions $f, F_1, ..., F_m : U \to \mathbb{R}^n$, where $m < n$. And let
i)$F_1(\vec{a}) = ... = F_m(\vec{a})$,
ii)$M \stackrel{\text{def}}{=} \{x \in U : F_1(x) = ... = F_m(x) = 0\}$,
iii) the matrix $\left(\frac{\partial F_i(a)}{\partial x_j}\right)_{ij}, i \in \{1, ..., m\}, j \in \{1, ..., n\}$ has the rank equal to m,
iv)$f, F_1, ..., F_m$ have continuous first derivatives.
If f is thought of as a function on the set M and if f has a critical point (local minimum, maximum or saddle point) in $\vec{a}$, then there exist $\lambda_1, ..., \lambda_m \in \mathbb{R}$ such that

$$\vec{\nabla} f(\vec{a}) = \sum_{j=1}^{m} \lambda_j \vec{\nabla} F_j(\vec{a}). \tag{C.2}$$

In this case, we have $m = 1$ and $f = H_{CE2}$. The set M is determined by

$$F_1(X, Y, Z) = 1 - X^2 - Y^2 - Z^2 = 0. \tag{C.3}$$

Let us find all the possible critical points of H_{CE2}. Using equation (C.2), we have

$$\frac{\partial\left(H_{CE2} - \lambda_1 F_1\right)}{\partial X} = p - 2X\lambda_1 = 0. \tag{C.4}$$

For $\lambda_1 \neq 0$ (i.e. $p \neq 0$), we get

$$X = \frac{p}{2\lambda_1} \tag{C.5}$$

Next, using equation (C.2), we get

$$\frac{\partial\left(H_{CE2} - \lambda_1 F_1\right)}{\partial Y} = \frac{\kappa p^2}{12}Y - 2Y\lambda_1 = 0. \tag{C.6}$$

There are two options satisfying equation (C.6):
I)

$$\frac{\kappa p^2}{12} = 2\lambda_1 \implies \lambda_1 = \frac{\kappa p^2}{24}, \tag{C.7}$$

II)

$$Y = 0. \tag{C.8}$$

Next, considering equation (C.2), we get

$$\frac{\partial\left(H_{CE2}-\lambda_1 F_1\right)}{\partial Z} = -\frac{\kappa p^2}{12} Z - 2Z\lambda_1 + \kappa Z, \tag{C.9}$$

$$= Z\cdot\left(\kappa - \frac{\kappa p^2}{12}\right) - 2\lambda_1 Z = 0. \tag{C.10}$$

Thus either

a)

$$Z = 0 \tag{C.11}$$

or

b)

$$\lambda_1 = \frac{1}{2}\left(\kappa - \frac{\kappa p^2}{12}\right). \tag{C.12}$$

We consider only the case $p \neq 0$. Then the following four options are all the possible critical points:

I) a)

$$\begin{aligned} X &= 12/\left(\kappa p\right), \\ Y &= \pm\sqrt{1-\left(\frac{12}{\kappa p}\right)^2}, \\ Z &= 0, \end{aligned} \tag{C.13}$$

I) b)

$$\begin{aligned} p &= \pm\sqrt{6}, \\ X &= \pm 2\sqrt{6}/\kappa, \\ Y^2 + Z^2 &= 1 - \frac{24}{\kappa^2}, \end{aligned} \tag{C.14}$$

II) a)

$$\begin{aligned} X &= \pm 1, \\ Y &= 0, \\ Z &= 0, \\ H_{CE2} &= \pm p \end{aligned} \tag{C.15}$$

II) b)

$$\begin{aligned} X &= p\cdot\left(\kappa - \kappa p^2/12\right)^{-1}, \\ Y &= 0, \\ Z &= \pm\sqrt{1-X^2}, \\ H_{CE2} &= \frac{\kappa}{2} - \frac{\kappa p^2}{24} + \frac{1}{2}\cdot\frac{p^2}{\kappa - \kappa p^2/12}. \end{aligned} \tag{C.16}$$

D. Angular momentum Wigner distribution and coherent states

In order to understand the visualisation techniques used in section 3.2.5, we present fragments of the theory of coherent spin states. The more scrutinized discussion is in paper [37]. And we also describe the angular momentum Wigner distribution, described in papers [38, 39]. Many of the statements in this appendix we present without proof and support for their validity could be found in the sources cited.

D.1 Coherent states of harmonic oscillator

Coherent spin states are an analogue of coherent states of a one-dimensional harmonic oscillator [12, 37, 40]

$$|\alpha\rangle \stackrel{\text{def}}{=} e^{-|\alpha|^2/2} e^{\alpha \widehat{a}^\dagger} |E_0\rangle , \tag{D.1}$$

where α is an arbitrary complex number and $\widehat{a}^\dagger$ is the creation operator known from a harmonic oscillator. The ground state of a one-dimensional harmonic oscillator is $|E_0\rangle$.

We remind that

$$\widehat{a}^\dagger |E_n\rangle = \sqrt{n+1}\, |E_{n+1}\rangle , \tag{D.2}$$

$$\widehat{a} |E_n\rangle = \sqrt{n}\, |E_{n-1}\rangle , \tag{D.3}$$

where $|E_n\rangle , n \in \mathbb{N}_0$ are the energy eigenstates of a one-dimensional harmonic oscillator and $\widehat{a}$ is a harmonic oscillator annihilation operator.

The operators $\widehat{a}$ and $\widehat{a}^\dagger$ satisfy

$$\widehat{a}\widehat{a}^\dagger - \widehat{a}^\dagger \widehat{a} = \widehat{I}. \tag{D.4}$$

We recall the position and momentum operators [12]

$$\widehat{x} = \sqrt{\frac{1}{2m\omega}} (\widehat{a}^\dagger + \widehat{a}),\ \widehat{p} = i\sqrt{\frac{m\omega}{2}} (\widehat{a}^\dagger - \widehat{a}), \tag{D.5}$$

where ω is the angular frequency of the oscillator and m is the mass of the particle associated with the oscillator.

Using equation (D.2), we transcribe equation (D.1) into

$$|\alpha\rangle = \sum_{n=0}^{+\infty} f_n(\alpha) |E_n\rangle , \tag{D.6}$$

$$f_n(\alpha) \stackrel{\text{def}}{=} e^{-|\alpha|^2/2} \frac{\alpha^n}{\sqrt{n!}}. \tag{D.7}$$

The complex conjugate of $f_3(\alpha)$, i.e. the function $f_3^*(\alpha)$, is visualized in figure D.1.

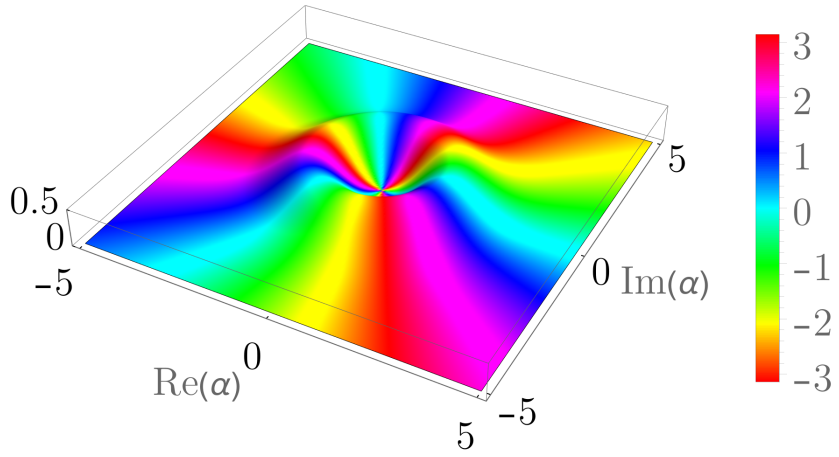

Figure D.1: The dependence of the scalar product $\langle\alpha|E_3\rangle = f_3^*(\alpha)$ on α. The landscape represents the absolute value $|\langle\alpha|E_3\rangle|$ and the colour represents the phase $\arg\langle\alpha|E_3\rangle \in (-\pi, \pi]$.

If we attempt to identify the functions $f_n(\alpha)$ (D.7) with the states of a *two*-dimensional harmonic oscillator with two (rescaled) coordinates $x_1, x_2 \in \mathbb{R}$, we find that the states $\langle x_1, x_2|\psi^{(n)}\rangle = f_n(\alpha = x_1 + ix_2)/\sqrt{\pi}$ form just a *proper* subset of the energy and angular momentum eigenstates of a *two*-dimensional harmonic oscillator [37].

The states $|\alpha\rangle$ span the whole Hilbert space $\mathcal{H}_{1D}$ of a *one*-dimensional harmonic oscillator since

$$\frac{1}{\pi}\iint \mathrm{dIm}(\alpha)\mathrm{dRe}(\alpha)\,|\alpha\rangle\langle\alpha| = \sum_{n=0}^{+\infty}|E_n\rangle\langle E_n| = \widehat{I}. \tag{D.8}$$

The states $|\alpha\rangle$ form an overcomplete set in $\mathcal{H}_{1D}$. It, leisurely speaking, means that there is too much states indexed by α, i.e. more than is needed. We show the overcompleteness by the simple but instructive example. If the states $|\alpha\rangle$ form the basis, i.e. the set that is *not* overcomplete, then each state $|\psi\rangle$ is uniquely determined by some function $C_\psi(\alpha), \alpha \in \mathbb{C}$ the following way

$$|\psi\rangle = \iint \mathrm{dIm}(\alpha)\mathrm{dRe}(\alpha)\mathrm{C}_\psi(\alpha)\,|\alpha\rangle\,. \tag{D.9}$$

We show that the uniqueness of $C_{|\psi\rangle}$ is not a property of the set $\{|\alpha\rangle\}$. We define

$$C_{\rho_0,\rho_1}(\alpha) \overset{\text{def}}{=} \begin{cases} 0 & \text{if} \quad |\alpha| < \rho_0, \\ N(\rho_0,\rho_1) & \text{if} \quad \rho_0 \le |\alpha| \le \rho_1, \\ 0 & \text{if} \quad \rho_1 \le |\alpha|. \end{cases} \tag{D.10}$$

From the equations

$$\begin{aligned} \iint \mathrm{dIm}(\alpha)\mathrm{dRe}(\alpha)C_{\rho_0,\rho_1}\,|\alpha\rangle &= N(\rho_0)\int_{\rho_0}^{\rho_1}\mathrm{d}\rho\int_0^{2\pi}\mathrm{d}\varphi\sum_{n=0}^{+\infty}e^{-\rho^2/2}\frac{\rho^{n+1}e^{in\varphi}}{\sqrt{n!}}\,|E_n\rangle \\ &= 0 + |E_0\rangle\,N(\rho_0,\rho_1)2\pi\int_{\rho_0}^{\rho_1}\rho e^{-\rho^2/2}\mathrm{d}\rho \qquad \text{(D.11)} \\ N(\rho_0,\rho_1) &= \left(2\pi\int_{\rho_0}^{\rho_1}\rho e^{-\rho^2/2}\mathrm{d}\rho\right)^{-1}, \qquad \text{(D.12)} \end{aligned}$$

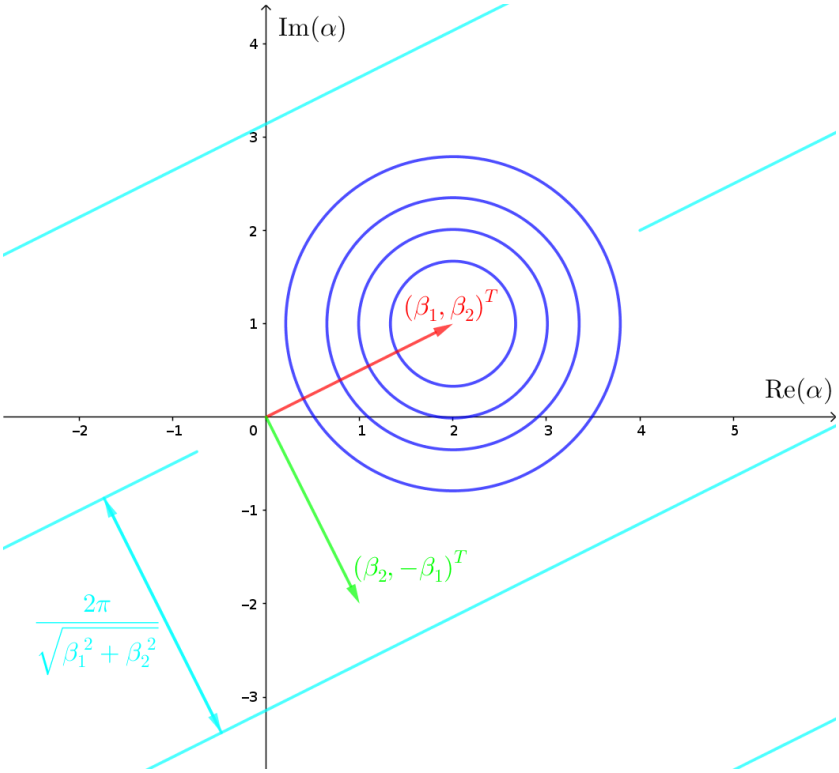

Figure D.2: A schematical representation of the function $g(\alpha) \stackrel{\text{def}}{=} \langle\alpha|\beta\rangle$. We define $\beta_1 \stackrel{\text{def}}{=} \text{Re}(\beta), \beta_2 \stackrel{\text{def}}{=} \text{Im}(\beta)$. In this particular example $\beta = 2 + i$. The blue circles represent the Gaussian shape of the landscape $|g(\alpha)| = e^{-|\alpha-\beta|^2/2}$. The straight turquoise solid lines represent the points of the same phase $\arg g(\alpha) = 0$, the distance between these lines is $2\pi/|\beta|$. The phase of the function $g(\alpha)$ increases in the direction of the vector $(\beta_2, -\beta_1)^T$.

we see that all the $\rho_1 > \rho_0 \geq 0, \rho_1, \rho_0 \in \mathbb{R}$ define functions $C_{\rho_0,\rho_1}(\alpha)$ that define the same state $|E_0\rangle = |\alpha = 0\rangle$, i.e. the state $|E_0\rangle$ does not define $C_{|E_0\rangle}(\alpha)$ uniquely.

The consequence of overcompleteness is that the set $\{\langle\alpha|\}, \alpha \in \mathbb{C}$ is not orthogonal

$$\langle\alpha|\beta\rangle = e^{-|\alpha-\beta|^2/2} e^{i\text{Im}(\alpha^*\beta)}. \tag{D.13}$$

The function $g(\alpha) \stackrel{\text{def}}{=} \langle\alpha|\beta\rangle$ can be described schematically. Let us define $\alpha_{1,2}, \beta_{1,2} \in \mathbb{R}$ by $\alpha = \alpha_1 + i\alpha_2$ and $\beta = \beta_1 + i\beta_2$. The absolute value $|g(\alpha))|$ is characterized by a Gaussian shape centred in the position β, i.e. $|g(\alpha)| = e^{-|\alpha-\beta|^2/2}$. The phase is equal to zero on the line $\alpha_2 = \alpha_1\beta_2/\beta_1$ and increases in the direction characterized by the vector in the two-dimensional complex plane $(\beta_2, -\beta_1)^T$, generally the phase is equal to the scalar product $(\alpha_1, \alpha_2)(\beta_2, -\beta_1)^T = \text{Im}(\alpha^*\beta)$. The contours of the same phase form straight lines parallel to the line $\alpha_2 = \alpha_1\beta_2/\beta_1$ and have distances between each other equal to $2\pi/|\beta|$. The function $g(\alpha)$ is schematically described in figure D.2 and visualized in figure D.3, where we used $\beta = 2 + i$.

The harmonic oscillator coherent states $|\alpha\rangle$ are states with the mean values

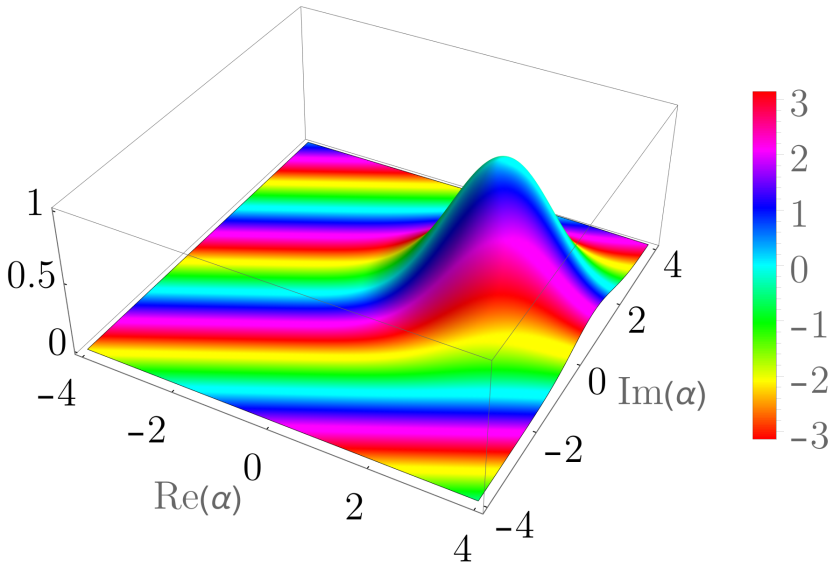

Figure D.3: The dependence of the scalar product $\langle\alpha|\beta = 2 + i\rangle$ on α. The landscape represents the absolute value $|\langle\alpha|2 + i\rangle|$ and the colour represents the phase $\arg\langle\alpha|2 + i\rangle \in (-\pi, \pi]$.

of position and momentum determined the following way

$$\langle\alpha|\widehat{x}|\alpha\rangle = \sqrt{\frac{2}{m\omega}}\mathrm{Re}\alpha, \tag{D.14}$$

$$\langle\alpha|\widehat{p}|\alpha\rangle = \sqrt{2m\omega}\mathrm{Im}\alpha. \tag{D.15}$$

The variations of position and momentum for the coherent states are

$$\langle\alpha|\left(\widehat{x} - \langle\alpha|\widehat{x}|\alpha\rangle\right)^2|\alpha\rangle = \frac{1}{2m\omega}, \tag{D.16}$$

$$\langle\alpha|\left(\widehat{p} - \langle\alpha|\widehat{p}|\alpha\rangle\right)^2|\alpha\rangle = \frac{m\omega}{2}. \tag{D.17}$$

Generally in quantum mechanics for any Hermitian operators $\widehat{A}$ and $\widehat{B}$ the following inequality relation holds [12]

$$\left\langle\psi\middle|\left(\widehat{A} - \left\langle\psi\middle|\widehat{A}\middle|\psi\right\rangle\right)^2\middle|\psi\right\rangle\left\langle\psi\middle|\left(\widehat{B} - \left\langle\psi\middle|\widehat{B}\middle|\psi\right\rangle\right)^2\middle|\psi\right\rangle \geq \frac{1}{4}\left(\left\langle\psi\middle|\widehat{C}\middle|\psi\right\rangle\right)^2,$$

$$\widehat{C} \stackrel{\mathrm{def}}{=} \left[\widehat{A}, \widehat{B}\right]. \tag{D.18}$$

The harmonic oscillator coherent states have the property that the product of variances of position and momentum has its lowest possible value

$$\left\langle\alpha\middle|\left(\widehat{x} - \langle\alpha\,|\,\widehat{x}\,|\,\alpha\rangle\right)^2\middle|\alpha\right\rangle\left\langle\alpha\middle|\left(\widehat{p} - \langle\alpha\,|\,\widehat{p}\,|\,\alpha\rangle\right)^2\middle|\alpha\right\rangle = \frac{1}{4}, \forall\alpha \in \mathbb{C}, \tag{D.19}$$

$$[\widehat{x}, \widehat{p}] = i\widehat{I}. \tag{D.20}$$

The well known representation of a quantum state related to the phase space of position and momentum is the Wigner distribution function of that state. The Wigner distribution function (of a one-dimensional problem) is defined by [12]

$$W(x, p) = \frac{1}{\sqrt{2\pi}}\int_{-\infty}^{+\infty}\left\langle x + \frac{\xi}{2}\middle|\widehat{\rho}\middle|x - \frac{\xi}{2}\right\rangle e^{+p\xi}\mathrm{d}\xi, \tag{D.21}$$

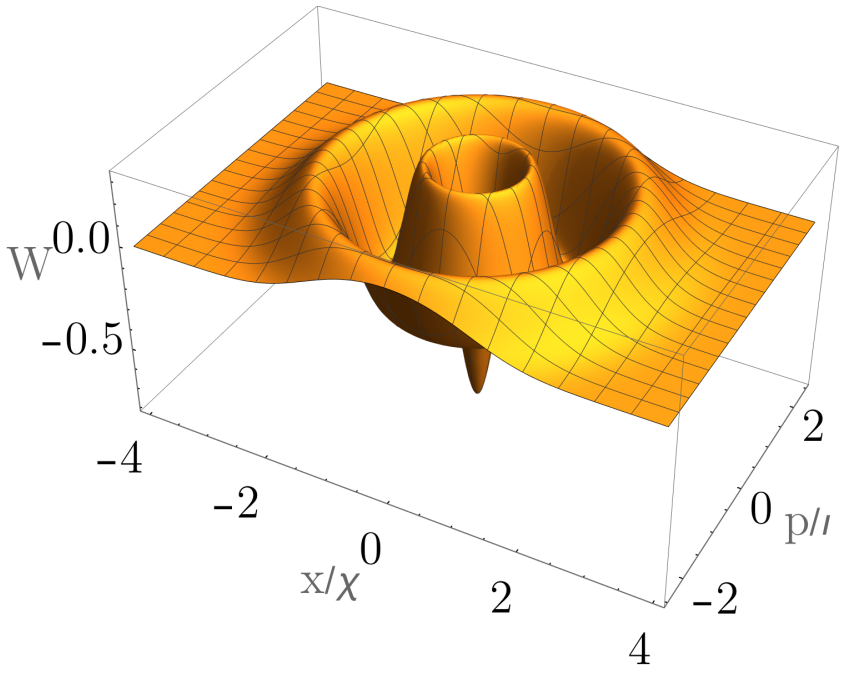

Figure D.4: The Wigner distribution function of the eigenenergy state $|E_3\rangle \in \mathcal{H}_{1D}$. The rescaling constants are $\chi = \sqrt{1/(m\omega)}, \iota = \sqrt{m\omega}$. Compare with figure D.1 knowing $\langle\alpha|(\widehat{x}/\chi, \widehat{p}/\iota)|\alpha\rangle = (\alpha_1\sqrt{2}, \alpha_2\sqrt{2})$.

where $\widehat{\rho}$ is the density operator (also called density matrix). For pure states (characterized by vector $|\psi\rangle$) the density operator reads $\widehat{\rho} = |\psi\rangle\langle\psi|$.

The Wigner distribution function for the state $|E_3\rangle$ is in figure D.4 and the Wigner distribution function for the state $|\alpha = 2 + i\rangle$ is in the figure D.5. In the following we will construct the harmonic oscillator coherent state analogue for angular momentum states and also the Wigner distribution function analogue for angular momentum states. It is our hope that the objects constructed for harmonic oscillator will provide intuition and justification for the objects constructed for angular momentum states.

D.2 Coherent spin states

The coherent spin states indexed by $\mu \in \mathbb{C}$ are defined by

$$|\mu\rangle \stackrel{\text{def}}{=} \frac{1}{(1+|\mu|^2)^j} e^{\mu \widehat{J}_-} |m = +j\rangle \tag{D.22}$$

$$= \frac{1}{(1+|\mu|^2)^j} \sum_{m=-j}^{+j} \left[\binom{2j}{m+j} \right]^{\frac{1}{2}} \mu^{j-m} |m\rangle \,, \tag{D.23}$$

where the lowering operator $\widehat{J}_-$ is defined by (3.9). We used [12]

$$\widehat{J}_\pm |m\rangle = \sqrt{j(j+1) - m(m\pm 1)}\, |m \pm 1\rangle \,. \tag{D.24}$$

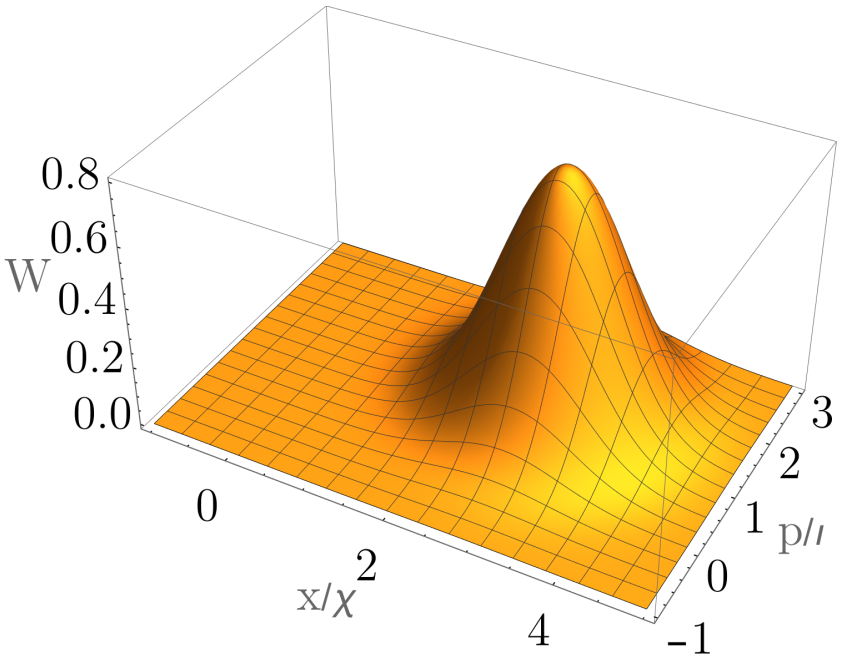

Figure D.5: The Wigner distribution function of the coherent state $|\alpha = 2 + i\rangle \in \mathcal{H}_{1D}$. The rescaling constants are $\chi = \sqrt{1/(m\omega)}, \iota = \sqrt{m\omega}$. Compare with figure D.3 knowing $\langle\alpha|(\widehat{x}/\chi, \widehat{p}/\iota)|\alpha\rangle = (\alpha_1\sqrt{2}, \alpha_2\sqrt{2})$.

We remind the definition of the binomial coefficient

$$\binom{n}{k} \stackrel{\text{def}}{=} \frac{n!}{k!(n-k)!}, \forall n \in \mathbb{N}, k \in \{0, 1, ..., n\}, \tag{D.25}$$

$$\binom{2j}{m+j} = \frac{(2j)!}{(m+j)!(j-m)!}. \tag{D.26}$$

Without proof (though the proof is not very difficult), we note that the following equations hold [37]

$$\langle\mu|\lambda\rangle = \frac{(1+\lambda^*\mu)^{2j}}{(1+|\lambda|^2)^j(1+|\mu|^2)^j}, \tag{D.27}$$

$$|\langle\mu|\lambda\rangle| = \left(1 - \frac{|\lambda-\mu|^2}{(1+|\lambda|^2)(1+|\mu|^2)}\right)^{2j} \tag{D.28}$$

$$\frac{2j+1}{\pi}\iint \frac{\mathrm{dIm}(\mu)\mathrm{dRe}(\mu)}{(1+|\mu|)^2}|\mu\rangle\langle\mu| = \sum_{m=-j}^{+j}|m\rangle\langle m| = \widehat{I}, \tag{D.29}$$

$$\langle\lambda|\widehat{J}_z|\mu\rangle = j\frac{1-\lambda^*\mu}{1+\lambda^*\mu}\langle\lambda|\mu\rangle, \tag{D.30}$$

$$\langle\lambda|\widehat{J}_+|\mu\rangle = \frac{2j\mu}{1+\lambda^*\mu}\langle\lambda|\mu\rangle, \tag{D.31}$$

where $\mu, \lambda \in \mathbb{C}$.

Instead of parametrization by complex number $\mu \in \mathbb{C}$, we parametrize the coherent spin states by two angles θ, ϕ (determining a position on the Bloch

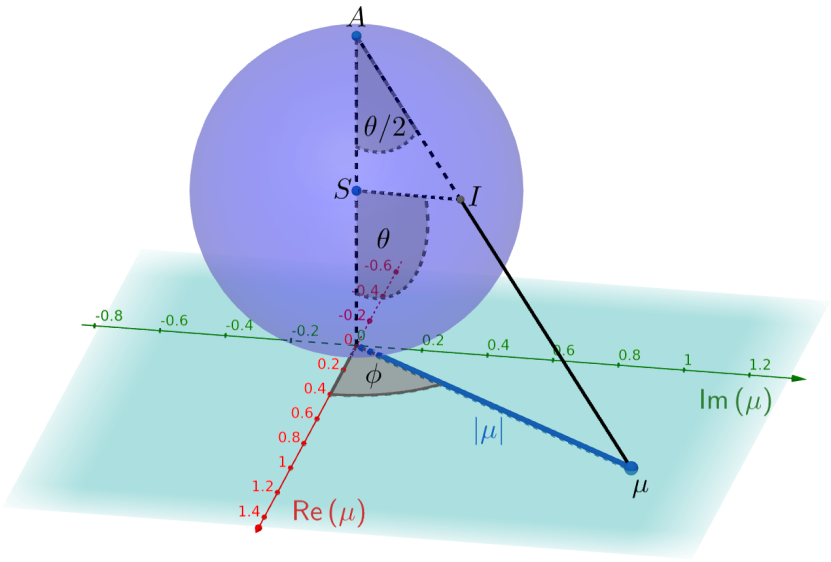

Figure D.6: A geometrical construction of the parametrization of the coherent spin states prescribed by $\mu = \tan(\theta/2)e^{i\phi}$. The sphere in the figure has the radius $|SA| = 1/2$. Note that the state $|\theta = 0, \phi = 0\rangle = |m = +j\rangle$ is mapped to the lower pole of the sphere in this figure. The Bloch sphere is equivalent to the sphere in this figure rotated so that the poles of the spheres are interchanged (and resized).

sphere) the following way

$$\mu = \tan\left(\frac{\theta}{2}\right) e^{i\phi},\ 0 \leq \theta < \pi,\ 0 \leq \phi < 2\pi. \tag{D.32}$$

The above parametrization (D.32) is visualized in figure D.6. Using equation (D.23), we derive that the coherent spin states parametrized by equation (D.32) are

$$\boxed{|\theta, \phi\rangle = e^{ij\phi} \sum_{m=-j}^{+j} \left[\binom{2j}{m+j}\right]^{\frac{1}{2}} \left(\cos\frac{\theta}{2}\right)^{j+m} \left(\sin\frac{\theta}{2}\right)^{j-m} e^{-im\phi} |m\rangle}. \tag{D.33}$$

We note again some useful equalities [37]

$$\langle\theta, \phi|\theta', \phi'\rangle = \left[\left(\cos\frac{\theta}{2}\right)\left(\cos\frac{\theta'}{2}\right) + \left(\sin\frac{\theta}{2}\right)\left(\sin\frac{\theta'}{2}\right) e^{i(\phi'-\phi)}\right]^{2j}, \tag{D.34}$$

$$|\langle\theta, \phi|\theta', \phi'\rangle| = \left(\frac{1 + \vec{n}(\theta, \phi) \cdot \vec{n}(\theta', \phi')}{2}\right)^{j}, \tag{D.35}$$

$$\vec{n}(\theta, \phi) \overset{\text{def}}{=} (\sin\theta\cos\phi, \sin\theta\sin\phi, \cos\theta)^T. \tag{D.36}$$

The important equality, which is analogous to equalities (D.14, D.15), is

$$\boxed{\left\langle \theta, \phi \middle| \widehat{\vec{J}} \middle| \theta, \phi \right\rangle = j\vec{n}(\theta, \phi)}, \tag{D.37}$$

where $\vec{n}(\theta, \phi)$ (D.36) is a unit vector pointing in the direction characterized by the angles θ and ϕ.

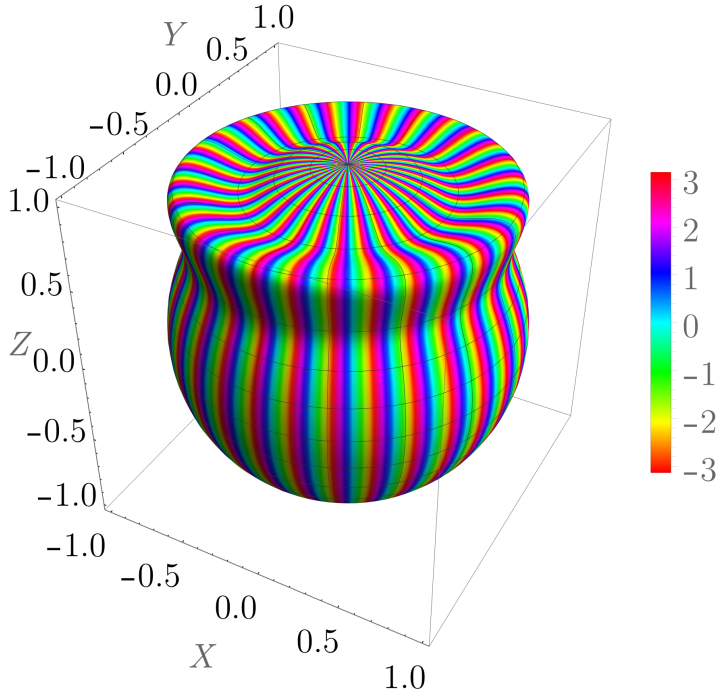

Figure D.7: A plot of the scalar product $\langle \theta, \phi | j = 100, m = 70 \rangle$. The landscape represents the function $1 + |\langle \theta, \phi | j = 100, m = 70 \rangle|$. The phase $\arg \langle \theta, \phi | j = 100, m = 70 \rangle$ is distinguished by colour.

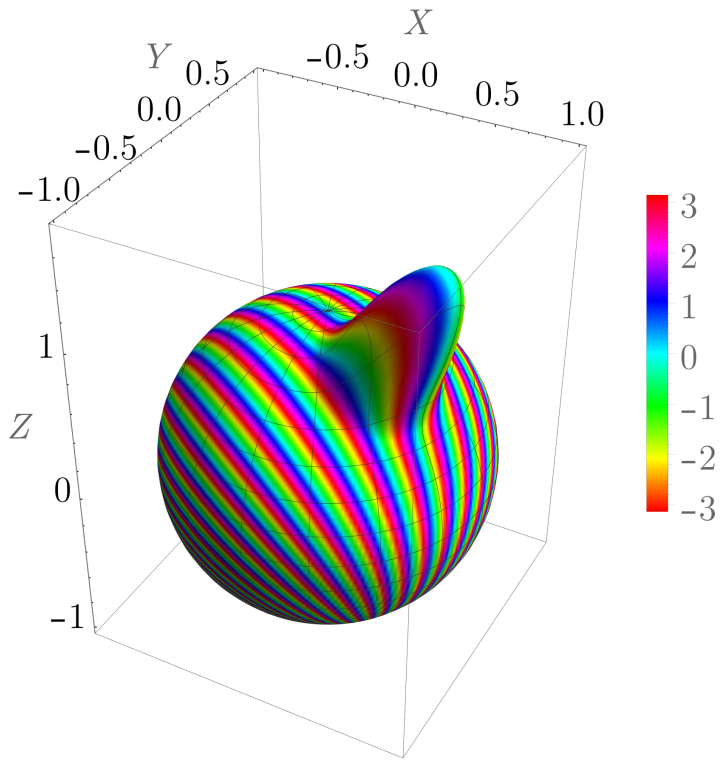

Figure D.8: A plot of the scalar product $h(\theta, \phi) \stackrel{\text{def}}{=} \langle \theta, \phi | \theta' = \frac{\pi}{6}, \phi' = -\frac{\pi}{7} \rangle$. The landscape represents the function $1 + |h(\theta, \phi)|$. The phase $\arg h(\theta, \phi)$ is represented by colour. In this figure $j = 100$.

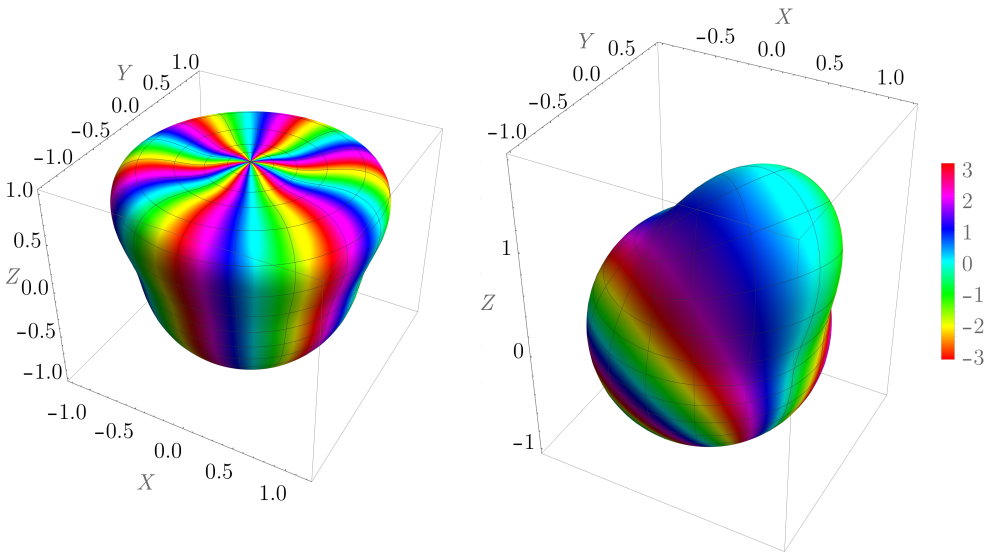

Figure D.9: The left plot represents the scalar product $\langle\theta,\phi|j=15,m=9\rangle$. The landscape represents the function $1+|\langle\theta,\phi|j=15,m=9\rangle|$. The phase $\arg\langle\theta,\phi|j=15,m=9\rangle$ is distinguished by colour. The right plot represents the scalar product $h_{15}(\theta,\phi)\overset{\text{def}}{=}\langle\theta,\phi|\theta'=\frac{\pi}{6},\phi'=-\frac{\pi}{7}\rangle$. The landscape represents the function $1+|h_{15}(\theta,\phi)|$ and the phase $\arg h_{15}(\theta,\phi)$ is represented by colour. In this figure $j=15$.

The completeness relation (D.29), expressed using the new parametrization, reads

$$\frac{2j+1}{4\pi}\int_0^{\pi}\int_0^{2\pi}\mathrm{d}\theta\mathrm{d}\phi\sin\theta\,|\theta,\phi\rangle\langle\theta,\phi| \;=\; \frac{2j+1}{4\pi}\iint\mathrm{d}\Omega\,|\theta,\phi\rangle\langle\theta,\phi| = \widehat{I},$$
$$\mathrm{d}\Omega \overset{\text{def}}{=} \mathrm{d}\theta\mathrm{d}\phi\sin\theta. \tag{D.38}$$

Analogues of figures D.1 and D.3 are figures D.7 and D.8. In figures D.7 and D.8 we present the states with high $j=100$ since for high j the shapes are enhanced. The states for $j=15$ are plotted in figure D.9.

D.3 Angular momentum Wigner distribution

We define the multipole operators the following way

$$\boxed{\widehat{T}_{kq}\overset{\text{def}}{=}\sum_{m=-j}^{+j}\sum_{m'=-j}^{+j}(-1)^{j-m}\sqrt{2k+1}\begin{pmatrix}j & k & j\\ -m & q & m'\end{pmatrix}|m\rangle\langle m'|}, \tag{D.39}$$

where $\begin{pmatrix}j & k & j\\ -m & q & m'\end{pmatrix}$ is the standard $3j$ symbol (its relation to Clebsch–Gordan coefficients and other properties are e.g. in [12]). The indices k,q has the range $k=0,...,2j$ and $q=-k,...,k$. Some more information regarding the multipole operators could be found in [41].

All the angular momentum operators could be expressed in terms of multipole operators

$$\widehat{A} = \sum_{k=0}^{2j} \sum_{q=-k}^{+k} A_{kq} \widehat{T}_{kq}. \tag{D.40}$$

The coefficients A_{kq} could be found using

$$\boxed{A_{kq} = \mathrm{Tr}\left(\widehat{T}_{kq}^{\dagger} \widehat{A}\right)}, \tag{D.41}$$

which is a consequence of equality [39]

$$\mathrm{Tr}\left(\widehat{T}_{kq}^{\dagger} \widehat{T}_{lr}\right) = \delta_{kl}\delta_{qr}. \tag{D.42}$$

The paper [39] defines various generalized phase-space distributions. By requiring

$$\mathrm{Tr}\widehat{A} = \sqrt{\frac{2j+1}{4\pi}} \int W(\theta,\phi)\mathrm{d}\Omega \tag{D.43}$$

and

$$\mathrm{Tr}\left[\widehat{A}^{(1)}\widehat{A}^{(2)}\right] = \int W^{(1)}(\theta,\phi)W^{(2)}(\theta,\phi)\mathrm{d}\Omega, \tag{D.44}$$

we choose from the distributions defined in [39] the distribution defined by[1]

$$\boxed{W(\theta,\phi) = \sum_{k=0}^{2j} \sum_{q=-k}^{+k} Y_{kq}^{*}(\theta,\phi) A_{kq}}. \tag{D.45}$$

In this thesis, we use only the distribution $W(\theta,\phi)$ constructed for the density operator of the system $\widehat{\rho}$, i.e. $\widehat{A} = \widehat{\rho}$.

Figure D.10 supports the use of the angular momentum Wigner distribution defined by (D.45) (and (D.41, D.39), $\widehat{A} = \widehat{\rho}$).

The state presented in the right plot in figure D.9 has the angular momentum Wigner distribution in plot f) in figure D.10. The state presented in the left plot in figure D.9 has the angular momentum Wigner distribution in plot g) in figure D.10.

The one-dimensional harmonic oscillator Wigner distribution in figure D.4 should be compared with plots c) and e) in figure D.10. Plot c) in figure D.10 is a three times shifted state $|m = +j\rangle$ (see equation (D.23)), i.e.

$$|m = +j\rangle = \widehat{J}_{-}^{3} |m = +j\rangle \,/ |\widehat{J}_{-}^{3} |m = +j\rangle\,|. \tag{D.46}$$

And similarly, $|M_y = 2, j = 5\rangle$ (the eigenstate of the operator $\widehat{J}_y$ with the eigenvalue 2) is a three times shifted state $|M_y = 5, j = 5\rangle$, i.e.

$$|M_y = 2, j = 5\rangle = \frac{\left(\widehat{J}_z - i\widehat{J}_x\right)^3 |M_y = 5, j = 5\rangle}{\left|\left(\widehat{J}_z - i\widehat{J}_x\right)^3 |M_y = 5, j = 5\rangle\right|}. \tag{D.47}$$

[1]The original papers [38, 39] define the distribution $\widetilde{W}(\theta,\phi) \stackrel{\mathrm{def}}{=} \sum_{k=0}^{2j} \sum_{q=-k}^{+k} Y_{kq}(\theta,\phi) A_{kq}$. When matching the distribution with the states $|m\rangle$ and $|\theta,\phi\rangle$, we found the definition (D.45) more convenient. The equalities (D.43, D.44) still hold since $Y_{kq}^{*}(\theta,\phi) = Y_{kq}(\theta,-\phi)$.

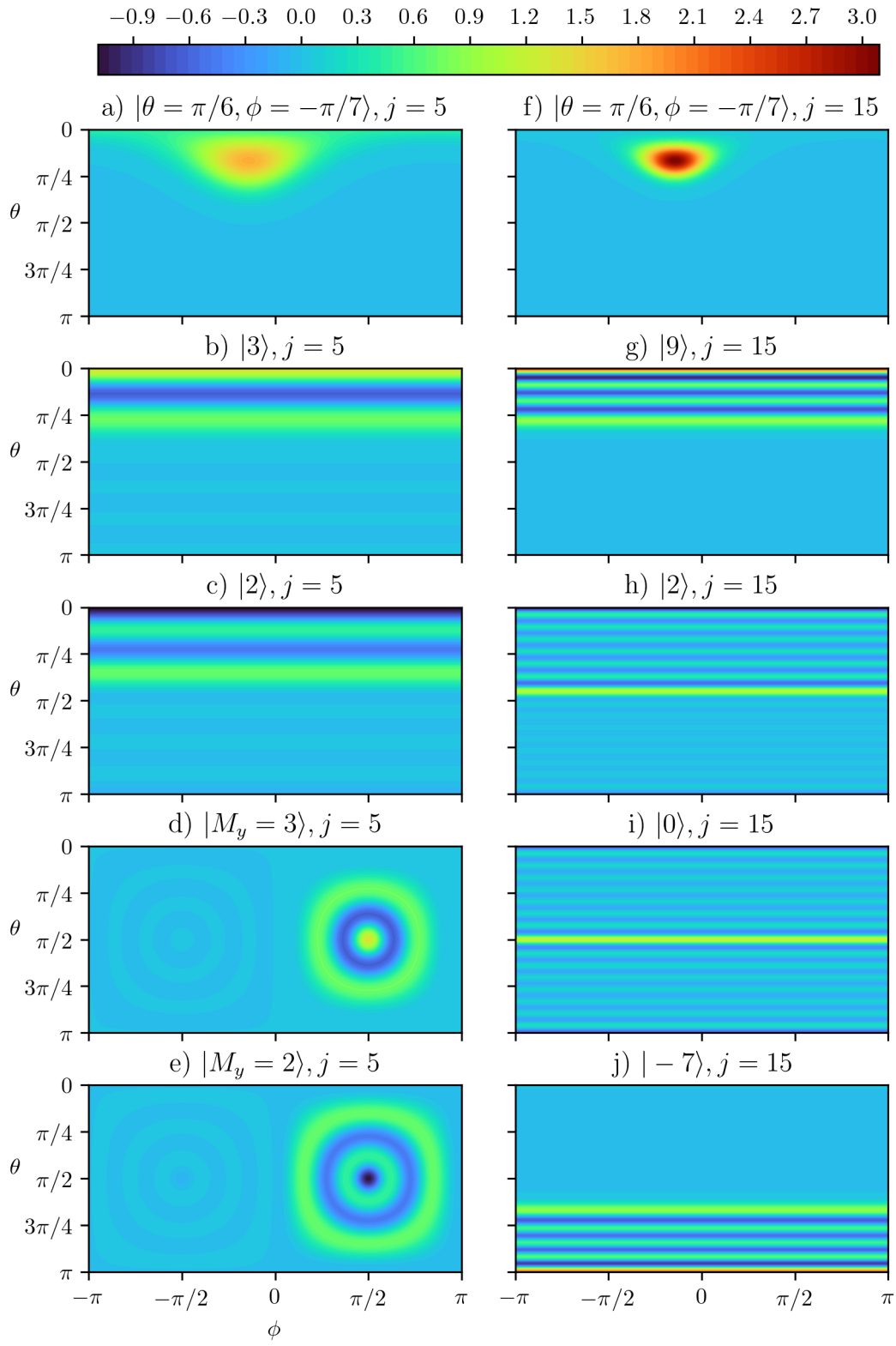

Figure D.10: Examples of various angular momentum Wigner distributions. The left column presents the states with $j = 5$ and the right column presents the states with $j = 15$. The first row presents coherent spin states. The states $|M_y\rangle$ are eigenstates of the operator $\widehat{J}_y$, i.e. $\widehat{J}_y |M_y\rangle = M_y |M_y\rangle$.

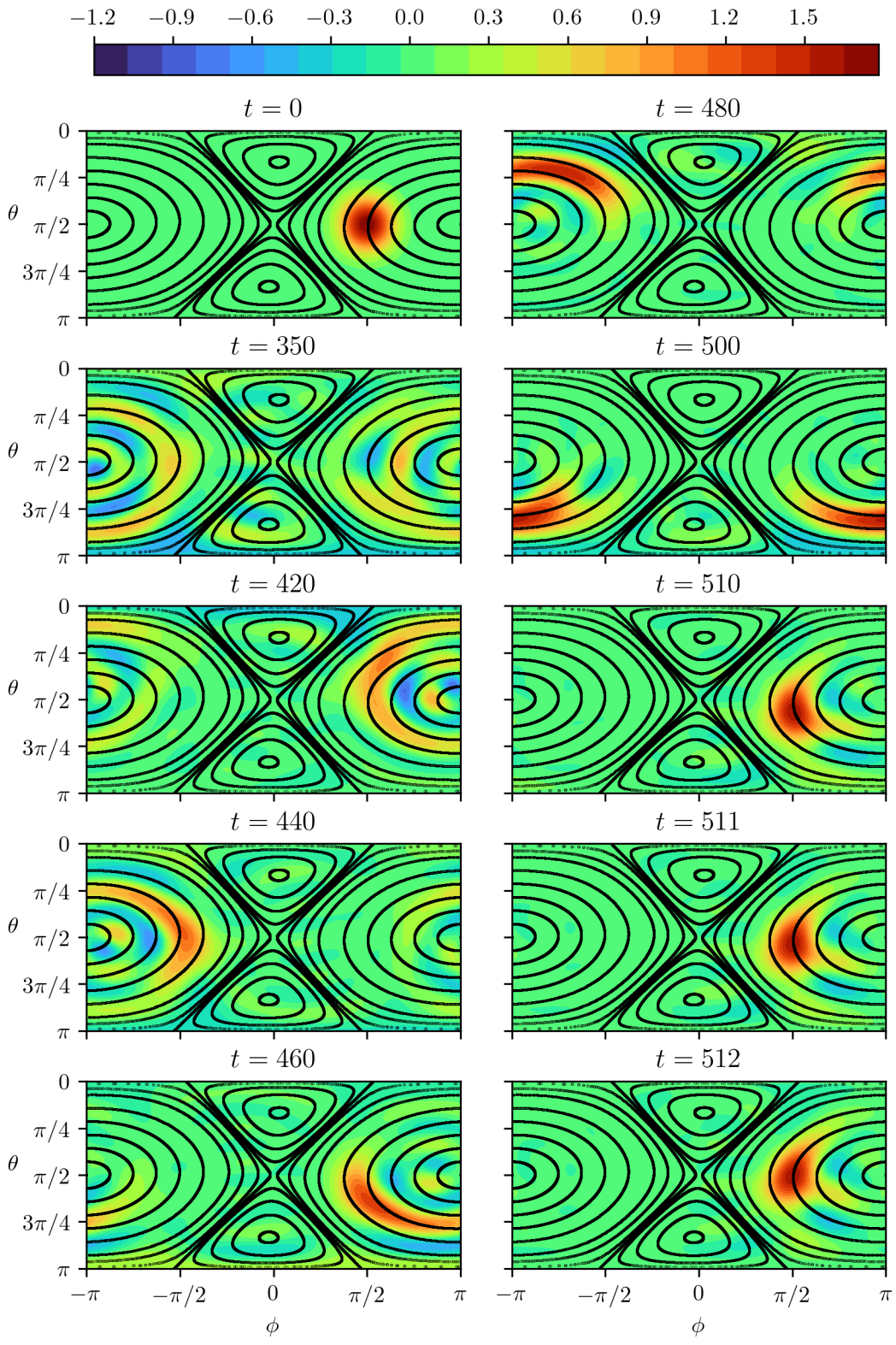

Figure D.11: A closer look into the Poincaré recurrence already identified in figure 3.10. The precise classical regular (not chaotic) trajectories in black compared with the evolution of the angular momentum Wigner function. We used the parameters of the kick top system $\kappa = 0.2, p = 0.1, j = 5$.

Bibliography

[1] G. Floquet. Sur les équations différentielles linéaires à coefficients périodiques. *Annales scientifiques de l'École Normale Supérieure*, 2e série, 12:47, 1883.

[2] J.H. Shirley. Solution of the Schrödinger equation with a Hamiltonian periodic in time. *Phys. Rev.*, 138:B979, 1965.

[3] S. Chaudhury, A. Smith, B.E. Anderson, S. Ghose, and P.S. Jessen. Quantum signatures of chaos in a kicked top. *Nature*, 461:768, 2009.

[4] N. Goldman and J. Dalibard. Periodically driven quantum systems: effective Hamiltonians and engineered gauge fields. *Phys. Rev. X*, 4:031027, 2014.

[5] J.N. Bandyopadhyay and T.G. Sarkar. Effective time-independent analysis for quantum kicked systems. *Phys. Rev. E*, 91:032923, 2015.

[6] P. Weinberg, M. Bukov, L. D'Alessio, A. Polkovnikov, S. Vajna, and M. Kolodrubetz. Adiabatic Perturbation Theory and Geometry of Periodically-Driven Systems. *Phys. Rep.*, 688, 2017.

[7] V.M. Bastidas, P. Pérez-Fernández, M. Vogl, and T. Brandes. Quantum criticality and dynamical instability in the kicked-top model. *Phys. Rev. Lett.*, 112:140408, 2014.

[8] V.M. Bastidas, G. Engelhardt, P. Pérez-Fernández, M. Vogl, and T. Brandes. Critical quasienergy states in driven many-body systems. *Phys. Rev. A*, 90:063628, 2014.

[9] P. Cejnar, M. Macek, S. Heinze, J. Jolie, and J. Dobeš. Monodromy and excited-state quantum phase transitions in integrable systems: collective vibrations of nuclei. *J. Phys. A: Math. Gen.*, 39:L515, 2006.

[10] M.A. Caprio, P. Cejnar, and F. Iachello. Excited state quantum phase transitions in many-body systems. *Ann. Phys.*, 323:1106, 2008.

[11] P. Cejnar and P. Stránský. Impact of quantum phase transitions on excited-level dynamics. *Phys. Rev. E*, 78:031130, 2008.

[12] P. Cejnar. *A Condensed Course of Quantum Mechanics*. Karolinum Press, Charles University in Prague, 2014.

[13] J.J. Sakurai and J. Napolitano. *Modern quantum mechanics*. Addison-Wesley, Boston, 2011. Page 345.

[14] M. Holthaus. Floquet engineering with quasienergy bands of periodically driven optical lattices. *J. Phys. B: At. Mol. Opt. Phys.*, 49:013001, 2015.

[15] S. Rahav, I. Gilary, and S. Fishman. Effective Hamiltonians for periodically driven systems. *Phys. Rev. A*, 68:013820, 2003.

[16] M. Bukov, L. D'Alessio, and A. Polkovnikov. Universal high-frequency behavior of periodically driven systems: from dynamical stabilization to Floquet engineering. *Adv. Phys.*, 64:139, 2015.

[17] M. Grifoni and P. Hänggi. Driven quantum tunneling. *Phys. Rep.*, 304:229, 1998.

[18] G. Santoro. Introduction to Floquet, 2019. Lecture notes, available at `https://www.ggi.infn.it/sft/SFT_2019/LectureNotes/Santoro.pdf`.

[19] N.W. Ashcroft and N.D. Mermin. *Solid State Physics*. Harcourt College Publishers, Orlando, 1976.

[20] C. Cohen-Tannoudji, B. Diu, and F. Laloë. *Quantum Mechanics, Volume 2: Angular Momentum, Spin, and Approximation Methods*. Wiley-VCH, 2 edition, 2019.

[21] H.J. Lipkin, N. Meshkov, and A.J. Glick. Validity of many-body approximation methods for a solvable model: (I). Exact solutions and perturbation theory. *Nuclear Physics*, 62:188, 1965.

[22] P. Cejnar and P. Stránský. Quantum phase transitions in the collective degrees of freedom: nuclei and other many-body systems. *Phys. Scr.*, 91:083006, 2016.

[23] J. Dolejší. Dynamics of externally driven quantum systems. Bachelor's thesis, Charles University, Faculty of Mathematics and Physics, Institute of Particle and Nuclear Physics, 2018.

[24] F. Haake. *Quantum Signatures of Chaos (Springer Series in Synergetics)*. Springer, 3rd edition, 2010.

[25] F. Haake and D.L. Shepelyansky. The kicked rotator as a limit of the kicked top. *Europhys. Lett.*, 5:671, 1988.

[26] G.M. Lando and A.M.O. de Almeida. Semiclassical evolution in phase space for a softly chaotic system, 2019. arXiv:1907.06298 `https://arxiv.org/abs/1907.06298`.

[27] G.M. Lando and A.M.O. de Almeida. Quantum-chaotic evolution reproduced from effective integrable trajectories. *Phys. Rev. Lett.*, 124:010402, 2020.

[28] QuantumOptics.jl. Quantum kicked top. Available at `https://docs.qojulia.org/examples/quantum-kicked-top/#`.

[29] S. Krämer, D. Plankensteiner, L. Ostermann, and H. Ritsch. QuantumOptics. jl: A Julia framework for simulating open quantum systems. *Comput. Phys. Commun.*, 227:109, 2018.

[30] P. Bocchieri and A. Loinger. Quantum recurrence theorem. *Phys. Rev.*, 107:337, 1957.

[31] G. Casati, B. V. Chirikov, F.M. Izraelev, and J. Ford. Stochastic behavior of a quantum pendulum under a periodic perturbation. In G. Casati and J. Ford, editors, *Stochastic Behavior in Classical and Quantum Hamiltonian Systems*, page 334, Berlin, Heidelberg, 1979. Springer Berlin Heidelberg.

[32] B. Chirikov and D. Shepelyansky. Chirikov standard map. *Scholarpedia*, 3:3550, 2008. Revision #197507. Available at `http://www.scholarpedia.org/article/Chirikov_standard_map`.

[33] A.A.M. Cuyt, V. Petersen, B. Verdonk, H. Waadeland, W.B. Jones, F. Backeljauw, and C. Bonan-Hamada. *Handbook of Continued Fractions for Special Functions*. Springer, 2008. Page 344.

[34] D.H. Sattinger and O.L. Weaver. *Lie Groups and Algebras with Applications to Physics, Geometry, and Mechanics (Applied Mathematical Sciences, 61)*. Springer, 1986.

[35] R. Scharf. The Campbell-Baker-Hausdorff expansion for classical and quantum kicked dynamics. *J. Phys. A: Math. Gen.*, 21:2007, 1988.

[36] A. Milton. *Handbook of Mathematical Functions, With Formulas, Graphs, and Mathematical Tables*. Dover Publications, Inc., USA, 1970.

[37] J.M. Radcliffe. Some properties of coherent spin states. *J. Phys. A: Gen. Phys.*, 4:313, 1971.

[38] J.P. Dowling, G.S. Agarwal, and W.P. Schleich. Wigner distribution of a general angular-momentum state: Applications to a collection of two-level atoms. *Phys. Rev. A*, 49:4101, 1994.

[39] G.S. Agarwal. Relation between atomic coherent-state representation, state multipoles, and generalized phase-space distributions. *Phys. Rev. A*, 24:2889, 1981.

[40] K.E. Cahill and R.J. Glauber. Ordered expansions in boson amplitude operators. *Phys. Rev.*, 177:1857, 1969.

[41] W. Hanle and H. Kleinpoppen. *Progress in Atomic Spectroscopy: Part A (Physics of Atoms and Molecules)*. Plenum Press, New York and London, 1978. Page 86.